論文 / 著書情報
Article / Book Information

題目(和文)	
Title(English)	Identification of ferrochelatase as a novel target of salicylic acid-induced mitochondrial injury
著者(和文)	GUPTAVIPUL
Author(English)	Vipul Gupta
出典(和文)	学位:博士(理学), 学位授与機関:東京工業大学, 報告番号:甲第9355号, 授与年月日:2013年12月31日, 学位の種別:課程博士, 審査員:山口 雄輝,工藤 明,川上 厚志,立花 和則,小倉 俊一郎
Citation(English)	Degree:Doctor (Science), Conferring organization: Tokyo Institute of Technology, Report number:甲第9355号, Conferred date:2013/12/31, Degree Type:Course doctor, Examiner:,,,,
学位種別(和文)	博士論文
Type(English)	Doctoral Thesis

東京工業大学
Tokyo Institute of Technology

Identification of ferrochelatase as a novel target of salicylic acid-induced mitochondrial injury

サリチル酸が引き起こすミトコンドリア損傷の新規標的因子 **ferrochelatase** の同定

Supervisor

Professor Yuki YAMAGUCHI

Submitted in total conformity with the requirement for the degree of

Doctor of Science

By

Vipul GUPTA
Student ID: 09D52013
Department of Biological Information
Graduate School of Bioscience and Biotechnology
Tokyo Institute of Technology

September 2013

Contents

Abbreviations

SA	Salicylic acid
m-HBA	*meta*-hydroxybenzoic acid
p-HBA	*para*-hydroxybenzoic acid
PpIX	Protoporphyrin IX
NADH	Nicotinamide adenine dinucleotide
NAD(P)H	Nicotinamide adenine dinucleotide phosphate
ATP	Adenosine triphosphate
FECH	Ferrochelatase
AMO	Antisense morpholino oligonucleotide
PBS	Phosphate buffered saline
WST-8	2-(2-methoxy-4-nitrophenyl)-3-(4-nitrophenyl)-5-(2,4-disulfophenyl)-2H-tetrazolium ,monosodium salt]
1-Methoxy PMS	1-Methoxy-5-methylphenazinium methylsulfate
FCCP	Carbonyl cyanide p-trifluoromethoxyphenylhydrazone
Ub	Ubiquitin
UPLC	Ultra-high performance liquid chromatography

Chapter 1. General introduction

1.1 Identification of drug targets

Generally, medicinal drugs exert their effects by interacting with specific proteins in the body, but many of the currently available drugs have been introduced into the market without prior knowledge of their target proteins or the mechanism of action. For proper efficacy and specificity, the mechanism of action of a drug should be completely understood. In order to understand the mechanism, it is important to know the following points: (i) how a drug reaches to the site of its action, (ii) what cellular targets are bound by the drug, (iii) what effect the drug has on the target molecules, and (iv) what phenotypic changes the drug induces.

Target elucidation and validation for medicinal drugs can give us valuable information about the biological and biochemical reactions pertaining to the drug. In addition, the information can also help understand any side effects of the drug and thus can provide a new insight for developing more potent drugs with lower side effects based on its structure-activity relationship (Morrison and Weiss, 2006). Keeping this in mind, we have been working hard to develop a technology that can provide a comprehensive and reproducible methodology for target elucidation (Sakamoto et al., 2009) and here I used this technology to elucidate a novel target of non-steroidal anti-inflammatory drug (NSAID), salicylic acid.

1.2 Salicylic acid

Salicylic acid or 2-hydroxybenzoic acid or ortho-hydroxybenzoic acid ($C_7H_6O_3$; molecular weight = 138.12; **Figure 1-1**) is a non-steroidal anti-inflammatory, anti-pyretic and analgesic drug that has been used for centuries to treat pain and fever. It occurs naturally in plant as an important signal molecule in plant defense responses (Durner et al., 1997). It is a small, colorless molecule consisting of a hydroxyl and a carboxyl group with a hydrophobic benzene ring. Salicylic acid belongs to the family of non-steroidal anti-inflammatory drugs, which nevertheless share certain therapeutic effects. This class includes many derivatives of salicylic acid and represents one of the most widely prescribed over-the-counter medicines that are used as analgesic, antipyretic and anti-inflammatory drugs.

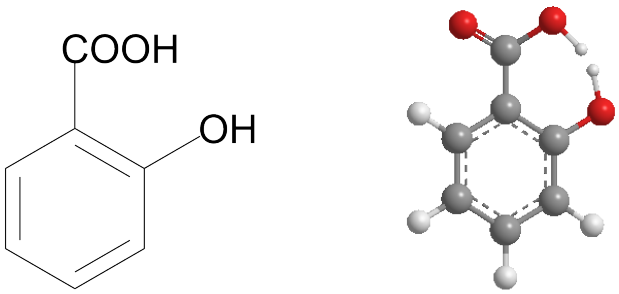

Figure 1-1. Salicylic acid (SA) or 2-hyroxybenzoic acid or *ortho*-hydroxybenzoic acid.

One of the most popular member of this family is aspirin (acetyl salicylic acid). Aspirin ($t_{1/2\ plasma}$ = 15 ~ 30 min), after oral administration is rapidly de-acetylated by plasma and cellular esterase to salicylic acid ($t_{1/2\ plasma}$ = 2 ~ 30 h) increasing its plasma concentration (Needs and Brooks, 1985), leading to an assumption that anti-inflammatory effects of aspirin are largely mediated by salicylate (Higgs et al., 1987).

1.2.1 Historical perspective

The therapeutic effect of willow bark (*Salix alba*) has been appreciated for many centuries after it was first reported about 3500 years ago. Legendary physician *Hippocrates* (~460 B.C.–370 B.C.), who is also considered as the father of modern medicine, mentioned the use of the willow bark extract as a treatment for pain, headache and fever. In the early 19th century, the advancement in chemistry led to the successful extraction of natural compounds from their sources. In the same era, two Italian researchers, *Brugnatelli and Fontana*, started the identification of the active component responsible for the therapeutic effect of willow bark. They successfully extracted an impure form of the active chemical substances. But it was in 1828 when *Johann Buchner* extracted the pure form as a bitter tasting yellow crystal, which he named as salicin (**Figure 1-2**).

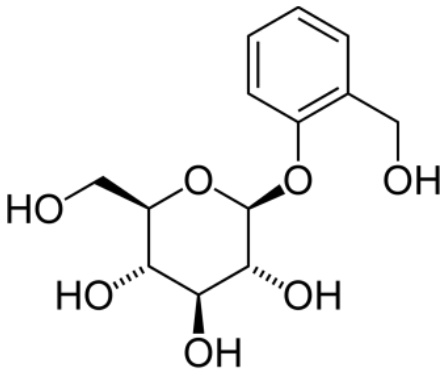

Figure 1-2. Salicin was extracted as the main constituent responsible for therapeutic effect of willow bark.

A decade later in 1838, Italian scientist *Raffaele Piria* at the Sorbonne in Paris successfully hydrolyzed salicin, splitting it into sugar and phenolic component and succeeded in oxidizing the hydroxymethyl group of the phenolic fragment to extract pure salicylic acid (**Figure 1-3**).

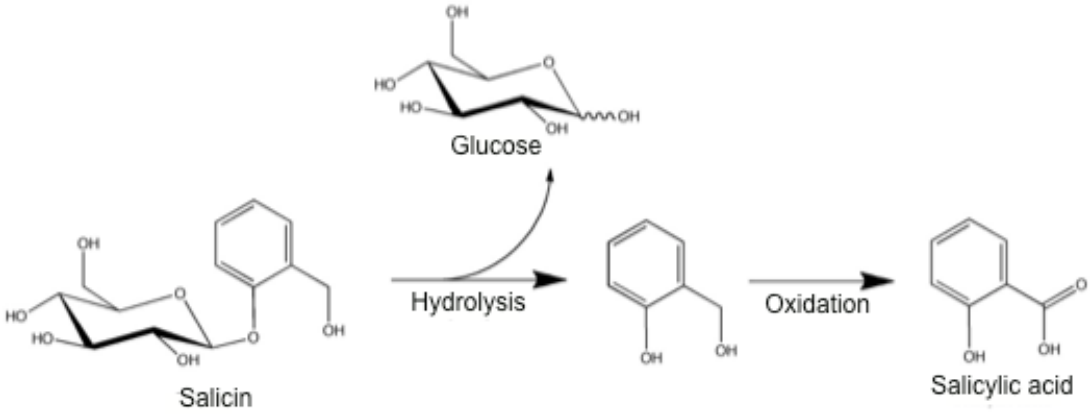

Figure 1-3. Salicylic acid was synthesized from salicin by hydrolyzing glucose moiety and oxidizing the product to form salicylic acid.

In the late 19th century, renowned German scientist *Hermann Kolbe* along with *Friedrich von Heyden* developed a process to chemically synthesize salicylic acid on large scale (**Figure 1-4**). With a cheaper cost and high benefit, salicylic acid became a general prescription for all kinds of pain ailments for that period. However, despite of its efficacy to treat pain, salicylic acid could not become a remedy, basically, because of its foul smell and side effects such as irritation of stomach.

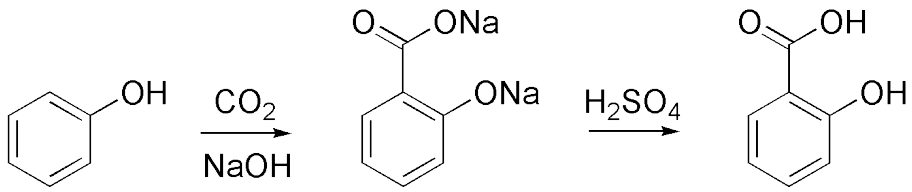

Figure 1-4. Salicylic acid was chemically synthesized by *Kolbe process*. Sodium phenolate was heated in the presence of carbon dioxide (CO_2) under high pressure followed by reaction with sulfuric acid (H_2SO_4). Salicylic acid was formed as the final product.

To neutralize the side effect of salicylic acid, it was chemically modified by *Felix Hoffmann*, a synthetic organic chemist at Bayer. He successfully synthesized acetylsalicylic acid and named it as “Aspirin” (**Figure 1-5**). This accomplishment was also said to be his personal effort to reduce the problem faced by his father while taking sodium salicylate.

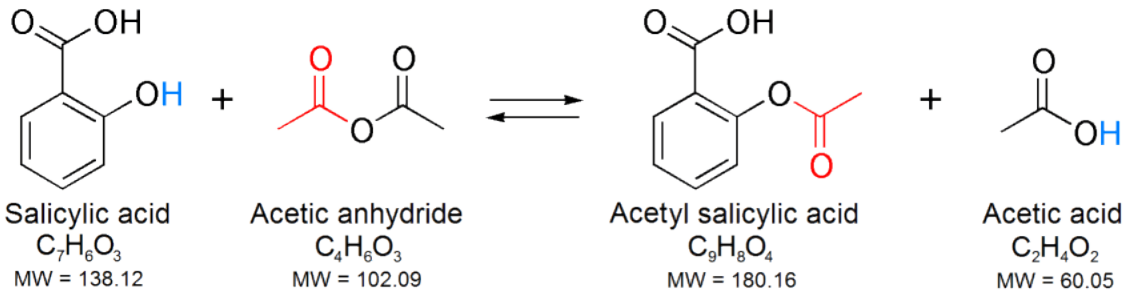

Figure 1-5. Synthesis of aspirin (acetyl salicylic acid) from salicylic acid.

French chemist *Charles Frederic Gerhardt* was the first to synthesize acetylsalicylic acid in 1853, by neutralizing salicylic acid with sodium hydroxide and acetyl chloride. But he was unable to identify the structure and medicinal benefits of this compound and thus left this discovery. Finally, the early 20th century marked the rise of aspirin as a wonder drug, and it became a standard item in every household’s medicine cabinet.

1.2.2 Pharmacological effects

Salicylic acid is known for its potent analgesic, antipyretic and anti-inflammatory activity (Grosser et al., 2009; Needs and Brooks, 1985). Epidemiological data also suggest the link between the increased and prolonged use of aspirin and salicylic acid and a decreased cancer risk (Elder et al., 1996; Bellosillo et al., 1998; Klampfer et al.,

1999). In addition, aspirin (Bellosillo et al., 1998; Piqué et al., 2000; Zimmermann et al., 2001) and salicylic acid (Elder et al., 1996; Bellosillo et al., 1998; Klampfer et al., 1999) inhibit cell proliferation and induce apoptosis in many cancer cell lines including colon cancer (Elder et al., 1996) and leukemia cells (Bellosillo et al., 1998; Klampfer et al., 1999; Piqué et al., 2000) and is therefore often used as a cancer treatment. Moreover, aspirin administration in severe rheumatoid causes several fold increase in plasma concentration of salicylic acid, which in addition to analgesia, causes various adverse events, such as gastrointestinal toxicity, renal toxicity, hepatic injury, and neurological and respiratory imbalances (Grosser et al., 2009; Needs and Brooks, 1985).

Salicylic acid is known to have detrimental effect on mitochondria such as inhibition of ATP synthesis, mitochondrial swelling, and disruption of mitochondrial membrane potential (Braun et al., 2012; Doi and Horie, 2010; Klampfer et al., 1999). Salicylic acid-induced mitochondrial damage contributes to the anti-inflammatory actions of salicylic acid by inhibiting oxidative phosphorylation and thereby reducing cellular ATP levels and consequently, induces the release of adenosine, an autocoid with strong anti-inflammatory properties (Cronstein, 1994), into extracellular fluids in sufficient quantities to exert anti-inflammatory effects (Cronstein, 1994, Cronstein et al., 1999, Amann and Peskar, 2002). However, the molecular mechanism through which salicylic acid induces mitochondrial injury is not well understood. Although several proteins, such as cyclooxygenase (COX), IκB kinase (IKK-β), and adenosine monophosphate-activated protein kinase (AMPK), are now recognized as therapeutic targets of aspirin and/or salicylic acid, a comprehensive understanding of the complex pharmacological mechanism of action of salicylic acid has not yet been achieved and it is evident that there might be unknown targets of salicylic acid that mediates its other effects such as anti-mitochondrial activity.

1.2.3 Known targets of salicylic acid

1.2.3.1 Cyclo-oxygenase (COX)

NSAIDs are known to induce analgesic, antipyretic and anti-inflammatory activity by inhibiting prostaglandin synthesis. Cyclo-oxygenase (COX; prostaglandin-endoperoxide synthase, EC 1.14.99.1) is responsible for the formation of prostaglandin in cells from arachadonic acid. Almost all the NSAIDs, reversibly or irreversibly, inhibit COX activity and prostaglandin production. Although belonging to the same class of drugs, salicylic acid has almost no inhibitory activity against purified COX (Mitchell et al., 1993). Aspirin inhibits COX by acetylation of serine residue present in the active site of prostaglandin synthase (Loll et al., 1995). Although salicylic acid lacks the acetyl group and has no significant effect on purified COX, still it shares similar anti-inflammatory effects *in vivo* (Mitchell et al., 1993). Considering the short half-life of aspirin (Grosser et al., 2009; Needs and Brooks, 1985), the major pharmacological action of aspirin can be because of its metabolite, salicylic acid (Higgs et al., 1987). Nevertheless, the pathway through which salicylic acid inhibits prostaglandin synthesis is still unknown, and current information only suggests that other targets that indirectly affect COX activity might account for the anti-inflammatory actions of salicylic acid.

1.2.3.2 IκB kinase β (IKK-β)

A well-known protein target of salicylic acid and aspirin is IκB kinase β (IKK-β), a subunit of IκB kinase (IKK) and a key enzyme in the nuclear factor (NF)-κB pathway (Kopp and Ghosh, 1994; Yin et al., 1998). NF-κB pathway controls the transcription of genes involved in the immune and inflammatory responses to external stimuli such as

cytokines - interleukins (IL-1, IL-6, IL-8), interferon β and TNF-alpha. NF-κB is a homo- or heterodimeric complex formed by the Rel-like domain-containing proteins RELA/p65, RELB, NFKB1/p105, NFKB1/p50, REL and NFKB2/p52 and the heterodimeric p65-p50 complex appears to be most abundant one (Beinke et al., 2004). NF-κB complexes are held in the cytoplasm in an inactive state bound to a NF-κB inhibitor, IκB. Upon induction by external stimuli, IκB is phosphorylated by IκB kinase (IKK) enzyme leading to the proteosomal degradation of IκB by ubiquitination (**Figure 1-6**) and thus liberating the active NF-κB complex, which translocates to the nucleus and stimulates the gene expression (**Figure 1-6**). Salicylic acid and aspirin bind to IKK-β and inhibits its IκB phosphorylation activity by reducing ATP binding (Kopp and Ghosh, 1994; Yin et al., 1998).

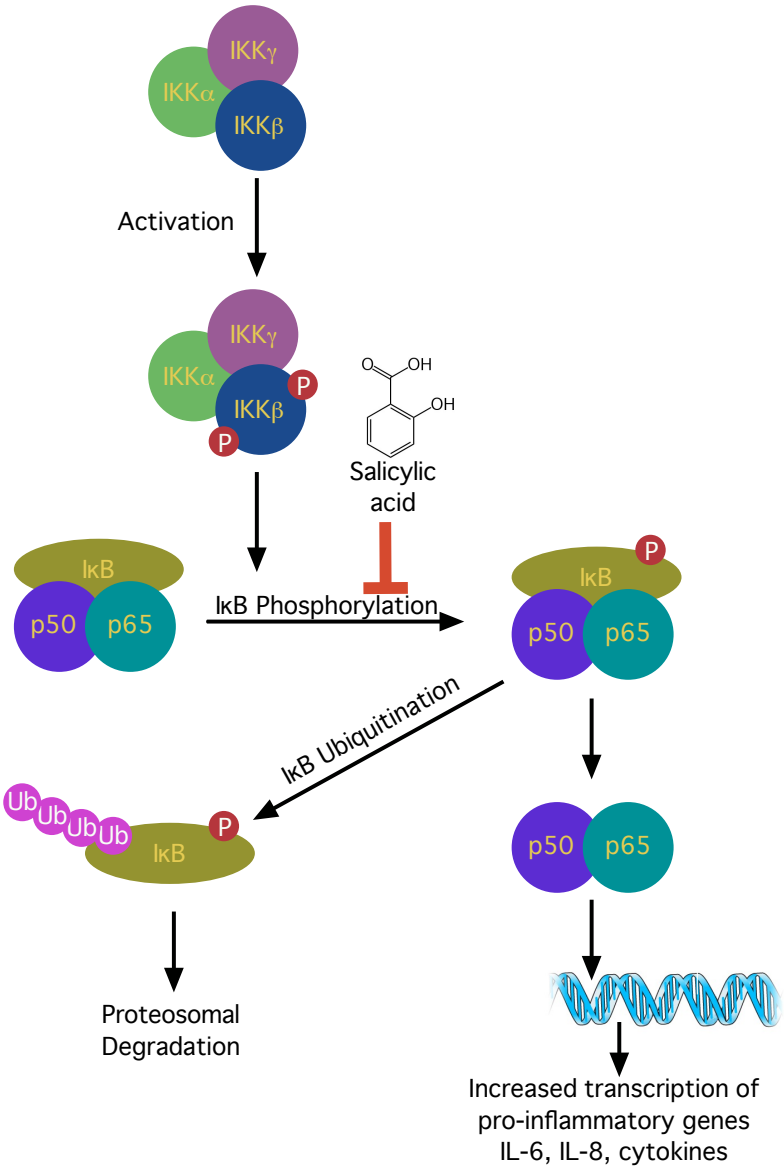

Figure 1-6: Pathway of NF-κB activation and its inhibition by salicylic acid. Cytokines such as TNF-α and environmental hazards such as ionizing radiation or toxins activates the nuclear translocation of NF-κB via activation of the inhibitor-of-NF-κB (IκB) kinase complex (IKK). IKK phosphorylates IκB bound to NF-κB, which consists of a dimer of Rel family proteins such as p65 and p50. This phosphorylation is the signal for ubiquitination of IκB. This marks IκB for proteosomal degradation, which then results in the release of NF-κB and its translocation to the nucleus where it binds to specific DNA elements and activates the transcription of NF-κB-dependent genes. Abbreviation: Ub, ubiquitin.

Later, it was shown that the anti-inflammatory action of salicylic acid is not entirely dependent on NF-κB pathway, but other factors might also play a central role in its activity (Cronstein et al., 1999). This was based on the experiment in which it was shown that anti-inflammatory actions of salicylic acid can still be observed in NF-κB p105/p50 (NF-κB1) deficient mice (Cronstein et al., 1999; Langenbach et al., 1999). Also, mice deficient in COX activity showed similar kind of results (Cronstein et al., 1999). Thus, based on these results, it is possible that other factors are involved in salicylic acid induce anti-inflammatory actions.

1.2.3.3 Adenosine monophosphate-activated protein kinase (AMPK)

Adenosine monophosphate-activated protein kinase (AMPK), a cellular energy regulator protein, was identified as a new target of salicylic acid (Hawley et al., 2012). AMPK is found in all eukaryotes as a heterotrimer composed of a catalytic α subunit and regulatory β and γ subunits (Steinberg and Kemp, 2009; Hardie et al., 2012; Steinberg et al., 2013). Upon activation under metabolic stress, AMPK *switches off* ATP-consuming processes and *switches on* ATP-generating pathways, thereby increasing ATP production in cells. Salicylic acid has been shown to reduce circulating free fatty acids and/or triglycerides in humans with type 2 diabetes and to increase fatty acid metabolism during fasting in healthy humans (Steinberg and Kemp, 2009; Hardie et al., 2012; Steinberg et al., 2013). Salicylic acid, but not aspirin, was found to allosterically activate AMPK in cells (Hawley et al., 2012; Steinberg et al., 2013). Salicylic acid-induced activation of AMPK was shown to be responsible for an increased fat metabolism in mice (Hawley et al., 2012). However, this finding contradicts the previous reports showing that salicylic acid inhibits oxidative phosphorylation and thus reduces ATP production in cells. Moreover, the possible link between this finding and the anti-inflammatory and anti-mitochondrial function of salicylic acid remains unknown.

1.3 Purpose of this study

This study is focused on the identification of novel target of salicylic acid that can connect the unknown links between different, yet important, pathways that leads to its pharmacological action. Although it has been known for long that salicylic acid inhibits mitochondrial ATP synthesis and disrupts mitochondrial membrane potential, the mechanism of its action is poorly understood. The currently known targets of salicylic acid such as COX, IKK-β, and AMPK, are unlikely to account for its anti-mitochondrial activity. Thus, this study will aim to provide a relevant model for salicylic acid–induced mitochondrial injury.

The novel target is validated by several sets of biophysical and biochemical experiments. This includes the use of newly developed FG beads affinity purification technology, *in vitro* enzyme inhibition assay, X-ray crystallography, Isothermal Titration Calorimetry (ITC). In addition, cell-based assay systems are used to validate the interaction at the cellular level. Furthermore, animal experiments are performed to investigate the physiological relevance of this interaction. I believe that this study has broad implications in complex pharmacological effects of salicylic acid.

Chapter 2. Identification of novel salicylic acid-binding protein

2.1 Introduction

Investigations to understand the mechanism of salicylic acid action has been carried out for decades with an aim to completely elucidate the events that are related, directly or indirectly, to its action. With a broad spectrum of effects that includes anti-inflammatory, anti-cancer and anti-diabetic effects, salicylic acid can be a potential lead compound in development of novel drugs. However, this again requires the knowledge of its action inside the cells. As described in chapter 1, apart from inhibiting prostaglandin synthesis and nuclear factor (NF)-κB pathway, salicylic acid is well known to induce mitochondrial injury. This includes inhibition of ATP synthesis, mitochondrial swelling and the disruption of mitochondria membrane potential. Salicylic acid inhibits prostaglandin synthesis in intact cells but does not inhibit purified cyclooxygenase activity. In addition, mice model lacking the NF-κB pathway still shows some of the effects of salicylic acid. Thus, these targets do not fully explain the mechanism of salicylic acid action and, therefore, there might be some possibility that salicylic induces its effects by interaction to other proteins. To better understand the mechanism of action of drugs such as salicylic acid, we previously developed high performance affinity beads that allow one-step affinity purification of drug target proteins from crude cell extracts (Sakamoto et al., 2009). By using this methodology, we successfully identified new molecular targets of pharmacological drugs and elucidated novel cellular mechanisms responsible for their actions (Ito et al., 2010; Sakamoto et al., 2009; Shimizu et al., 2000; Uga et al., 2006).

Here, using one-step affinity purification methodology, I show ferrochelatase (FECH) as a novel protein target of salicylic acid. FECH specifically binds to salicylic acid beads and inhibits purified recombinant FECH activity. Moreover, salicylic acid, compared to its isomers, shows specific inhibitory effect on FECH. I also show that salicylic acid can bind to FECH from a different organism, thus showing that this interaction is cell type- and species- independent.

2.2 Materials and methods

2.2.1 Cell culture, antibodies, and reagents

Human erythroleukemia K562 cells were cultured in RPMI 1640 medium supplemented with 10% fetal bovine serum. 293T cells were cultured in DMEM supplemented with 10% fetal bovine serum. Rabbit polyclonal antibody against FECH was obtained from Abcam. Sodium salicylate was dissolved in ultrapure water, buffer, or directly in medium, as appropriate. Stock solutions of *meta*-hydroxybenzoic acid (*m*-HBA) and *para*-hydroxybenzoic acid (*p*-HBA) were prepared in 1 M NaOH, and the pH was adjusted to 7.4. Stock solutions of PpIX (10 mM in dimethyl sulfoxide, Frontier Scientific) and zinc acetate (10 mM in milliQ) were prepared and stored at −20°C until use.

2.2.2 Preparation of salicylic acid-immobilized beads

Salicylic acid was immobilized on carboxylated ferrite-glycidyl methacrylate (FG) beads by using 200 mM *N*-hydroxysuccinimide and 200 mM 1-ethyl-3-(3-dimethylaminopropyl)-carbodiimide. Beads were then incubated with 30 mM 5-amino salicylic acid (Nacalai Tesque) in *N,N*-dimethylformamide for 24 h at room temperature. Unreacted carboxylic acids were masked with 1 M 2-ethanolamine in *N,N*-dimethylformamide, and the resulting beads were stored at 4°C until use.

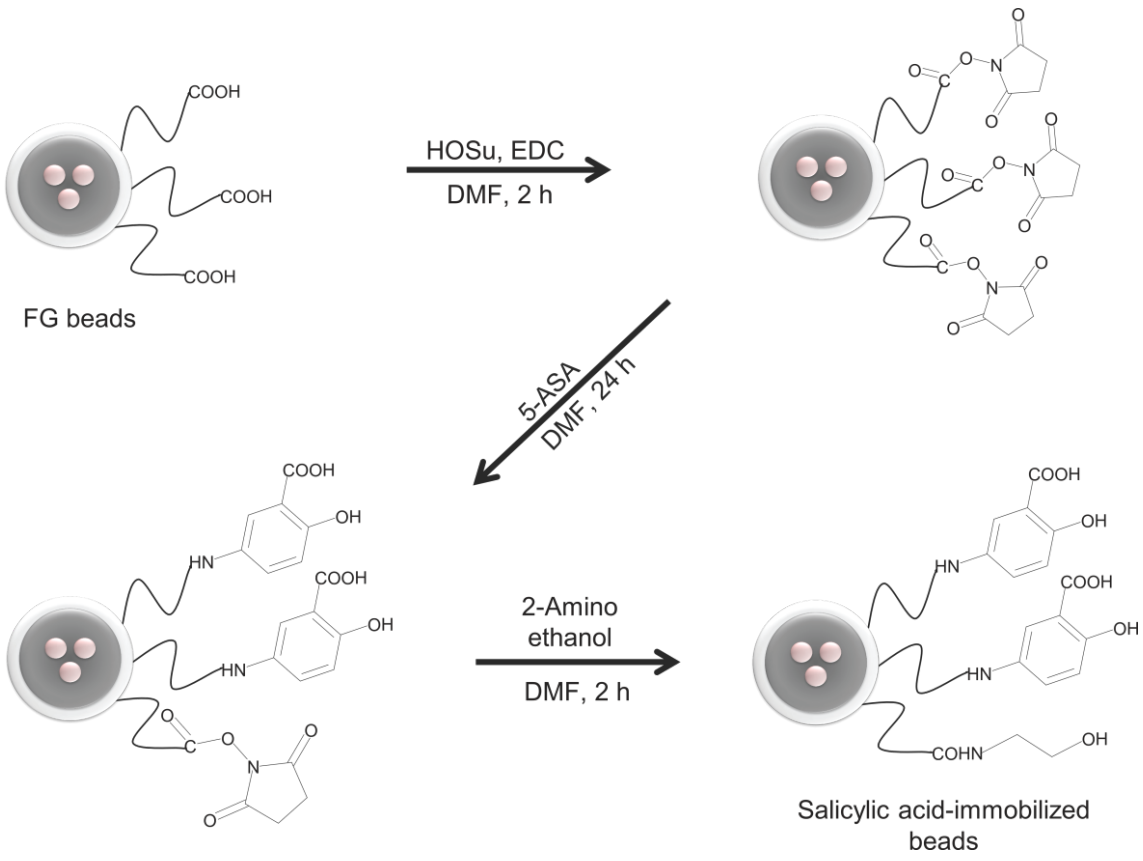

Figure 2-1: Chemistry of salicylic acid immobilization on FG beads. Control beads without salicylic acid were prepared by adding DMF only instead of 5-ASA. Beads were stored in milliQ at 4°C.

2.2.3 Preparation of input lysate for affinity purification

2.2.3.1 K562 cell extracts

K562 crude cell extracts were prepared in buffer IB-A (20 mM Hepes, pH 7.9, 100 mM KCl, 0.1% Triton X-100, and 10% glycerol). Briefly 1 x 10^7 cells were harvested, washed 2 times with Phosphate Buffered saline (PBS) and lysed using 3 times pellet volume of buffer IB-A by pipetting and incubation on ice for 15 min. After centrifugation at 20,400 x g 4°C 10 min, supernatant was collected and protein concentration was measured by Bradford using BSA as standard. The extract was

stored at -80°C until use.

2.2.3.2 Rat brain/liver mitochondria extract

Rats were sacrificed by a blow on the head, decapitated, and immediately exsanguinated. The liver and brain were quickly removed, cleansed of connective tissue and stored at -80°C until use. For mitochondria preparation liver and brain tissues were weighed and thawed in 10 times volume of pre-chilled buffer A (250 mM sucrose, 10 mM Tris-HCl pH 7.4). The tissues were minced with scissors to small fragments and homogenized in pre-chilled Potter homogenizer with pestle using Mazela Z-2200 homogenizer at 400 rpm. After 2 times of homogenization, the homogenate was collected in 15 ml tube and centrifuged at 80 x g, 4°C,10 min to remove cells debris and tissue fragments. The supernatant was collected and equal volume of buffer B (350 mM sucrose, 10 mM Tris-HCl pH 7.4) was added followed by centrifugation at 700 x g, 4°C, and 10 min. The supernatant was carefully collected and transferred to a 2 ml eppendorf tube and centrifuged at 7000 x g, 4°C, and 10 min. The pellets were washed twice in buffer A. To prepare mitochondria extracts, the pellets were lysed in buffer IB-A (20 mM Hepes, pH 7.9, 100 mM KCl, and 0.1% Triton X-100, and 10% glycerol) by pipetting and incubation on ice for 15 min. After centrifugation at 20,400 x g 4°C 10 min, supernatant was collected and protein concentration was measured by Bradford using BSA as standard. The extract was stored at -80°C until use.

2.2.4 Affinity purification

Affinity purification was performed to isolate salicylic acid-binding protein from cell extracts. The basic protocol includes 4 steps (i) equilibration, (ii) binding, (iii) washing and, (iv) elution.

(i) **Equilibration:** Control or salicylic acid-immobilized beads (0.2 mg) were taken in 1.5 ml eppendorf tubes and suspended in buffer IB-A (20 mM Hepes, pH 7.9, 100 mM KCl, 0.1% Triton X-100, and 10% glycerol). The suspended beads were spin-down and collected by magnetic separation until the supernatant becomes clear.

(ii) **Binding:** Cell or mitochondria extract were diluted to a final concentration of 1 mg/ml and 200 μl of the lysate was incubated with the salicylic acid-immobilized beads for 2 h at 4°C. After binding, beads were subjected to magnetic collection using magnetic separator. After beads collection, the clear supernatant was pipette out discarded.

(iii) **Washing:** Collected beads were suspended in 500 μl of the buffer IB-A, spin-down and kept in ice for 5 min. After beads collection, the clear supernatant was pipette out discarded. For best results this step was performed for 3 times.

(iv) **Elution:** For the elution of bound proteins from the beads, the beads were suspended and 40 μl of SDS sample buffer (50 mM Tris-HCl pH 8.0, 10% 2-mercaptomethanol, 2% sodium dodecyl sulphate, 0.1% bromophenol blue, 10% glycerol) was added. After vortex and spin down, the beads were boiled at 98°C for 5 min and spin down. To identify the salicylic acid binding protein, an aliquot of the boil elution sample was subjected to SDS-PAGE followed by either silver staining or immunoblotting.

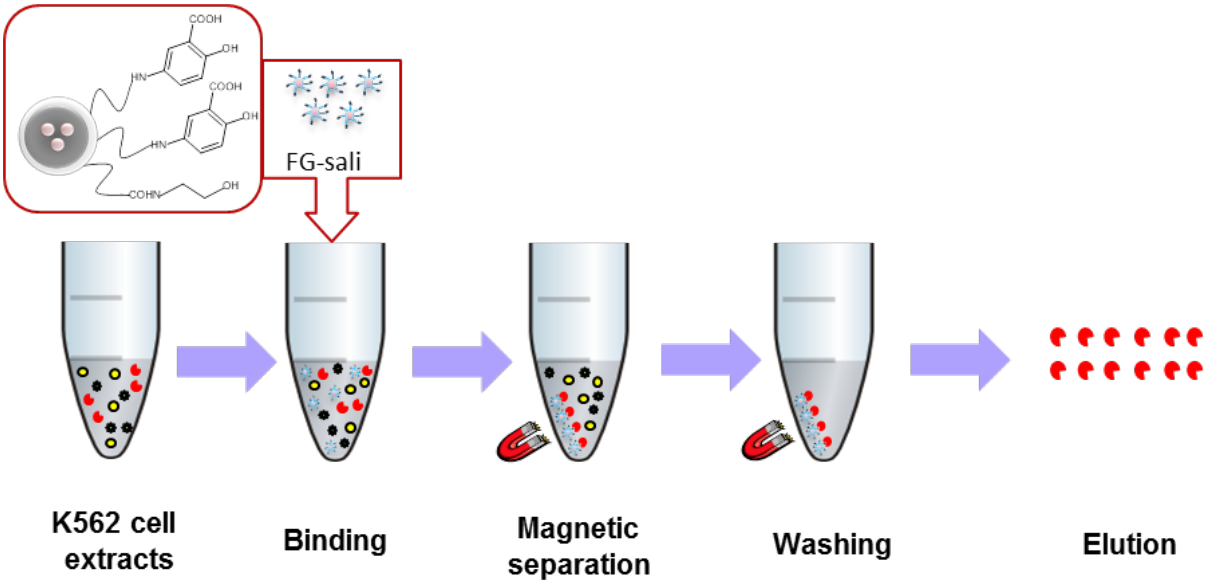

Figure 2-2: A pictorial representation of the binding assay scheme. Salicylic acid-immobilized beads are incubated with K562 cell extract and binding is performed for 2 h. After binding, beads are collected by magnetic separation and washed twice or thrice to remove non-binding proteins. Finally, bound proteins are eluted and identified.

All the above steps were performed on ice unless otherwise mentioned. For salicylic acid competition assay, the input lysate was pre-incubated with 5 – 50 mM of salicylic acid for 1 h at 4°C and affinity purification was performed.

2.2.5 Identification of salicylic acid-binding protein

2.2.5.1 Sodium dodecyl sulfate polyacrylamide gel electrophoresis (SDS-PAGE)

Sodium dodecyl sulphate-polyacrylamide gel electrophoresis (SDS-PAGE) was performed using Mini PROTEAN 3 system (Bio-Rad). The polyacrylamide gel is cast as a separating gel (or resolving gel) topped by stacking gel. A 12.5% separating gel was made by mixing 2 ml of Sol. A (30% acrylamide/0.8%

N,N'-methylenebisacrylamide), 1.5 ml of Sol. B (1.5 M Tris-HCl pH 8.8 and 0.4% SDS) and 1.5 ml of milliQ. After gently mixing the solution 40 μl of 10% APS (ammonium persulphate) and 10 μl of TEMED (*N,N,N',N'*-tetramethylethylenediamine) was added and the gel was poured gently in an glass gel cassette. The gel was allowed to polymerize for 45 min to 1 h. The stacking gel was prepared by mixing 0.45 ml of Sol A, 0.7 ml of Sol C (0.5 M Tris-HCl pH 6.8 and 0.4% SDS) and 1.8 ml of milliQ. After gently mixing the solution, 21 μl of 10% APS and 8 μl of TEMED were added and the solution was pour on top of the separating gel. A 15 well comb was inserted and the stacking gel was allowed to polymerize for 30-45 min. The glass cassette was placed into the slots of the Electrode Assembly and put in a Mini Tank. Both the inner and outer chamber of the mini tank was filled with 800 ml of SDS running buffer (20 mM Tris(hydroxymethyl)aminomethane, 154 mM glycine, 0.1% SDS). After loading the samples, the complete unit was connected to a power supply with proper polarity and the electrophoresis was performed at a constant current of 20 ~ 30 mA for 60 min.

2.2.5.2 Silver staining

Protein bands on the polyacrylamide gel were detected by silver staining technique. The nanogram-level detention of protein depends on binding of silver to various chemical groups (e.g., sulfhydryl and carboxyl moieties). Here, silver staining was performed using Sil-Best Stain One (Nacalai tesque) according to the following manufacture's instruction:

1. After gel electrophoresis, the gel was placed in clean plastic glass container containing fixing solution I (45% ethanol and 5% acetic acid) and agitated slowly for 20 min.
2. After pouring out the fixing solution I, the gel was soaked in fixing solution II (90% ethanol) for 10 min.
3. The fixing solution II was discarded and the gel was soaked in 40 ml of 1X pretreatment solution (stock 100X) for 10 min and then washed two times in milliQ for 5 min.
4. After washing, the gel was soaked in 40 ml of silver staining solution (2 ml Silver A solution 20X, 2 ml Silver B solution 20X, 36 ml milliQ) for 15 min and then rinsed 3 times in milliQ for 2 min.
5. After washing, the gel was treated with 40 ml of developing solution (stock 20X) and when the desired staining intensity was reached, the developing was stopped by addition of 2 ml of 10% acetic acid and agitated slowly for 15 min.
6. Finally the gel was rinsed in milliQ and dried using methanol/glycerol solution.

2.2.5.3 Immunoblotting (IB)

Protein samples, separated by SDS-PAGE, were electophorecially transferred to a PVDF membrane (Millipore, immobilon transfer membrane) using a Mini Transfer-Bolt System (Bio-Rad) in the presence of transfer buffer (20 mM Tris(hydroxymethyl)aminomethane, 154 mM Glycine, 20% Methanol) at 4°C and constant voltage of 100V for 1 h. After transfer was completed, the membrane was soaked in blocking buffer (50 mM Tris-HCl pH 7.5, 150 mM NaCl, 5% non-fat skim milk) for 1 h. The membrane was then incubated with primary antibody (specific for protein of interest) diluted in blocking buffer for 1 h. The blot was washed 3 x times

with TBS-T buffer (50mM Tris-HCl pH 7.5, 150 mM NaCl, 0.1% Tween 20) and incubated with Horseradish peroxidase–antibody conjugate directed against the primary antibody. After washing the bolt 3 times with TBS-T buffer, proteins were detected using ECL system (GE healthcare).

2.2.6 Construction of high expression histidine-tagged FECH plasmid

Human ferrochelatase (FECH, EC 4.99.1.1) was cloned from the cDNA library from Jurkat cell line and inserted into pGEX-6P-1 (GE Healthcare Life Sciences) which has Glutathione-*S*-transferase (GST) as a fusion tag under a *tac* promoter (hereafter called as GST-hFECH). The GST-hFECH plasmid was further modified using inverse polymerase chain reaction method with primers mentioned below, so that N-terminally truncated His-tagged matured form FECH could be expressed. A point mutation, R115L, shown to increase the solubility and stability of the FECH was inserted (Burden et al., 1999). Hereafter we call this construct as FECH R115L. FECH R115L was expressed under the control of the *tac* promoter. Essentially, the same construct was used in previous studies.

Primer used for truncating GST from pGEX-6P-1:

Forward:

ggggGAATTCTTAACTTTAAGAAGGAGATATATCCATGGCTCACCATCACCATCACCATCAACCGCAGAAGAGGAAGCCG

EcoR1 Enhancer SD M A ----------6X- His tag----------61 62

Reverse:

tttCTCGAGTCACAGCTGCTGGCTGGTGAAGAAG

Xho1 STOP

2.2.7 Expression of R115L and GST-hFECH

Plasmids, GST-hFECH and FECH R115L, were transformed in *E coli* BL21 (DE3).

For FECH R115L expression, a single colony was cultured in LB containing 100mg/ml of ampicillin at 37ºC for 10~12 h. An aliquot of this culture was transferred to fresh LB (with ampicillin) and cultured at 37ºC until the OD is 0.4 ~ 0.6. IPTG 0.1mM (final concentration) was added and protein expression was performed at 25ºC for 24 h. Bacteria pellets were collected, washed with PBS and pellets were stored at -80ºC until use.

For GST-FECH expression, a single colony was cultured in LB containing 100mg/ml of ampicillin at 37ºC for 10~12 h. An aliquot of this culture was transferred to fresh LB (with ampicillin) and cultured at 37ºC until the OD is 0.4 ~ 0.6. IPTG 1mM (final concentration) was added and protein expression was performed at 25ºC for 4~6 h. Bacteria pellets were collected, washed with PBS and pellets were stored at -80ºC until use.

2.2.8 Preparation of *E. coli* extract for affinity purification

Crude *E. coli* extracts were prepared from bacterial pellets, prepared in **2.2.7**, expressing either GST-FECH or FECH R115L. Pellets were thawed and washed in ice-chilled PBS lysed using 5 volumes of buffer IB-A (20 mM Hepes, pH 7.9, 100 mM KCl, 0.1% Triton X-100, and 10% glycerol) by pipetting, incubation on ice for 15 min followed by sonication. After centrifugation at 20,400× g 4°C 10 min, supernatant was collected and protein concentration was measured by Bradford using BSA as standard. Affinity purification was performed as in **2.2.4**.

2.2.9 Protein purification

This protocol describes the purification of FECH R115L from 1 L bacteria culture. *E. coli* pellets were thawed and washed in ice-chilled PBS. The cell pellet was suspended in 30 ml of buffer IB-B (50 mM Tris-MOPS pH 8.0, 100 mM KCl, 1.0%

sodium cholate, 10 mM Imidazole, Glycerol 10%). The cell suspension was sonicated on ice for 20 min and centrifuged at 20,400× g for 30 min at 4ºC. The supernatant was collected, filtered using 0.45 μm syringe driven filter (Millex-HV, Millipore) and incubated with 2 ml of 50% slurry Ni-NTA beads (Qiagen) pre-equilibrated with buffer IB-B for 1 h at 4°C. The mixture was loaded on a column and the supernatant was cleared by gravity-flow. The column was then washed with 30 ml of the buffer IB-B and bound FECH R115L was eluted with 4 ml of IB-C (50 mM Tris-MOPS, pH 8.0, 100 mM KCl, 1.0% (w/v) sodium cholate, 250 mM imidazole). The purity of protein was analyzed by SDS-PAGE and coomassie blue staining, and concentration was determined by either Bradford or UV absorbance.

GST-hFECH was affinity purified from *E. coli* crude lysate prepared (20 mM Hepes, pH 7.9, 100 mM KCl, 0.1% Triton X-100, and 10% glycerol). Briefly, bacteria lysate expressing GST-hFECH was incubated with glutathione-immobilized sepharose beads. After binding, beads were washed in 20 mM Hepes, pH 7.9, 100 mM KCl, 0.1% Triton X-100, and 10% glycerol and bound protein was eluted by 5 – 10 mM of reduced glutathione in 20 mM Hepes, pH 7.9, 100 mM KCl, 0.1% Triton X-100, and 10% glycerol. The purity of protein was analyzed by SDS-PAGE and coomassie blue staining.

2.2.10 UV-spectroscopy

UV-visible spectroscopy was performed using a DU700 series spectrophotometer (Beckman Coulter). FECH R115L concentrations were determined using the previously defined extinction coefficient 46,900 $M^{-1} \cdot cm^{-1}$ at 278 nm (Burden et al., 1999) or Bradford assay using BSA as a standard. The presence of the [2Fe-2S] cluster was detected by the presence of its characteristic spectra at 330 nm, 460 nm, and 550 nm (Burden et al., 1999; Dailey et al. 1994).

2.2.11 Cell-free FECH enzymatic activity

Enzymatic activity was measured as the amount of Zn-PpIX produced by aerobic incorporation of zinc into PpIX by recombinant FECH, as described previously (Li et al., 1987). Briefly, all reactions were performed in buffer IB-D (250 mM Tris-HCl, pH 8.2, 1% TritonX-100, and 1.75 mM palmitic acid). Buffer IB-D containing purified recombinant FECH (1 µg) with or without salicylic acid was first incubated at 4°C for 1 h and then at 25°C for 5 min. After the addition of PpIX and zinc acetate to the final concentration of 10 µM for each reagent, the reaction (250 µl) was further incubated for 5 min, stopped by the addition of a DMSO:methanol mixture (750 µl; 30:70 v/v), and centrifuged at 7000 rpm for 10 min. The supernatant was filtered through a 0.22 µm centrifugal filter (Milllipore), and the filtrate was applied to a Waters 600 high performance liquid chromatography (HPLC) system (Waters) equipped with a 4.6 × 150 mm 5C_{18}–AR-II column (Nacalai Tesque). The sample was resolved with a linear gradient of ammonium acetate/methanol that ranged from 0.25 M ammonium acetate (pH 5.16)/75% methanol to 0.05 M ammonium acetate (pH 5.16)/95% methanol. Zn-PpIX and PpIX were monitored by the absorbance at 416 and 400 nm, respectively. Their identities were confirmed by applying a mixture of commercially available Zn-PpIX and PpIX as the standard to the column.

2.3 Results

2.3.1 Isolation of novel salicylic acid binding protein

To identify novel salicylic acid-binding proteins, salicylic acid-immobilized beads were prepared by conjugating 5-amino salicylic acid (5-ASA) on the ferrite affinity beads (FG beads) with free carboxyl group as described in **2.2.2**. Affinity purification was performed using the basic protocol as described in **2.2.3**. Control beads, without conjugated 5-ASA, were used to check the specificity of the affinity purification. Briefly, K562 cells extract was incubated with control or salicylic acid-immobilized beads, and after extensive washing, bound proteins were eluted using sodium dodecyl sulfate (SDS) containing sample buffer. The eluted sample was subjected to SDS-PAGE and silver staining. A polypeptide with an apparent molecular weight of ~40 kDa (arrow) was found associated with the salicylic acid beads, **Figure 2-3A** (Lane 2, arrow). By contrast the polypeptide band was absent in the control beads (**Figure 2-3A**, Lane 1, arrow). Further, to confirm the binding specificity between the salicylic acid-immobilized beads and the 40 kDa protein, a competition affinity purification assay was performed by pre-incubating K562 cell lysate with different concentrations of free salicylic acid. This sample was then incubated with the salicylic acid-immobilized beads and the basic procedure of affinity purification was performed. As shown in **Figure 2-3A** (Lane 2, 3, 4 and 5, arrow), the binding of the 40 kDa polypeptide was clearly inhibited by increasing concentrations of free salicylic acid. Finally, this polypeptide was identified as ferrochelatase (FECH), an inner mitochondrial membrane protein involved in the heme biosynthetic pathway. The identity of FECH was further confirmed by immunoblot analysis with an antibody against human FECH (**Figure 2-3A**, bottom). To further investigate if FECH interaction to salicylic acid is species-dependent or independent, affinity purification

using rat liver/brain mitochondria extracts were performed. Extracts of rat liver/brain mitochondria were prepared as described in **2.2.3.2**. FECH from these extracts was also found to associate with the salicylic acid-immobilized beads confirmed by immunoblot analysis with human FECH antibody (**Figure 2-3B**). Thus, remarkably, these results clearly identify FECH as a novel salicylic acid-binding protein.

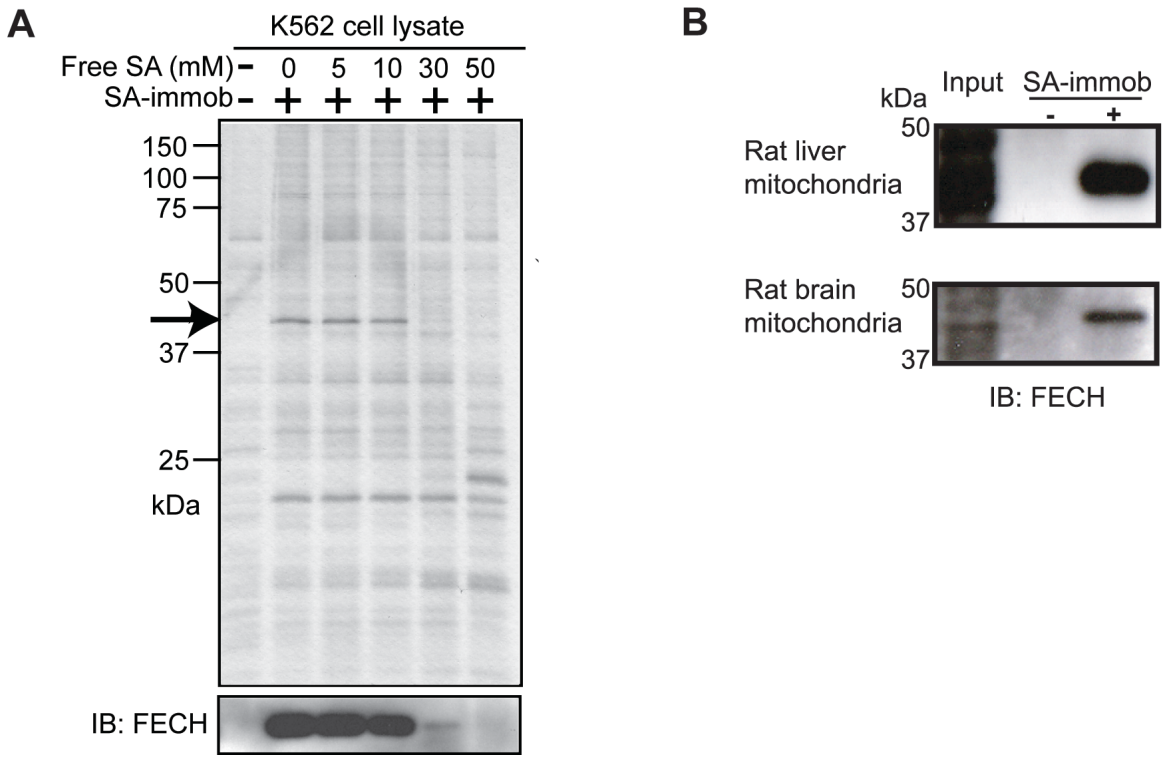

Figure 2-3: Ferrochelatase (FECH) is identified as a novel salicylic acid binding protein. (A) Salicylic acid (SA)-binding proteins were purified from K562 cell lysate with salicylic acid-immobilized (+) or control (−) beads. The indicated concentrations of free salicylic acid were added to the cell lysate before incubation with the beads. Eluted proteins were analyzed by silver staining (top) or immunoblotting (IB, bottom) with an anti-FECH antibody. (B) Species- and cell type-independent interaction of FECH with salicylic acid. Extract prepared from rat liver and brain mitochondria were incubated with salicylic acid-immobilized beads and affinity purification was performed. Eluted proteins were analyzed by immunoblotting (IB:FECH) with an anti-FECH antibody.

2.3.2 Salicylic acid inhibits recombinant FECH activity *in vitro*

Mammalian FECH from K562 was found to interact with salicylic acid-immobilized beads. To investigate the sustainability of this interaction *in vitro*, I constructed a plasmid expressing the R115L variant of recombinant human FECH. In cells, premature form of FECH is synthesized in cytoplasm and is proteolytically processed to its mature form while its translocation to the mitochondria (Dailey, 1988). This recombinant variant lacks the N-terminal mitochondrial signal peptide (amino acids 1-62), thus expressing a processed form of mammalian FECH that contains residues 61-423 (**Figure 2-4**). A 6x N-terminal histidine (His-) tag was added to ease the purification process. Essentially, the same construct was used previously to express high level of recombinant FECH (Burden et al., 1999; Wu et al., 2001). Although, the Arg115 residue makes a contact with the physiological substrate of FECH, PpIX, the R115L mutant and the wild-type enzyme share similar catalytic activity (Medlock et al., 2007b; Burden et al., 1999; Wu et al., 2001).

```
 53 MAHHHHHHQP QKRKPKTGIL MLNMGGPETL GDVHDFLLRL FLDRDLMTLP
103 IQNKLAPFIA KRLTPKIQEQ YRRIGGGSPI KIWTSKQGEG MVKLLDELSP
153 NTAPHKYYIG FRYVHPLTEE AIEEMERDGL ERAIAFTQYP QYSCSTTGSS
203 LNAIYRYYNQ VGRKPTMKWS TIDRWPTHHL LIQCFADHIL KELDHFPLEK
253 RSEVVILFSA HSLPMSVVNR GDPYPQEVSA TVQKVMERLE YCNPYRLVWQ
303 SKVGPMPWLG PQTDESIKGL CERGRKNILL VPIAFTSDHI ETLYELDIEY
353 SQVLAKECGV ENIRRAESLN GNPLFSKALA DLVHSHIQSN ELCSKQLTLS
403 CPLCVNPVCR ETKSFFTSQQ L
```

Figure 2-4: His-tagged FECH-R115L primary protein sequence. The amino numbering is started from 53 so that the FECH residues can be numbered to

the original position in wildtype FECH sequence. Highlighted in red is the His-tag at the N terminal. R115L mutation is highlighted in cyan.

To analyze the different between the expression and purification level of GST-hFECH and FECH R115L constructs, both plasmids were expressed in *E. coli.* BL21 under different conditions and affinity tag purification was performed as described in **2.2.7** and **2.2.9**. Compared to the GST-hFECH, the FECH R115L shows higher expression and purification efficiency (**Figure 2-5A**) and on a gel, stained with coomassie blue, a protein band with approximate molecular mass of 70 (**Figure 2-5A**, GST-hFECH, arrow) or 42 kDa (**Figure 2-5A**, FECH R115L, arrow) was detected. Previously purified recombinant FECH R115L has a characteristic reddish color indicative of the presence of the [2Fe-2S] cluster usually found in human FECH in the C terminal, bound to four cystine residues (Burden et al., 1999, Wu et al., 2001). The function of this cluster inside the protein is debatable; however, it has been shown important for protein stability. If present, this cluster shows characteristic visible spectral features at 320 nm and broad features around 550 nm (Burden et al., 1999). Thus to provide further evidence for the presence of cluster in FECH R115L, an aliquot of purified FECH R115L in buffer IB-B (see materials and methods) was subjected to a UV/VIS spectrophotometer. The visible absorption spectra is shown in **Figure 2-5B**. As expected, the spectra of FECH R115L showed an absorption peak at 330 nm; indicative of an intact [2Fe-2S] cluster.

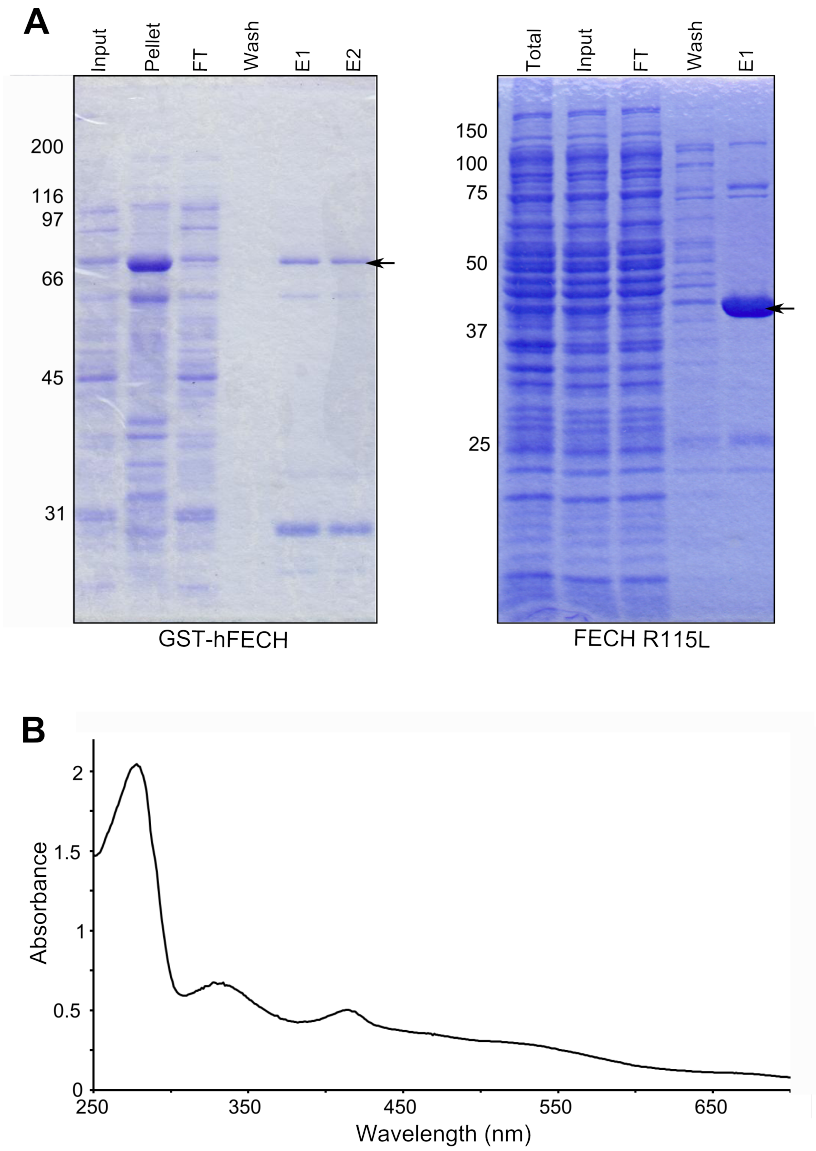

Figure 2-5: Expression, purification and characterization of recombinant FECH R115L. (A) Protein purification of GST- hFECH (left) and FECH R115L (right). Equal volume of bacteria culture expressing either of the two construct was lysed and affinity tag purification was performed as described in experimental procedures. FT – Flow through: E1, E2 – Elution samples. (B) Ultraviolet/visible light spectrum of purified recombinant FECH R115L. Protein was solubilized in buffer IB-B and subjected to a spectrophotometer.

Next, to gain insight of FECH•salicylic acid interaction, it was important to investigate whether salicylic acid inhibits the FECH enzymatic activity *in vitro*.

Because FECH from K562 cells binds with salicylic acid-immobilized beads, I checked the binding efficiency of the recombinant FECH R115L to the salicylic acid-immobilized beads. Affinity purification was performed by incubating salicylic acid-immobilized beads with extract from *E.coli* expressing FECH R115L protein. After affinity purification, the eluted sample was subjected to SDS-PAGE and bound FECH R115L was detected by immunoblotting analysis with an antibody against human FECH. As expected, FECH R115L was found to bind with the salicylic acid-immobilized beads. Moreover, the efficiency of binding was indistinguishable from that of GST-hFECH (compare **Figure 2-7A** and Figure xx). To further investigate the physiological importance of FECH•salicylic acid interaction, I next performed structure-function analysis between salicylic acid and its isomers *meta*-hydroxybenzoic acid (*m*-HBA, **Figure 2-7B**), and *para*-hydroxybenzoic acid (*p*-HBA, **Figure 2-7B**). To my knowledge, only a single study has compared the pharmacological actions of these three isomers (You, 1983). This previous study showed that salicylic acid, but not its isomers, caused the swelling of rat liver mitochondria. To check if *m*-HBA or *p*-HBA interacts efficiently with FECH R115L, a competition assay similar to **Figure 2-3A** was performed and the eluted samples were subjected to SDS-PAGE and immunoblotting. As shown in **Figure 2-7C**, free salicylic acid (SA) inhibited the association of FECH with salicylic acid-immobilized beads. By contrast, pre-incubation of *E.coli.* extract either with free *m*-HBA or with free *p*-HBA did not cause any appreciate inhibition on FECH•salicylic acid interaction (**Figure 2-7C)**.

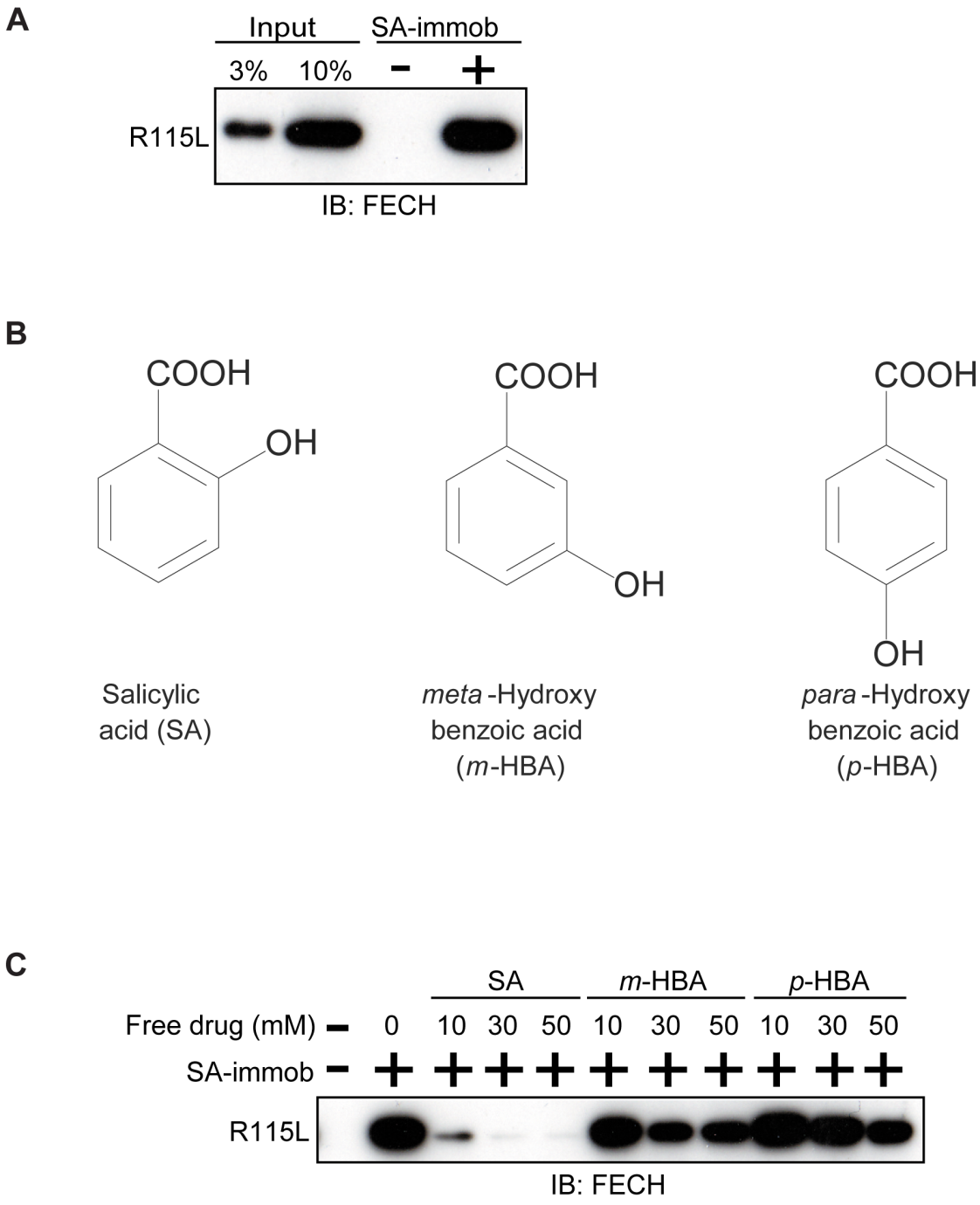

Figure2-7: Recombinant FECH R115L specifically binds with salicylic acid. (A) Affinity purification was carried out with recombinant FECH R115L. *E. coli* extract expressing FECH R115L was incubated with salicylic acid-immobilized beads and eluted samples were subjected to immunoblotting to an FECH antibody. (B) Salicylic acid and its isomers *meta*-hydroxybenzoic acid

(*m*-HBA), or *para*-hydoxybenzoic acid (*p*-HBA). (C) Free salicylic acid (SA), *m*-HBA, or *p*-HBA was preincubated with cell lysate derived from *E. coli* expressing FECH R115L and subjected to affinity purification with salicylic acid-immobilized beads.

Finally, the effect of salicylic acid on *in vitro* FECH enzymatic activity was investigated. As mentioned earlier, FECH is the terminal enzyme in heme biosynthesis pathway and produces heme by chelating ferrous into PpIX. However, in *in vitro* conditions ferrous ion is highly unstable and is readily oxidized to ferric ion that may hamper the FECH activity (Hunter, 2008). Consequently, for *in vitro* assays, the more stable metal ion substrate zinc is often utilized to assess ferrochelatase activity aerobically (Shi and Ferreira, 2004; Gora et al., 1996; Li et al., 1987; Medlock et al., 2007). To investigate the effect of salicylic acid on FECH enzymatic activity, the formation of a zinc protoporphyrin IX (Zn-PpIX) complex from zinc (Zn) and protoporphyrin IX (PpIX) was examined *in vitro* by using purified recombinant FECH R115L (**Figure 2-8A**). As expected, salicylic acid inhibited the formation of Zn-PpIX in a concentration-dependent manner (**Figure 2-8B**). Contrary to this, both *m*-HBA and *p*-HBA had little effect on FECH activity in the same concentration range as salicylic acid (**Figure 2-8B**). Thus consistent with the competition assay, salicylic acid substantially and specifically inhibits FECH activity.

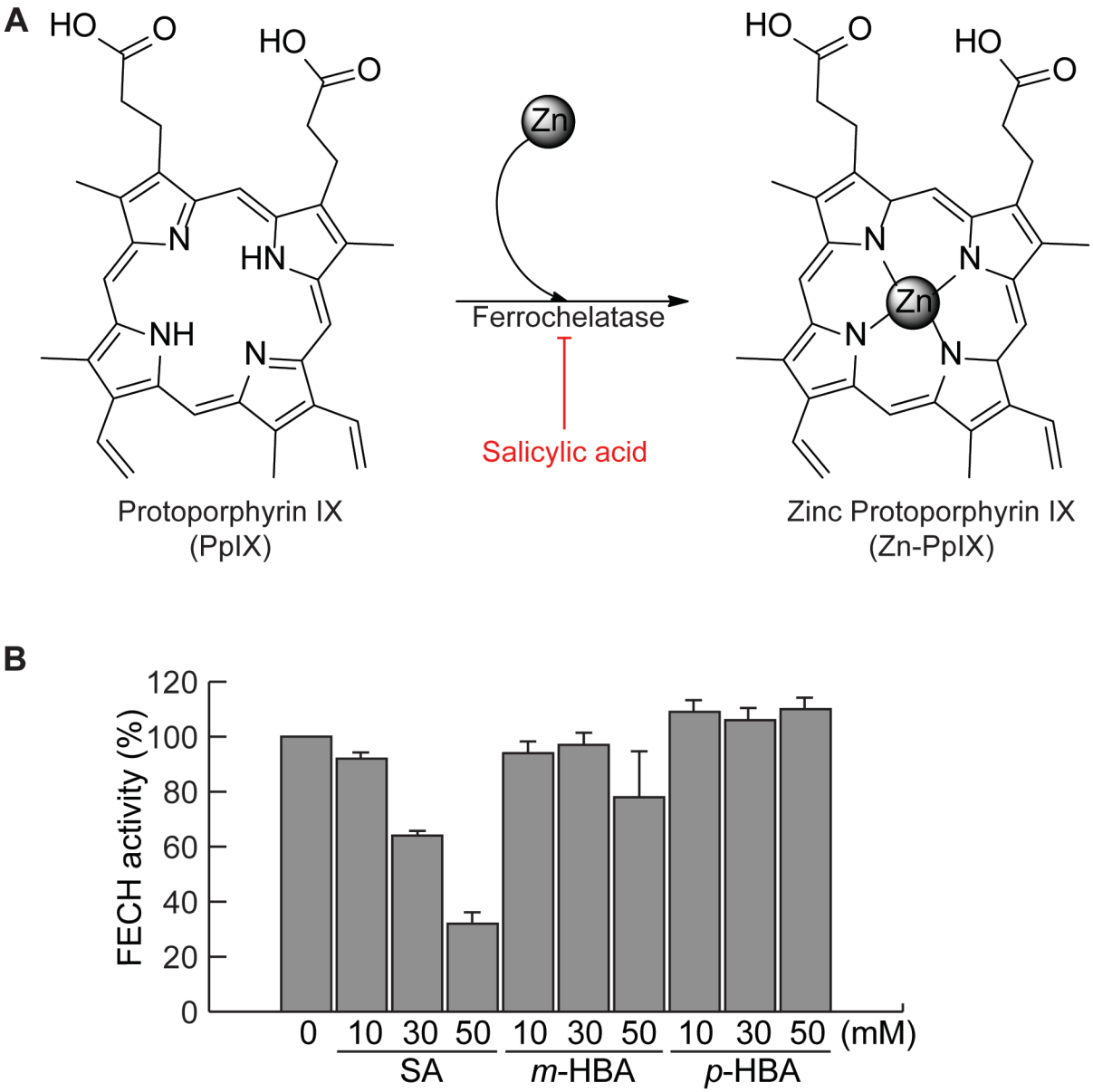

Figure 2-8. (A) The inhibitory effects of salicylic acid on recombinant FECH R115L activity was measured as the decrease in the amount of zinc protoporphyrin IX (Zn-PpIX) produced by aerobic incorporation of zinc (Zn) into protoporphyrin IX (PpIX). (B) Purified FECH R115L pre-incubated with indicated concentration of salicylic acid (SA), *meta*-hydroxybenzoic acid (*m*-HBA), or *para*-hydroxybenzoic acid (*p*-HBA) was assayed for Zn-PpIX formation as described in (A). The final product was subjected to HPLC analysis and the peak area was measured and plotted. The decrease FECH activity is plotted as the percent decrease in Zn-PpIX formation.

2.4 Conclusions

In this chapter, heme biosynthesis enzyme ferrochelatase (FECH) was identified as a novel protein target of salicylic acid. FECH is an inner mitochondrial membrane protein involved in the heme biosynthesis pathway. Heme is further incorporated in different hemoprotein that are vital to cell viability. Both human and murine FECH were found to interact with salicylic acid-immobilized beads. Salicylic acid was found to bind and inhibit the recombinant FECH activity *in vitro*. Although preliminary, these results point towards a significantly important, novel interaction. Since FECH is a mitochondrial protein and salicylic acid is also known to induce mitochondrial dysfunction, in the next chapter, I investigated whether this interaction plays any significant role in salicylic acid-induced mitochondrial dysfunction.

Chapter 3. Mechanism of salicylic acid induced FECH inhibition

3.1 Introduction

Determination of sperm whale myoglobin tertiary structure hallmarked the use of X-ray crystallography in the field of biology, which gave the authors, Max Perutz and John Kendrew the Chemistry Nobel Prize in 1962. Till now, more than 90,000 tertiary structures of proteins, nucleic acids and other biological macromolecules has been determined and stored in databases (www.rcsb.org/pdb). Tertiary structure of a protein gives a clear picture of the mechanism involved in its activity. Likewise, proteins in complex with either its substrate, or pharmaceutical drug, or both gives additional information as to how a compound binds to the protein and what changes, if any, are induced upon its binding. In the last chapter, I identified ferrochelatase (FECH) as a novel salicylic acid-binding protein. This chapter aims to investigate and establish a mechanism by which salicylic acid inhibits FECH activity.

The tertiary structures of FECH from *Bacillus subtilis* (Al-Karadaghi et al, 1997), humans (Wu et al, 2001), and *Saccharomyces cerevisiae* (Karlberg et al, 2002) have been determined by X-ray crystallography. Till now, about 15 human FECH structures either in apo form or in complex with its substrate have been determined and deposited in RCSB database (www.rcsb.org/pdb). Based on the structures, while bacterial FECH is monomer, human FECH is a homodimer (Al-Karadaghi et al, 1997; Wu et al, 2001). Moreover, unlike human FECH, bacterial FECH lacks [2Fe-2S] cluster and a C-terminal extension (Al-Karadaghi et al., 1997).

In this chapter, I determined the crystal structure of FECH salicylic acid

complex at 2.0 Å resolution. FECH exists as a homodimer and salicylic acid was found to bind at the dimer interface. Point mutations of amino acid at the dimer interface lead to the loss of salicylic acid binding and affects the FECH's dimerization status. In addition, a mechanism of how salicylic acid binding to the dimer interface inhibits its enzymatic activity is investigated.

3.2 Material and methods

3.2.1 Crystallization and structure determination

For crystallization, FECH R115L was purified as mentioned in **2.2.9**. Purified FECH R115L solubilized in buffer IB-B (50 mM Tris-MOPS pH 8.0, 100 mM KCl, 1.0% sodium cholate, 250 mM imidazole, glycerol 10%) was further purified using size exclusion chromatography using AKTA explorer with a HiLoad 16/600 Superdex 200 Prep Grade column. Eluates showing minimum contamination in CBB staining were mixed and concentrated using Amicon-Ultra-4 Centrifugal Filter Units (M.W.C.O. 30 kDa, Millipore) to a final concentration of 10 mg/ml. For the crystallization of the FECH•salicylic acid complex, purified FECH R115L (500 µM) was incubated with 10 mM sodium salicylate for 1 h at 4°C. Before crystallization, sample was filtered using an Ultrafree-MC centrifugal filter (Millipore). Crystallization was performed using sitting drop vapor diffusion method. Sitting drops were obtained by mixing 0.2 µL of FECH-salicylic acid mixture with equal volume of reservoir solution using an automatic crystallizer mosquito (TTP lab Tech) followed by incubation at 20°C. Initial screening of crystallization condition was performed with ready-to-use kits Crystal Screen II, PACT Suite, JCSG + Suite. Red crystals of the FECH•salicylic acid complex were obtained by incubating the protein-salicylic acid mixture in 0.1 M PCB buffer containing 10% PEG1500 as precipitant at 20°C for 3 days. For cryoprotection, the crystals were soaked in a reservoir solution containing 25% ethylene glycol. X-ray diffraction data were collected at the SPring-8 beamline BL41XU facility (wavelength 1.0 Å, temperature 100 K, Japan Synchrotron Radiation Research Institute (JASRI), Hyogo, Japan) and processed with HKL2000 software (Otwinowski and Minor, 1997). Other crystallographic calculations were performed with the CCP4 package (Collaborative Computational Project, 1994). The structure of the FECH-salicylic acid

complex was determined via the molecular replacement method, based on the structure of the apoenzyme (PDB code: 2HRC) (Medlock and Swartz et al., 2007) as a search model with Molrep. Model building was accomplished with Coot (Emsley and Cowtan, 2004), and refinement was performed by using REFMAC5 (Steiner et al., 2003) and Phenix (Afonine et al., 2012). Data collection and structure refinement statistics are summarized in **Table 3-1**. The Ramachandran statistics were 97.8/2.2/0 (%), corresponding to favored/allowed/outliers. The atomic coordinates for the R115L FECH-salicylic acid complex structure have been deposited in the Protein Data Bank, www.pdb.org (PDB ID code 3W1W).

Table 3-1. Data collection and refinement statistics, related to Figure 2.

	3W1W
Data collection	
Space group	$P2_12_12_1$
Cell dimensions	
a, b, c (Å)	87.53,93.63, 110.29
α, β, γ (°)	90, 90, 90
Resolution (Å)	50-2.00 (2.03–2.00)
R_{sym} *or* R_{merge}	0.081 (0.390)
$I / \sigma I$	31.2 (6.1)
Completeness (%)	99.6 (98.8)
Redundancy	7.1 (6.8)
Refinement	
Resolution (Å)	50–2.0
No. reflections	60798
R_{work} / R_{free}	0.185/0.223
No. atoms	
Protein	5799
Ligand/ion	251
Water	417
B-factors	
Protein	22.9
Ligand/ion	31.9

Water	28.0
R.m.s. deviations	
Bond lengths (Å)	0.008
Bond angles (°)	1.33

*Values in parentheses are for the highest-resolution shell.

3.2.2 FECH R115L mutants

FECH R115L mutants were constructed by PCR using FECH R115L plasmid as template and appropriate oligonucleotides with alanine mutation (as described in **Table 3-2**). *EcoRI* and *XhoI* digested FECH R115L plasmid was used as the vector. PCR products were also digested using *EcoRI* and *XhoI* and used as insert. All the designated mutations were validated by sequencing. All mutants were expressed in the same way as the FECH R115L as described in **2.2.7**. Similar methodology, as mentioned in **2.2.9**, was employed to purify the mutants. Affinity purification was performed using crude *E. coli* extracts expressing the mutants as in **2.2.8**.

Table 3-2: Primers used to introduce alanine mutation in FECH R115L. Marked in red colors is the position where alanine was inserted.

Mutant	Forward primer (5' → 3')	Reverse primer (5' → 3')
V270A	tgccgatgtctgtggccaacagaggcga	tcgcctctgttggccacagacatcggca
Q278A	ggcgacccatatcctgcggaggtaagcgccact	agtggcgcttacctccgcaggatatgggtcgcc
S281A	tatcctcaggaggtagccgccactgtccaaaaa	tttttggacagtggcggctacctcctgaggata
W301A	taccgactggtggcgcaatccaaggttggt	accaaccttggattgcgccaccagtcggta
L311A	tccgatgccctgggcaggtcctcaaacaga	tctgtttgaggacctgcccagggcatcgga

3.2.3 Cloning and expression of bacterial FECH

Bacterial FECH was cloned from *Escherichia coli* BL21 species using forward (*5'*GGGGGGAATTCATGCGTCAGACTAAAACCGG*3'*) and reverse (*5'*TTTCTCGAGTTAGCGATACGCGGCAACAA*3'*) primers. The PCR product was digested using restriction enzymes *EcoRI* and *XhoI* and ligated to *EcoRI*- and *XhoI*-digested pGEX-6P-1. The integrity of the insert sequence was checked by sequencing. Hereafter, the bacterial FECH is referred as GST-eFECH. For GST-eFECH expression, a single colony was cultured in LB containing 100mg/ml of ampicillin at 37ºC for 10~12 h. An aliquot of this culture was transferred to fresh LB (with ampicillin) and cultured at 37ºC until the OD is 0.4 ~ 0.6. IPTG 1mM (final concentration) was added and protein expression was performed at 25ºC for 4~6 h. Bacteria pellets were collected, washed with PBS and pellets were stored at -80ºC until use. Crude *E. coli* extracts expressing GST-eFECH were prepared from pellets and affinity purification was performed as in **2.2.8**.

3.2.3 Gel filtration

Gel filtration was performed by using an AKTA explorer (GE Healthcare) equipped with a Superdex 200 10/300 column (GE Healthcare). For **Figure 3-5**, 100 μL of either FECH R115L (5 mg/ml) or its mutants (3 –5 mg/ml) were loaded on the column and subjected to gel filtration in buffer IB-B. Protein peaks were detected by UV absorbance at 280 nm and compared with protein size markers (Sigma) consisting of apoferritin (443 kDa), alcohol dehydrogenase (150 kDa), ovalbumin (45 kDa), and α-lactalbumin (14.2 kDa).

Salicylic acid induced conformational change in FECH R115L (**Figure 3-8**)

was analyzed using gel filtration using a AKTA explorer (GE Healthcare) equipped with a Superdex 200 10/300 column (GE Healthcare). FECH R115L (5 mg/ml) was first incubated with the indicated concentration of either salicylic acid or *p*-HBA for 1 h at 4°C, and then 100 µl of the sample was loaded onto the column, with buffer IB-B (50 mM Tris-MOPS [pH 8.0], 100 mM KCl, 1.0% (w/v) sodium cholate, 250 mM imidazole) as the column buffer containing the indicated concentration of either salicylic acid or *p*-HBA. Eluate fractions (500 µl each) were collected, and peak fractions were analyzed by SDS-PAGE and Coomassie Brilliant Blue staining. The column was calibrated with protein size markers (Sigma) consisting of apoferritin (443 kDa), alcohol dehydrogenase (150 kDa), ovalbumin (45 kDa), and α-lactalbumin (14.2 kDa).

3.2.4 Isothermal titration calorimetry

ITC measurements were performed by using an iTC200 Titration Calorimeter (GE Healthcare). After a buffer change from buffer IB-B to buffer IB-D (25 mM Tris-HCl, pH 8.0, 100 mM KCl, 0.1% Triton X-100, and 1% glycerol), purified recombinant FECH was concentrated to 0.2 mM, dialyzed in buffer IB-D, and loaded into the sample cell. Salicylic acid (25 mM) dissolved in IB-D was used as the ligand solution. Titration between ligand and protein solution was performed by 19 injections of ligand (2 µl) solution into the sample cell at 3-min intervals. The experimental chamber was subjected to constant stirring at 307 rpm at 25.0±0.1°C. Data were plotted and analyzed with MicroCal Origin software version 7.0 (GE Healthcare, single binding site model).

3.3 Results

3.3.1 Overall structure of FECH-salicylic acid complex

The crystal structures of human FECH, either in free form or complexed with protoporphyrin IX, have been reported (Dailey et al., 2007; Medlock and Swartz et al., 2007; Medlock and Dailey et al., 2007; Medlock et al., 2009; Medlock et al., 2012; Wu et al., 2001). To determine the structural basis for the interaction between FECH and salicylic acid, the co-crystal structure was determined. After screening several buffer conditions, bright red crystals of FECH•salicylic acid complex were successfully produced in 0.1 M PCB buffer pH 4.8 at 20°C (**Figure 3-1**). Crystals were red in colour because of the presence of oxidised [2Fe-2S] cluster (Wu et al., 2001). These crystals were subjected to X-ray diffraction and data set to a 2.0 Å resolution was collected.

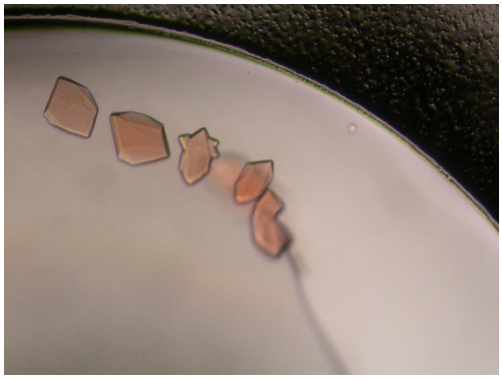

Figure 3-1. Co-crystals of FECH•SA complex. Crystallization was performed using the sitting drop vapour diffusion method, and crystals were grown at 20°C for 3 days.

The overall structure of FECH complexed with salicylic acid (FECH•salicylic acid) is essentially the same as the previously reported structure for the apoenzyme form of FECH (Wu et al., 2001; Medlock and Swartz et al., 2007) (**Figure 3-2**). Each

asymmetric unit of the structure consists of two FECH molecules forming a dimer, with the dimer interface situated on the non-crystallographic axis. Consistent with previous studies, a [2Fe-2S] cluster was found attached to each FECH protomer covalently through Cys196, Cys403, Cys406, and Cys411 with an unusual motif NH_2-Cys-X_{206}-Cys-X_2-Cys-X_4-Cys-COOH (where X and subscripted number represent number of residues between the coordinating Cys) (Wu et al., 2001) (**Figure 3-2**). In addition, one ethylene glycol molecule, five cholate molecules, and 417 water molecules were found in each asymmetric unit (**Figure 3-2**). The structure of the monomer contains approximately 48% α-helices and 14% β-sheets. Each monomer is comprised of two similar domains, each with a four-stranded parallel β-sheet flanked by an α-helix in a β-α-β motif. In addition, a clear electron density that is well fitted to a single molecule of salicylic acid is present between the two FECH protomers.

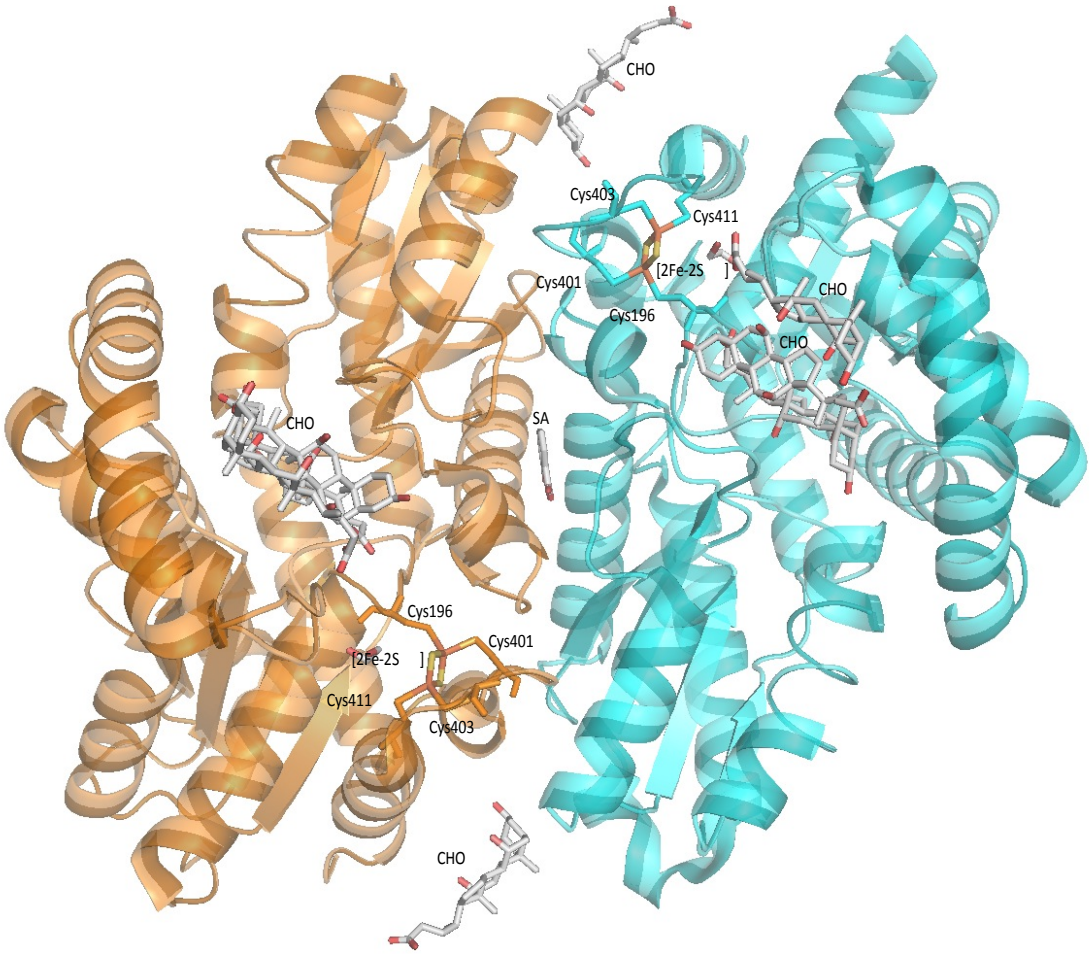

Figure 3-2. Overall structure of FECH•SA complex. FECH•SA complex exist as a dimer with two protomers colored in (chain B) and orange (chain A). A [2Fe-2S] cluster was present in each FECH monomer bound covalently through Cys196, Cys403, Cys406, and Cys411. In addition, one ethylene glycol molecule, five cholate molecules (CHO), and 417 water molecules were found in each asymmetric unit. Salicylic acid (SA) was found to bind to the dimer interface.

Human FECH is essentially a homodimer with the monomer subunits related by pseudo two-fold symmetry at the dimer interface. The dimer interface shows an extensive network of hydrogen bonds and hydrophobic interactions (Dailey et al., 2007; Medlock and Swartz et al., 2007; Medlock and Dailey et al., 2007; Medlock et al., 2009; Medlock et al., 2012; Wu et al., 2001). Apart from structural integrity, the FECH dimer interface is considered equally important for FECH activity (Wu et al.,

2001). In previous FECH structures, small and relatively hydrophobic or planar molecules, like benzene and imidazole have been observed at dimer interface (Dailey et al., 2007; Medlock and Swartz et al., 2007; Medlock and Dailey et al., 2007; Medlock et al., 2009; Medlock et al., 2012; Wu et al., 2001), thus showing that this region is accessible to small molecule such as salicylic acid. Because salicylic acid binding position is similar to the two-fold symmetry of FECH dimer (**Figure 3-3A**), it is possible to model salicylic acid in two opposite orientations **(Figure 3-3B)**. The final two structures obtained after refinement are essentially identical, and in both orientations, salicylic acid is surrounded by hydrophobic amino acids such as Val270, Pro277, Trp301, and Leu311 and a polar amino acid Ser281 originating from both protomers (**Figure 3-3B** and **Figure 3-3C**). A flip of 180° in salicylic acid is shown in **Figure 3-3B**. In both orientations, the hydroxyl group of salicylic acid forms a hydrogen bond with the side chain of Ser281 at a distance of 2.7 or 2.8 Å (**Figure 3-3B** and **Figure 3-3C**).

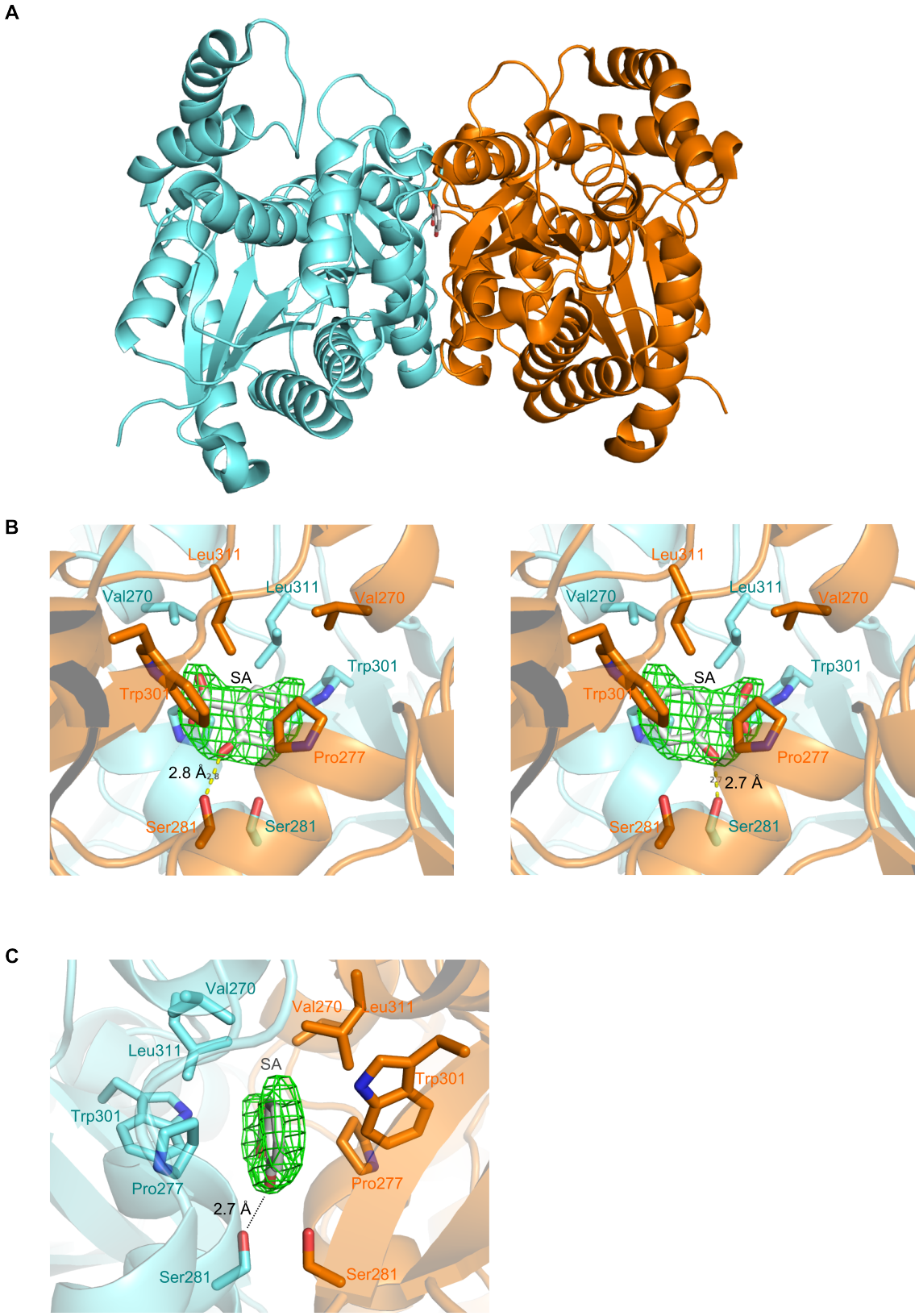

Figure 3-3: Salicylic acid binds to the dimer interface of FECH and can be modelled in two orientations. (A) Structure of the FECH•salicylic acid complex

showing the two-fold symmetry. Two protomers are shown in cyan (chain B) and orange (chain A), respectively, while salicylic acid is colored by elements. (B) Close-up view of the salicylic acid-binding region. The Fo-Fc omit map is shown at the 4.0 σ level in green color. Amino acid residues surrounding salicylic acid are shown in the stick model. A hydrogen bond between Ser281 of chain B and the hydroxyl group of salicylic acid is shown with a dotted line. (C) Right figure represents a 90° rotation of the FECH•SA structure that is depicted in (B). Left figure shows another possible orientation of SA viewed from the same angle. In both cases, SA forms a hydrogen bond with Ser281 at a distance of 2.7 Å and 2.8 Å.

3.3.2 Validation of salicylic acid binding site in FECH

Structural data show that salicylic acid interacts with FECH at the dimer interface. However, it is important to test the validity of the structural data. To do this, amino acid residues that seem to contact salicylic acid (Val270, Ser281, Trp301, and Leu311) were mutated to alanine. *E. coli* extract expressing either FECH R115L or its mutants were prepared, and binding assay was performed by using salicylic acid-immobilized beads. As shown in **Figure 3-4**, the W301A (R115L/W301A) and L311A (R115L/L311A) point mutations but not the S281A (R115L/S281A) point mutation, substantially reduced FECH R115L binding to salicylic acid-immobilized beads. The V270A (R115L/V270A) mutant binds to salicylic acid, albeit to a lesser extent than FECH R115L. These results suggest that the hydrogen bond between the hydroxyl group of salicylic acid and FECH Ser281 is dispensable and that the hydrophobic interactions of the benzene ring of salicylic acid with FECH Trp301 and Leu311 are critical to salicylic acid binding to the dimer interface.

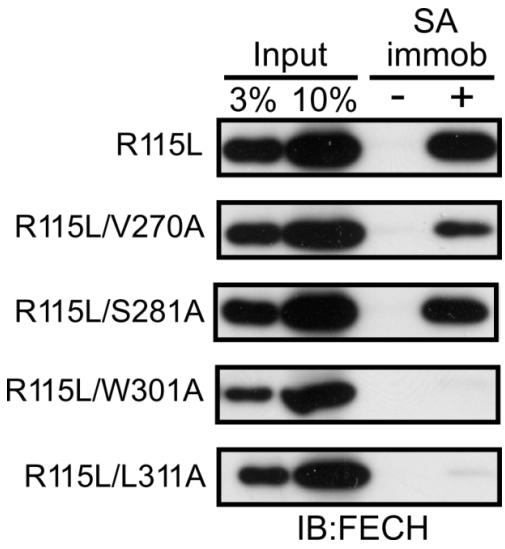

Figure 3-4. FECH R115L and its mutants were expressed in *E. coli*, and their lysates (input) were subjected to affinity purification with control beads (−) or salicylic acid-immobilized (+) beads. Samples were immunoblotted (IB) with anti-FECH antibody.

Because the amino acid residues studied above are located at the dimer interface, it is possible that the point mutations affected the dimerization status of FECH that might lead to the reduced interaction. To test this hypothesis gel filtration analysis was performed. The recombinant FECH R115L and mutant FECH R115L containing the mutations V270A, W301A, L311A and S281A were efficiently expressed in the *E. coli* BL21 strain and His purification was performed as described in **2.2.8**. The eluted samples were subjected to Superdex 200 gel filtration column and fractionated according to the protein size. Based on the UV-Vis absorbance at 280 nm, each of the proteins was eluted with a single, symmetrical peak. As shown in **Figure 3-5**, only FECH R115L and R115L/S281A migrated faster that R115L/V270A, R115L/W301A, and R115L/L311A. Based on the elution profile of standard protein markers, the observed molecular weight of FECH R115L and R115L/S281A was calculated to be ~90 kDa, while those of R115L/V270A, R115L/W301A, and

R115L/L311A were ~50 kDa, suggesting that these mutants exist largely as monomers (summarized in **Table 3-3**).

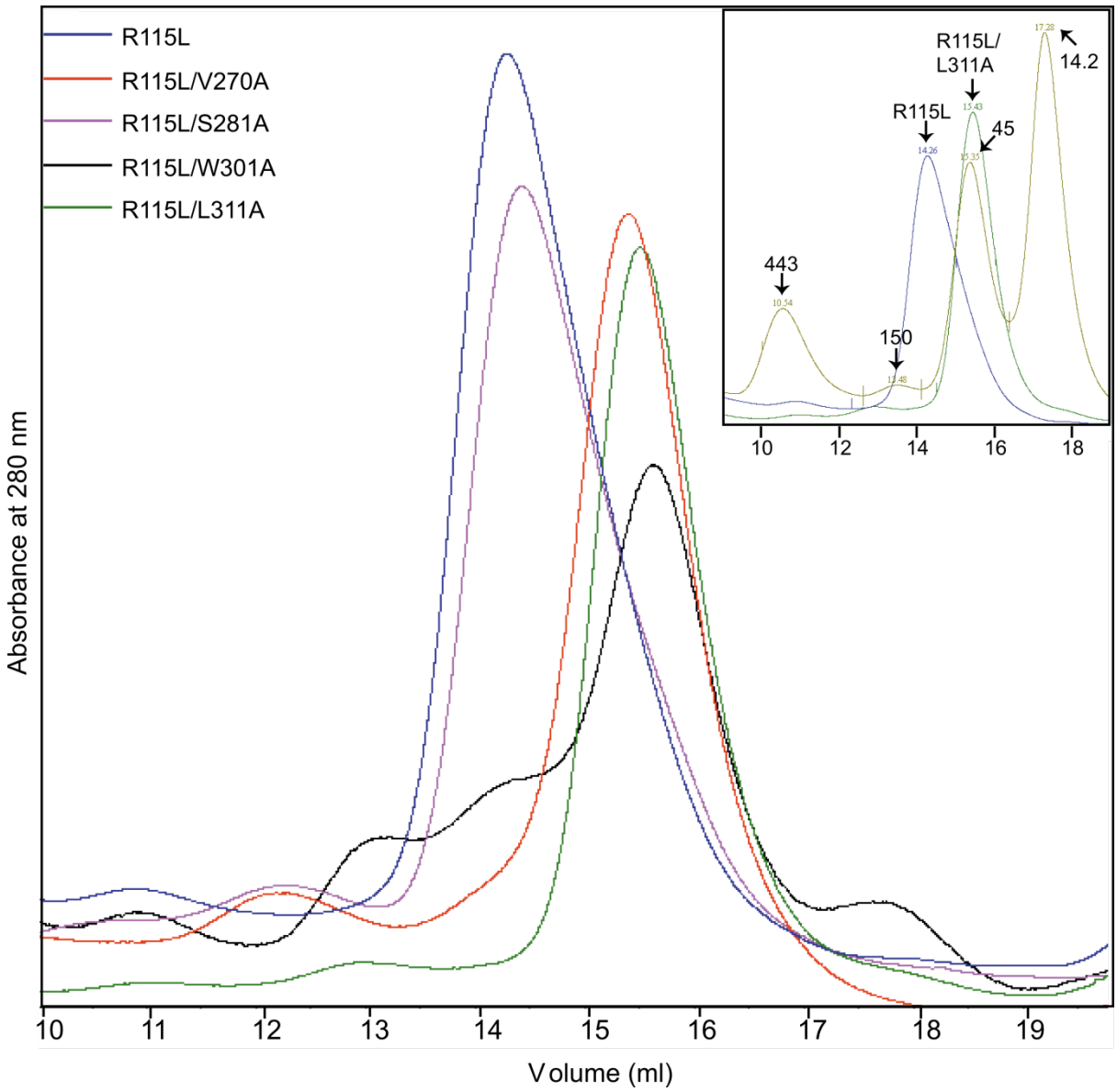

Figure 3-5. Purified recombinant FECH mutants were subjected to a Superdex 200 10/300 column (GE Healthcare). Elution profiles were analyzed by UV absorbance at 280 nm. In the inset, the elution profiles of some mutants were compared with those of protein size markers.

Nonetheless, except for S281A, none of these point mutants showed

detectable enzymatic activity (**Table 3-3**). This finding agrees with earlier studies demonstrating that the dimerization of FECH is essential for its function (Wu et al., 2001; Medlock and Swartz et al., 2007; Najahi-Missaoui and Dailey, 2005). Because the monomeric mutant R115L/V270A retained significant salicylic acid-binding activity, it was concluded that the dimerization of FECH is not required for its interaction with salicylic acid.

Table 3-3. Effects of alanine substitutions on FECH activity

Variant	Enzymatic activity[1]	Dimerization status[2]	Salicylic acid binding[3]
V270A	0%	Monomer	Weak
S281A	~70%	Dimer	Normal
W301A	0%	Monomer	Very weak
L311A	0%	Monomer	Very weak

[1] % of FECH R115L activity, measured as the amount of Zn-PpIX produced.

[2] Based on gel filtration data.

[3] Based on binding assays with salicylic acid-immobilized beads.

Finally, to investigate whether the amino acid residues W301 and L311 are directly involved in salicylic acid binding, binding assays were performed by again using the monomeric R115L/V270A FECH mutant. As expected, an additional W301A or L311A mutation introduced into R115L/V270A resulted in the loss of binding (Figure 3-6). Taken together, these results demonstrate that W301 and L311 are important both to salicylic acid binding and to FECH dimerization, raising the possibility that salicylic acid binding to FECH may affect its dimerization status.

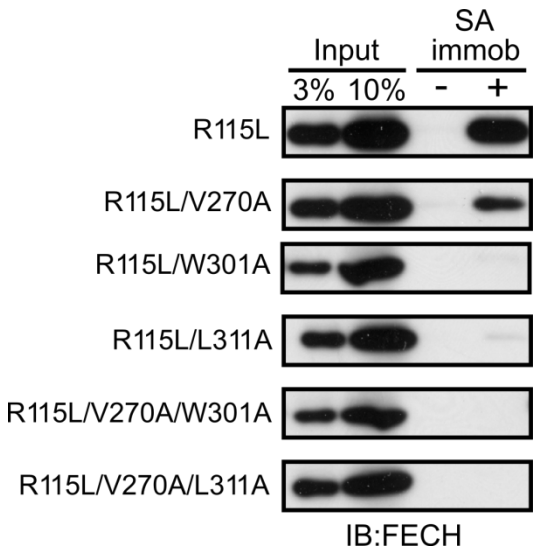

Figure 3-6. FECH R115L mutants, R115L/V270A/W301A and R115L/V270A/L311A, were expressed in *E. coli*, and their lysates (input) were subjected to affinity purification with control beads (−) or salicylic acid-immobilized (+) beads. Samples were immunoblotted (IB:FECH) with anti-FECH antibody. FECH R115L, R115L/V270A, R115L/W301A, R115L/L311A binding assay results are same as Figure 3-4 and are shown here for comparison.

3.3.3 Monomeric bacterial FECH binds to salicylic acid

FECH is widely conserved across species. Although the primary sequence alignment of FECH shows several deviations, structural features are largely conserved among species (Wu et al., 2001). In contrast to mammalian FECH, however, bacterial FECHs are known to function as monomers (Wu et al., 2001). Moreover, mammalian and bacterial FECHs share <20% identity and are particularly different in that bacterial FECHs lack the C-terminal extension that is important for their coordination with [2Fe-2S] cluster. Nevertheless, the secondary and tertiary structures of the core region of mammalian and bacterial FECHs are similar. This prompted me to investigate whether bacterial FECH also binds to salicylic acid. FECH from *E. coli*

BL21 was cloned and expressed as a GST-tagged protein and the extract prepared from *E. coli* expressing the GST-tagged bacterial FECH was subjected to binding assay with salicylic acid-immobilized beads. As a result, it was found that recombinant FECH derived from *Escherichia coli* binds to salicylic acid to the same extent as the human monomeric R115L/V270A FECH mutant (**Figure 3-7A**). Concordantly, amino acid residues critical for salicylic acid binding are conserved between mammalian and bacterial FECHs (**Figure 3-7B**). Since bacterial FECHs exist essentially as monomer, the above finding strengthens our conclusion that the dimerization of FECH is not required for salicylic acid binding.

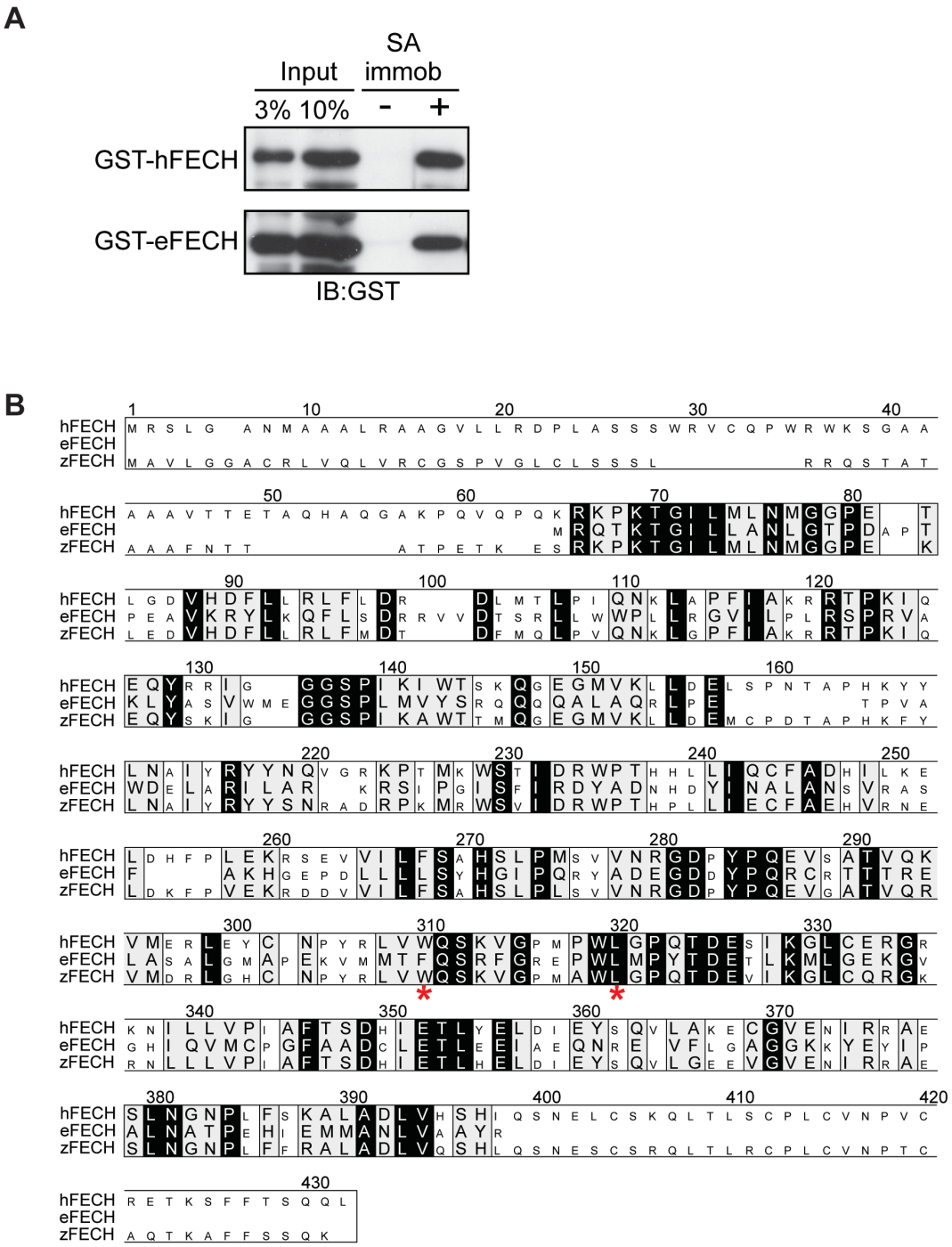

Figure 3-7. Salicylic acid binds to monomeric bacterial FECH. (A) Recombinant GST-tagged human wild-type FECH (GST-hFECH), and *E. coli* FECH (GST-eFECH) were subjected to salicylic acid-binding assays. Proteins were visualized by immunoblotting analysis with an anti-GST antibody. (B) Multiple sequence alignment for human, zebrafish and and *E. coli* ferrochelatases. Marked with red asterisk are the amino acids important for salicylic acid

binding in human (W301 and L311) that are conserved among all three sequences. Mammalian and zebrafish ferrochelatase have N-terminal mitochondrial targeting sequences and C-terminal extensions that are not present in *E. coli* ferrochelatase.

3.3.4 Salicylic acid induces conformational changes in FECH

Based on the above results, it is clear that mutation at the dimer interface destabilizes the dimer and renders the FECH inactive. This is in agreement to a previous report that any mutation affecting the dimer interface has a significantly greater impact on FECH activity (Najahi-Missaoui and Dailey, 2005). Since salicylic acid binding position in FECH is situated at the dimer interface, it is possible that salicylic acid can either (1) cause dissociation of dimer or (2) induce conformational changes in FECH molecule. To study this point further, gel filtration analysis was performed in the presence of different concentrations of salicylic acid. FECH R115L pre-incubated with indicated concentration of salicylic acid was loaded on the Superdex 200 column equilibrated with column buffer containing same concentration of salicylic acid. As shown in **Figure 3-8A**, the presence of salicylic acid clearly shifted the elution peak of FECH R115L from fraction #6 to fraction #7 at 30 and 100 mM salicylic acid concentration. To validate if this shift is specifically by salicylic acid, similar experiment was conducted with *para*-hydroxybenzoic acid (*p*-HBA). By contrast, *p*-HBA did not appreciably affect the elution profile of FECH R115L (**Figure 3-8B**), suggesting that the shift is specific and is mediated by salicylic acid binding to FECH. However, the shift in FECH R115L peak was not as dramatic as that caused by the L311A mutation (**Figure 3-7A** and **Figure 3-7B**) and salicylic acid also did not cause any appreciable shift in L311A peak, indicating that the drug may cause a conformational change in the dimer rather than its complete dissociation.

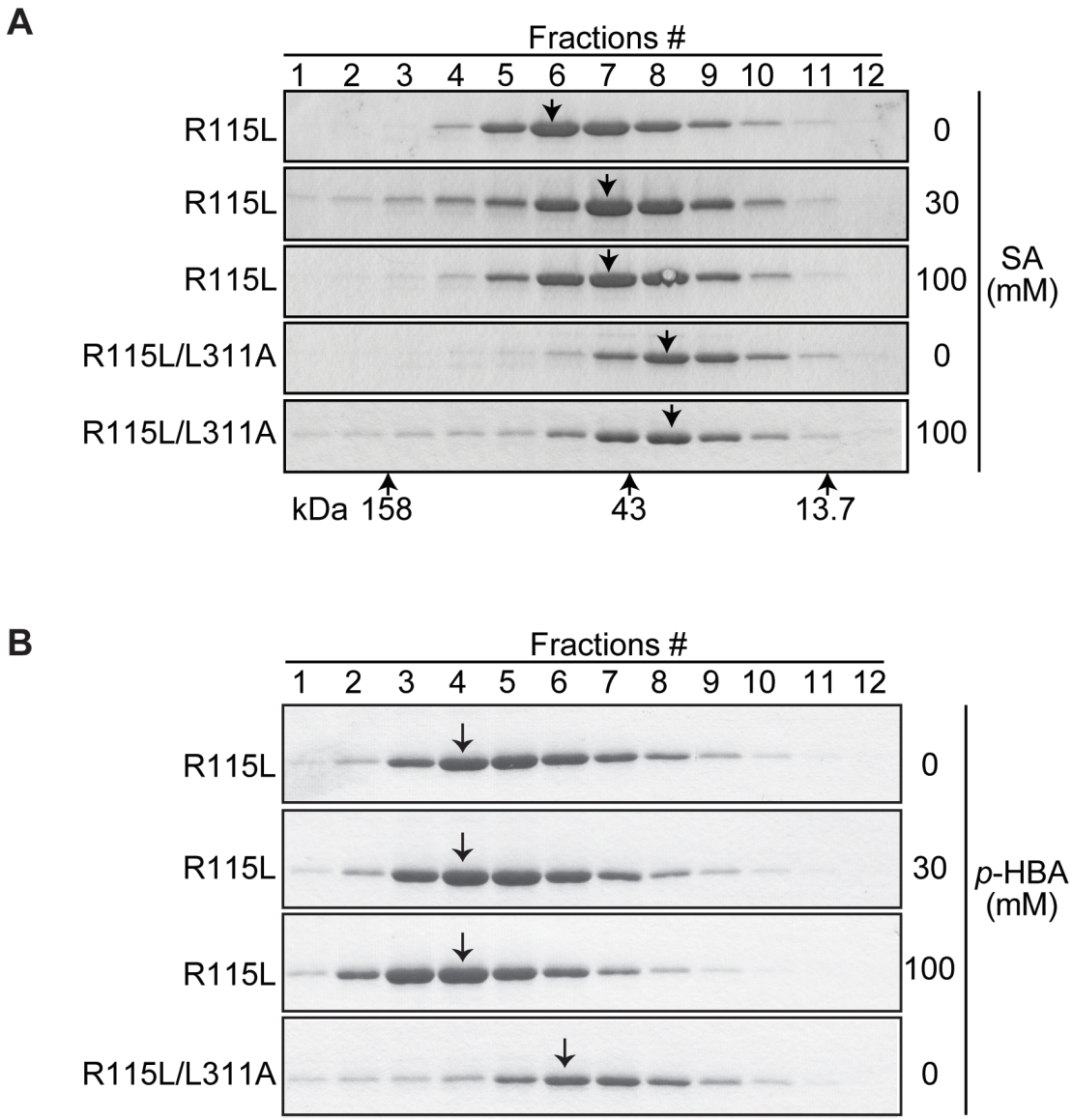

Figure 3-8. Salicylic acid induces conformational changes in FECH dimer. (A) Equal amounts of purified recombinant FECH R115L and L311A were incubated with or without the indicated concentrations of salicylic acid for 1 h at 4°C. They were then applied to a Superdex 200 10/300 gel filtration column (GE Healthcare). The same concentrations of salicylic acid were included in the column buffer. Eluate fractions (500 µl each) were collected and analyzed by SDS-PAGE and Coomassie Brilliant Blue staining. Peak positions are shown with down-arrows. The peak positions of gel filtration markers (158, 43, and 13.7 kDa) are shown with up-arrows. (B) Figure 3-8. Gel Filtration was performed as in (A), except *para*-hydroxybenzoic acid (*p*-HBA) was used instead of salicylic acid. Peak positions are shown with down-arrows.

3.3.5 Determination of binding constant (K_d) of FECH•salicylic acid by isothermal titration calorimetry

In severe cases of rheumatic fever and rheumatoid arthritis, high doses of aspirin are administered, resulting in its metabolite, salicylic acid, increasing to concentrations of 1–3 mM in the plasma and above 4 mM in the tissue (Baggott et al., 1992). Therefore, to obtain quantitative data on the FECH•salicylic acid interaction, isothermal titration calorimetry (ITC) was used. To estimate the dissociation constant (K_d) and the enthalpy change (ΔH), low c-value titrations were performed as described previously (Turnbull and Daranas, 2003), because the binding affinity was considered to be low and because it was not possible to increase the FECH concentration enough to perform the standard analytical method. In a typical ITC experiment with a c-value of 10 to 50, a sigmoidal curve is obtained when the ratio of total ligand and receptor concentrations ($[X]_t$ / $[M]_t$) is plotted against stepwise heat change (the Wiseman isotherm). An experiment with a low c-value results in a flatter line that is not suitable for curve fitting, as shown in **Figure 3-9**. When c-value is significantly smaller than 1, receptor occupancy is essentially independent of receptor concentration and principally dependent on the ratio of ligand concentration $[X]_t$ to K_d. When $[X]_t$ / K_d is plotted against stepwise heat change instead, low c-value data give a curve with a hyperbolic shape, and K_d and ΔH can be estimated from curve fitting. Binding stoichiometry (n), however, cannot be determined experimentally from this analysis. Therefore, to estimate thermodynamic parameters for the FECH-salicylic acid interaction, binding stoichiometry was fixed to 1, 5, 10, or 20 during the fitting procedure, and K_d and ΔH were obtained for each binding stoichiometry (**Table 3-4**). The estimated K_d value is in the range of 5 to 15 mM.

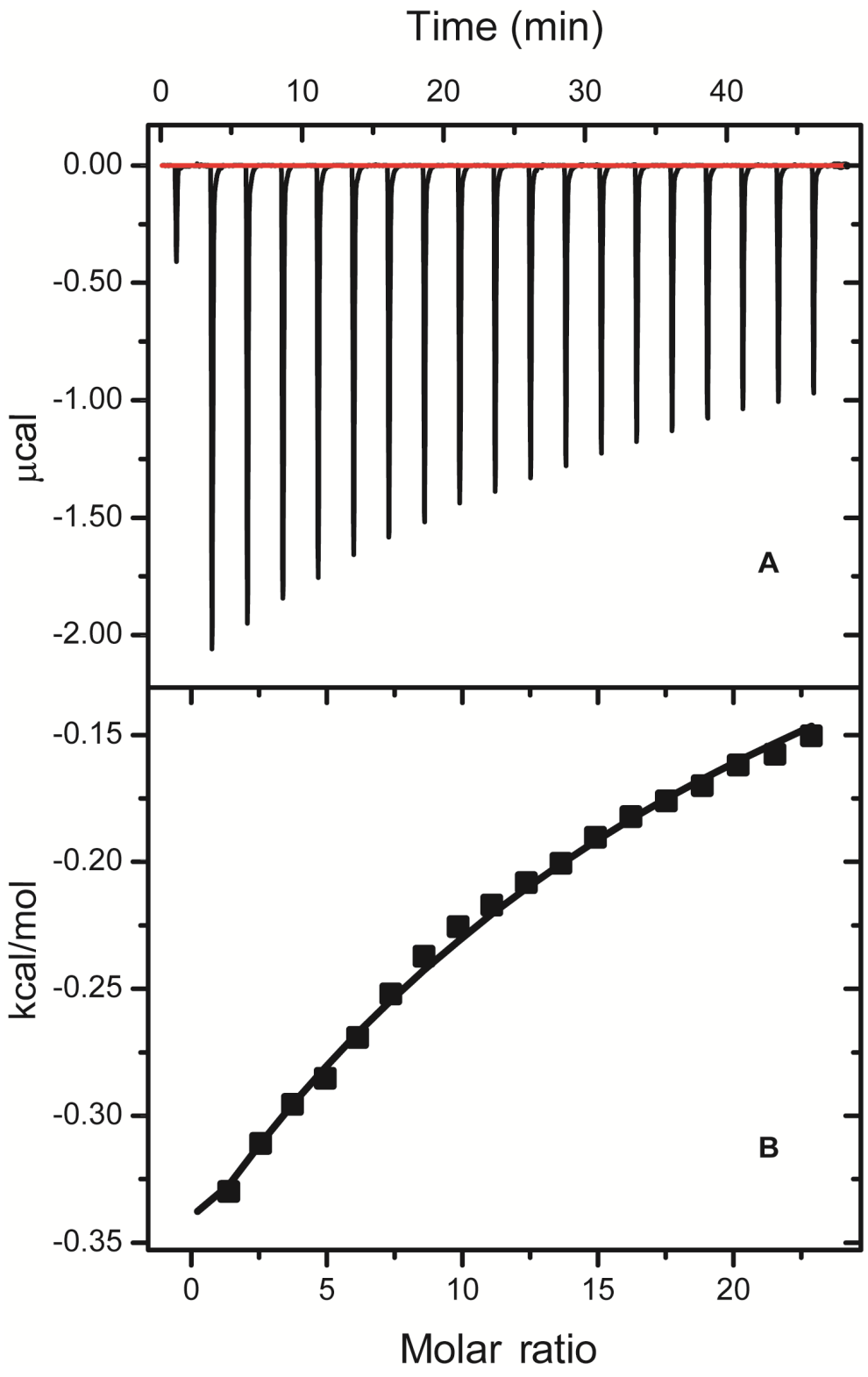

Figure 3-9. Analysis of binding parameters between FECH and salicylic acid by ITC. (A) Representative ITC data. Heat effects were recorded as a function of time during 19 successive 2 µl injections of 25 mM salicylic acid into the sample cell containing 200 µM FECH WT* or buffer at 25°C. The data obtained

by using buffer only were subtracted from those obtained by using FECH WT* and are indicated with red and black lines, respectively. (B) A plot of the calculated enthalpies per injection versus the molar ratios of ligand to protein in the sample cell is shown. The data were fitted according to a one site binding model (MicroCal origin software package).

Table 3-4. Selected thermodynamic parameters for the FECH-salicylic acid interaction

Stoichiometry (n)	K_a (M^{-1})[a]	Δ H (kcal/mol)
1	69±1.7	-23.4±0.5
5	79±2.5	-4.4±0.10
10	97±4.0	-2.0±0.06
15	129±8.0	-1.1±0.04
20	195±28.0	-0.7±0.05

[a] The equilibrium binding constant (1 / K_d)

It is important to note that most of the *in vitro* binding and enzyme assays performed in this study included 0.1–1.0% Triton X-100. FECH enzymatic activity buffer IB-D contains 1% TritonX-100, and 1.75 mM palmitic acid that has been shown to increase the FECH enzymatic activity (compared to the buffer containing either of these) and reduce non-enzymatic formation of Zn-PpIX (Li et al., 198). FECH binding assay with salicylic acid-immobilized beads was performed in buffer containing 0.1% Triton X-100. To investigate whether decreasing or increasing Triton X-100 concentration has any adequate effect on FECH salicylic acid interaction, binding assay under three Triton X-100 concentration – 0.02, 0.1 and 1 %. As shown in **Figure 3-10**, Triton X-100 is clearly inhibitory to the FECH/salicylic acid interaction, suggesting that the presence of the detergent underlies the weak affinity of salicylic acid for FECH *in vitro*. In our binding assay 0.1% Triton X-100 was found to be best suited for FECH•salicylic acid interaction. It may be possible that with increasing

concentration of Triton X-100, a certain fraction of the salicylic acid is entrapped in the micelle in the presence of Triton X-100, and is thus unable to interact with FECH.

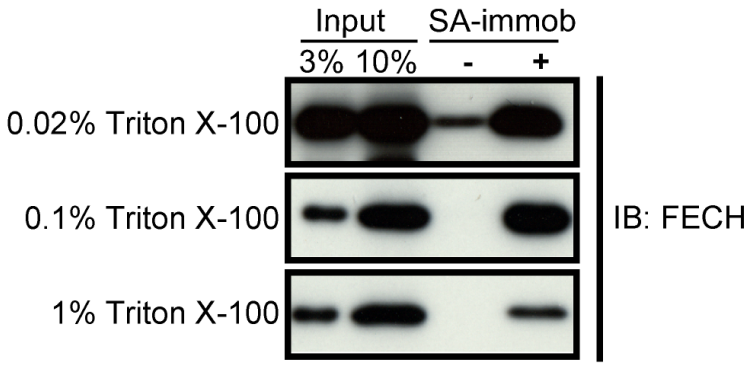

Figure 3-10. Affinity purification was performed with recombinant FECH R115L in IB-A buffer containing 1% Triton X-100. Results obtained by using 0.1% Triton X-100 instead of 1% Triton-X-100 (a reproduction of Figure 2-7) are shown for comparison.

3.4 Conclusions

From this chapter, a new insight into the mechanism of salicylic acid-mediated inhibition of FECH activity was obtained. Firstly, the tertiary structure of FECH•salicylic acid complex was determined, showing that salicylic acid binds to FECH dimer interface. Secondly, mutational analysis of the salicylic acid binding site revealed that amino acid W301 and L311 are important for salicylic acid interaction to FECH. Furthermore, it was also shown that dimerization is not a prerequisite for salicylic acid binding to FECH and salicylic acid can bind to the monomeric mutant FECH V270A. Also, mutation at the FECH dimer interface affects its homodimerization and renders FECH inactive. Based on these data, it was hypothesized that salicylic acid inhibits FECH activity by causing conformational changes at the dimer interface. The hypothesis was supported by the fact that salicylic acid induces shift in FECH elution peak on a gel filtration column. However, the findings apparently contradict the structural data, which did not reveal any conformational change in FECH upon salicylic acid binding. One explanation might be that the crystal structure obtained only represents an initial FECH•salicylic acid binding state. Regardless, the salicylic acid-induced structural change, evidenced by gel filtration analysis, may be related to its inhibitory effect on FECH's enzymatic activity. Finally, binding parameters of FECH•salicylic acid interaction is calculated by ITC and the K_d was calculated to be between 5 and 15 mM, which is similar or slightly higher than the physiological concentration of salicylic acid.

Chapter 4. Salicylic acid inhibits heme synthesis *in vivo*

4.1 Introduction

FECH is a ubiquitously expressed, inner mitochondrial membrane protein of the heme biosynthetic pathway that catalyzes the insertion of ferrous ions into protoporphyrin IX (PpIX) to form heme, through a complex series of steps initiated by condensation of glycine and succinyl CoA into δ-aminolevulinate (**Figure 4-1**). Heme then serves as the prosthetic group of various hemoproteins that are vital for cell viability such as oxygen carrying hemoglobin and myoglobin and energy producing cytochromes in the electron transport chain (Mobius et al. 2010). Decrease of 70% - 95% in FECH activity has been related to inherited disease erythropoietic protoporphyria (EPP) with prognosis characterized by PpIX accumulation in red blood cells (RBCs), plasma, bone marrow and other organs. Heme deficiency induce by lack of FECH activity inhibits the assembly of mitochondrial complex IV in human fibroblast cells that leads to impaired energy production, oxidative stress and corruption of Ca^{2+} homeostasis causing mitochondrial damage (**Figure 4-1**) (Atamna et al., 2001, 2002). Since, salicylic acid also causes similar mitochondrial injury; it will be interesting to investigate if salicylic acid inhibits heme synthesis in cells and *in vivo*.

In this chapter, I investigated the inhibitory effect salicylic acid on heme biosynthesis in human cell lines and animal models. At pharmacologically relevant concentrations, salicylic acid inhibits heme biosynthesis in K562 cells. In addition, at similar concentration and incubation time, salicylic acid substantially inhibits

mitochondrial activity in K562 cells. Both in 293T cells and zebrafish, knockdown of FECH lead to reduction of heme similar to the phenotype induced by salicylic acid. In addition, FECH overexpression in zebrafish partially restored heme production in both conditions. Salicylic acid also caused the accumulation of FECH substrate, protoporphyrin IX in salicylic acid treated zebrafish.

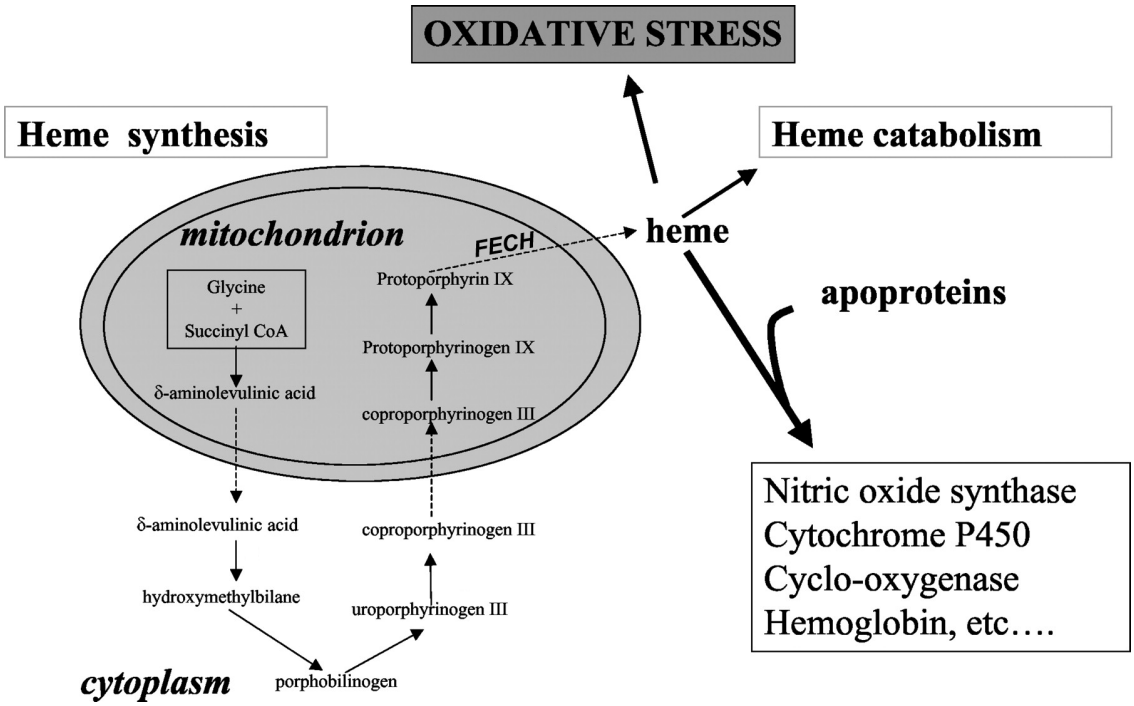

Figure 4-1: An overview of heme biosynthesis pathway in cells. Heme biosynthesis is initiated by the condensation of glycine and succinyl CoA. Ferrochelatase (FECH) catalyzes the terminal step of the pathway by chelating ferrous into PpIX to form heme. Heme is further incorporated by several proteins vital for cell viability (adapted from Wagener et al., 2003).

4.2 Materials and methods

4.2.1 Cell culture

Human erythroleukemia K562 cells were cultured in RPMI 1640 medium supplemented with 10% fetal bovine serum. 293T cells were cultured in DMEM supplemented with 10% fetal bovine serum.

4.2.2 FECH knock down in 293T cells

To knock down human FECH, the following sequences were used as a target of shRNA:

sh#1: 5'- CCAAGGAGTGTGGAGTTGAAA-3'

sh#2: 5'-GACCATATTGAAACGCTGTAT-3'

Lentiviral vectors expressing these shRNAs were produced and infected into 293T cells, followed by selection with puromycin for a few days. The resulting cells were then used for subsequent analyses.

4.2.3 Quantification of cellular heme content

Total heme was extracted and analyzed by ultra-high performance liquid chromatography (UPLC), essentially as described previously (Antonicka et al., 2003). K562 or 293T cells (2×10^6) were seeded onto six-well plates and cultured in RPMI medium supplemented with 10% FBS. The cells were then incubated with different concentrations of salicylic acid (SA), *m*-HBA, or *p*-HBA for 24 h at 37°C. After washing with phosphate buffered saline (PBS), cells were lysed by the sequential addition of acetone/HCl/water (175 µl; 77.5: 2.5: 20) and 50% acetonitrile (200 µl) with vigorous shaking. After centrifugation at 20,400 × g at 4°C for 10 min, the supernatant (200 µl) was collected and filtered through a 0.22 µm centrifugal filter

(Millipore). The pH of the sample was adjusted to ~3 – 4 by the addition of NH_4OH, and the sample was applied to a UPLC system equipped with a 2.1 × 50 mm C18 column (Waters). Heme was eluted at a flow rate of 0.2 ml/min by using a 30–50% acetonitrile gradient for the first minute, followed by a 50–95% acetonitrile gradient for the next 9 min. All column buffers contained 0.05% trifluoroacetic acid. The elution of heme was monitored by measuring the absorbance at 400 nm. The retention time of heme was confirmed by using commercially available hemin as the control (Frontier Scientific).

4.2.4 Quantification of NAD(P)H content

NAD(P)H content in cells was quantified by using the WST-8 assay (Nacalai Tesque). The assay is based on the extracellular reduction of WST-8 by NAD(P)H produced in the mitochondria (Berridge et al., 2005). K562 cells were seeded into 96-well plates (5000 cells/50 µl/well) in RPMI 1640 medium supplemented with 10% FBS. Salicylic acid (SA), *m*-HBA, or *p*-HBA (50 µl/well) was added to each well, and after 24 h of incubation at 37°C, WST-8 was added. The absorbance at 450 nm was determined by using a plate reader (Wallac 1420 ARVO SX). Data were reported as the percentage of the absorbance in untreated controls.

4.2.5 Mitochondrial membrane potential

Flow cytometry was used for the determination of mitochondrial membrane potential (MMP, ΔΨ). K562 cells (1 × 106 cells/ml/well) were seeded into six-well dishes in RPMI 1640 medium supplemented with 10% FBS. Salicylic acid (SA), m-HBA, p-HBA (10 mM), or FCCP (10 µM; Sigma) was added (in 1 ml of the same medium) and incubated for 24 or 48 h. Cells were stained with 10 µM Rhodamine 123 (Sigma) for 15 min at 37°C, washed with PBS, and analyzed with a FACScalibur

(Becton-Dickinson).

4.2.6 Zebrafish experiments

Zebrafish maintenance and breeding was performed as described previously (Westerfield, 1995). Embryos less than 5 days-post-fertilization (hpf) were cultured in E3 medium (5 mM NaCl, 0.17 mM KCl, 0.33 mM $CaCl_2$, 0.33 mM $MgCl_2$, 0.00001% methylene blue). For salicylic acid treatment, zebrafish embryos (1 hpf) were dechorionated by using 2 mg/ml protease type XIV (Sigma) and then immersed in E3 medium containing 0.5, 1, or 3 mM of salicylic acid for 47 h, as described previously (Ito et al., 2010). FECH Knockdown and rescue experiments were performed by microinjecting an antisense morpholino oligonucleotide (AMO; 1 to 2 ng) targeting zFECH (5'-CACGCGCCTCCTAAAACCGCCATTG-3'), with or without capped mRNA for zFECH (0.6 ng; Gene Tools, Philomath, OR, USA), as described previously (Ito et al., 2010). Heme was visualized by *o*-dianisidine staining (0.6 mg/ml *o*-dianisidine, 0.01 M sodium acetate pH 4.5, 0.65% H_2O_2, 40% v/v ethanol) of 48 hpf embryos, as described previously (Ransom et al., 1996). After staining, embryos were washed in PBS and fix with 4% paraformaldehyde for 1h. Finally, the embryos were cleared with 30 % to 70% glycerol solution. Accumulation of PpIX in living 48-hpf embryos was detected by fluorescence microscopy using its autofluorescence with illumination peak at 520-550 nm (Childs et al., 2000).

4.3 Results

4.3.1 Salicylic acid inhibits heme biosynthesis

Human chronic myelogenous leukemia (K562) cell lines were used to study the effect the salicylic acid on cellular heme synthesis. Although leukemic, these cells show proteomic similarity to both undifferentiated granulocytes and erythrocytes (Klein et al., 1976, Anderssion et al., 1979), and contain a functioning FECH protein. Thus, it is expected that on salicylic acid treatment, the cells will show reduction in level of heme. To investigate the effect of salicylic acid on cellular heme biosynthesis, K562 cells were treated with 1, 3 and 10 mM of salicylic acid and heme was extracted and subjected to UPLC, as mentioned in **4.2.3**. For comparative analysis, K562 cells were also incubated with 1, 3, and 10 mM of *m*-HBA and *p*-HBA, respectively to validate the specificity of the heme decrease. **Figure 4-2** shows that salicylic acid treatment for 24 h resulted in a substantial reduction in the heme content of K562 cells, with the maximum decrease of 64±3% observed at 10 mM. Alternatively, the effects of *m*-HBA and *p*-HBA were comparatively weak, with maximum decreases of 16±2% and 15±4%, respectively, at 10 mM. Hence, salicylic acid, but not *m*-HBA and *p*-HBA, inhibits FECH activity in cell-free assays and K562 cells.

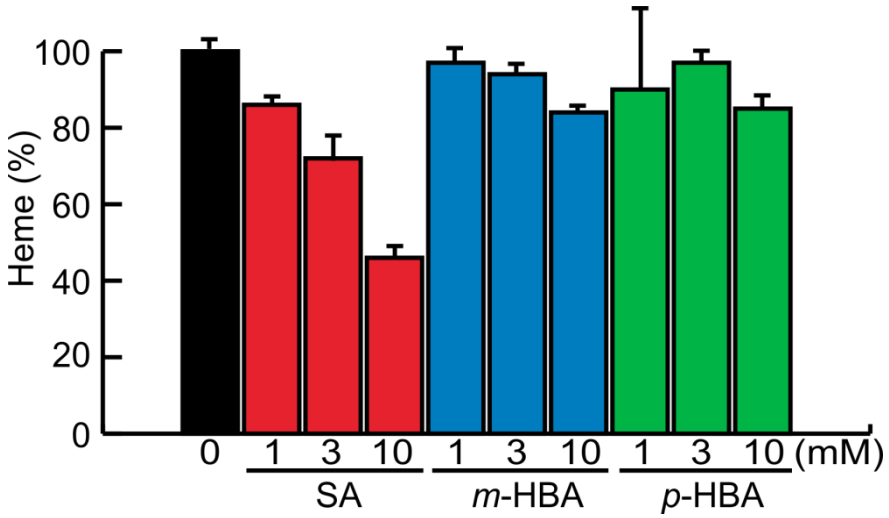

Figure 4-2: Salicylic acid inhibits heme biosynthesis and mitochondrial activity in K562 cells. K562 cells were treated with salicylic acid (SA, red), *m*-HBA (blue), or *p*-HBA (green) for 24 h, extracted, and subjected to UPLC. Heme was detected by measuring the absorbance at 400 nm (n=3; averages and SDs are indicated). The heme content in control K562 cells was set to 100%.

4.3.2 FECH is responsible for the inhibitory effect of salicylic acid on heme synthesis.

To investigate the functional link between FECH and salicylic acid more critically, we knocked down FECH in 293T cells by transducing lentiviral vectors expressing shRNAs directed towards two different regions of the coding region of FECH, starting from base pairs 1070-1090 and 1018-1038 respectively, as described in **4.2.2**. As shown in **Figure 4-3A**, both shRNAs effectively down-regulated FECH expression compared to the mock-treated cells. Also, FECH knockdown alone resulted in a reduction of the cellular heme level (data not shown). To study the effect of salicylic acid on FECH knockdown, 293T cells were first treated with lentiviral vectors expressing one of the two shRNAs. Thereafter, salicylic acid was added to the mock or shRNA treated cells at 1, 3, and 10 mM concentration. After 24 h incubation, cellular level of heme was measured with or without prior incubation of salicylic acid. Remarkably, FECH knockdown abolished salicylic acid-induced reduction of the heme level at all concentration of salicylic acid (**Figure 4-3B**), suggesting that FECH is responsible for the inhibitory effect of salicylic acid on heme synthesis, and mediating some of its pharmacological effects.

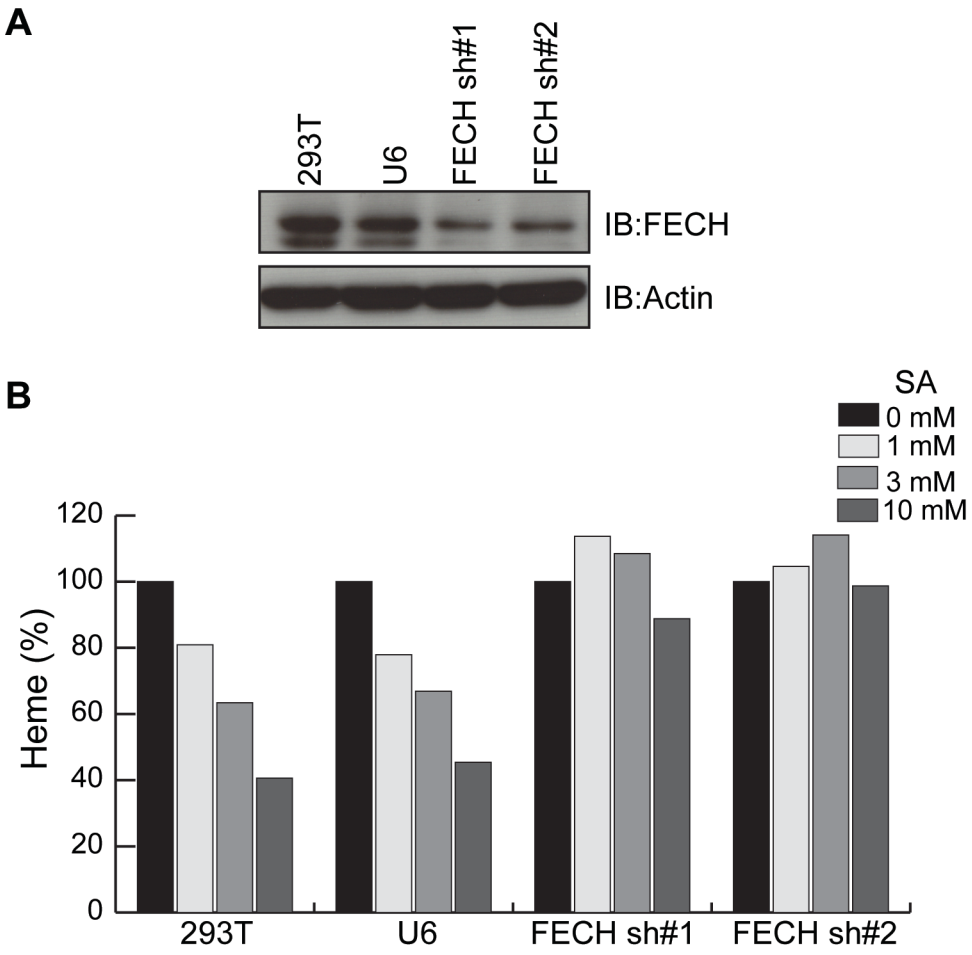

Figure 4-3: FECH is responsible for the inhibitory effect of salicylic acid on heme synthesis in 293T cells. (A) 293T cells were infected with lentiviral vectors expressing one of two shRNAs against FECH (FECH sh#1 and FECH sh#2) or a control vector (U6). After selection for a few days, cells were subjected to immunoblot analysis. "293T" represents untransduced 293T cells. (B) A fixed number of cells (FECH knockdown cells or control cells) were plated into multiwell plates, treated with the indicated concentrations of salicylic acid (SA) for 24 h, and subjected to UPLC analysis for the quantification of heme. Three independent experiments were performed, and a representative data set is shown.

4.3.3 Salicylic acid induces mitochondrial injury in K562 cells.

Salicylic acid-induced mitochondrial injuries were investigated in two different assays:

(i) the WST-8 (tetrazolium salt) assay, which measures NAD(P)H and hence general

mitochondrial energy metabolism, and (ii) the Rhodamine 123 assay, which measures mitochondrial membrane potential by using a fluorescent lipophilic cationic dye. In both assays, salicylic acid inhibits mitochondrial function (Braun et al., 2012; Klampfer et al., 1999).

To study the mitochondrial injury by salicylic acid, a general approach utilizing tetrazolium dyes was followed. An assay mixture containing the tetrazolium salt, WST-8, in association with an electron mediator. 1-methoxy PMS, was added to the cell culture. 1-methoxy PMS resides on the cell surface where it reacts directly with NADH (nicotinamide adenine dinucleotide reduced form) or NADPH (nicotinamide adenine dinucleotide phosphate reduced form). Reduced 1-methoxy PMS further reduces WST-8 present in the medium that gives a strongly coloured solution with a peak absorbance at 450 nm (**Figure 4-4A**). In cells, NADH or NAD(P)H are generated by the reaction of dehydrogenase enzymes and their substrates in different pathways, such as Krebs cycle (citric acid cycle), phosphopentose pathway and glycolysis. NAD(P)H is further used as electron donor in oxidative phosphorylation pathway. Thus, a decrease in NAD(P)H level is correlated with the abnormal mitochondrial activity. K562 cells were treated with 1, 3 and 10 mM of either salicylic acid (SA) or *m*-HBA or *p*-HBA for 24 h and after addition of WST-8 mixture, NAD(P)H level in cells were estimated based on absorbance at 460 nm. As shown in the **Figure 4-4B**, salicylic acid resulted in a significant dose-dependent decrease in cellular NAD(P)H levels, with an IC50 of ~3 mM after 24 h of incubation. By contrast, both *m*-HBA and *p*-HBA show only a modest inhibitory effect on the mitochondrial activity (**Figure 4-4B**).

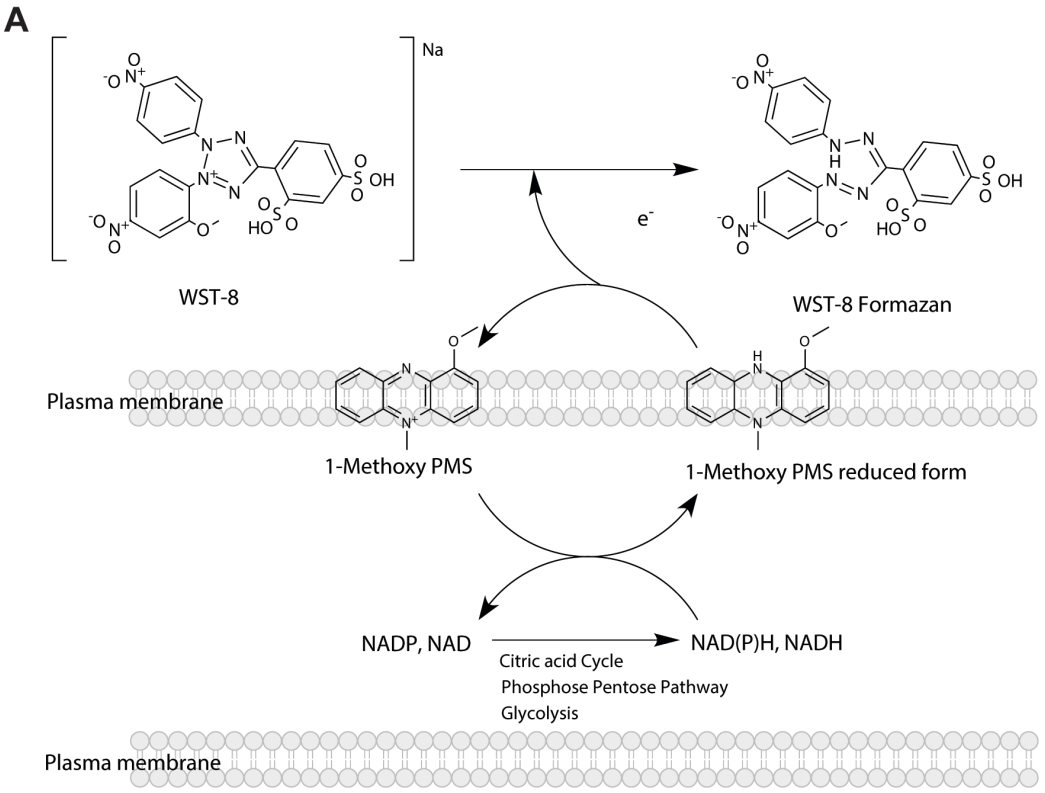

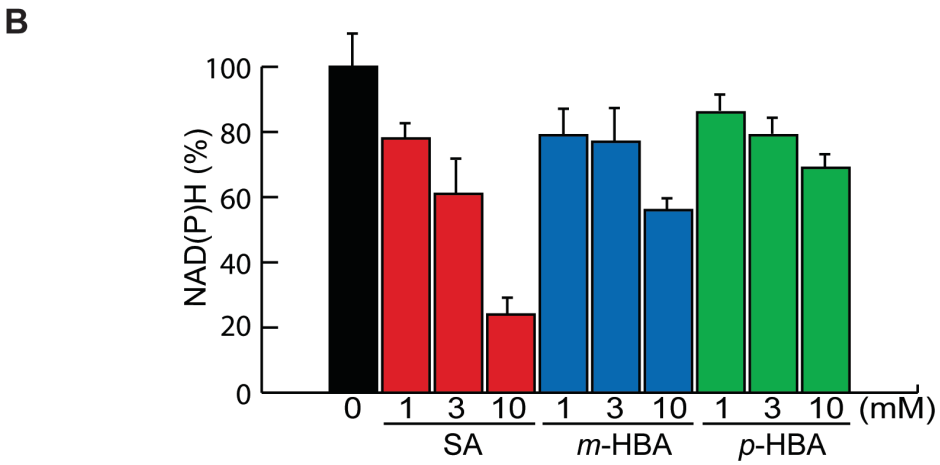

Figure 4-4: Salicylic acid inhibits mitochondrial NAD(P)H production activity (A) Biochemistry of NAD(P)H detection by WST-8 assay in cells. (B) K562 cells were similarly incubated with the indicated concentrations of SA (red), m-HBA (blue), or p-HBA (green) for 24 h. WST-8 assays were then performed to measure NAD(P)H content in the cells (n=4; averages and SDs are indicated). The NAD(P)H content in control K562 cells was set to 100%.

Rhodmaine 123 is a cell-permeant, fluorescent, aromatic, monovalent cationic dye that is used to measure the mitochondria membrane potential (**ΔΨm**), a key factor that drives the production of ATP in mitochondria energetics. Some of the advantages of using Rhodmaine 123 as an indicator of membrane potential is its availability, high sensitivity (high quantum yield), specificity (against other environmental changes), non-invasiveness, and low interference with underlying metabolic processes (Huang et al., 2007). In intact cells, respiring mitochondria easily take up Rhodamine 123 indicated by the increase in fluorescence, while any defect in mitochondria bioenergetics cause a reduction in the fluorescence (**Figure 4-5A**). To examine the effect of salicylic acid on mitochondria membrane potential, K562 cells treated with or without salicylic acid, *m*-HBA and *p*-HBA (10mM each) or with the known uncoupler, carbonyl cyanide *p*-trifluoromethoxyphenylhydrazone (FCCP, employed as the positive control).were subjected to rhodamine 123 assay. After 24 h incubation, a small reduction in membrane potential was induced by salicylic acid (**Figure 4-5B, left**). At 48 h, salicylic acid yielded a 52% decrease in fluorescence, which was comparable to that induced by FCCP. By contrast, *m*-HBA and *p*-HBA had only a modest effect on membrane potential, at both 24 h and 48 h (**Figure 4-5B, right**).

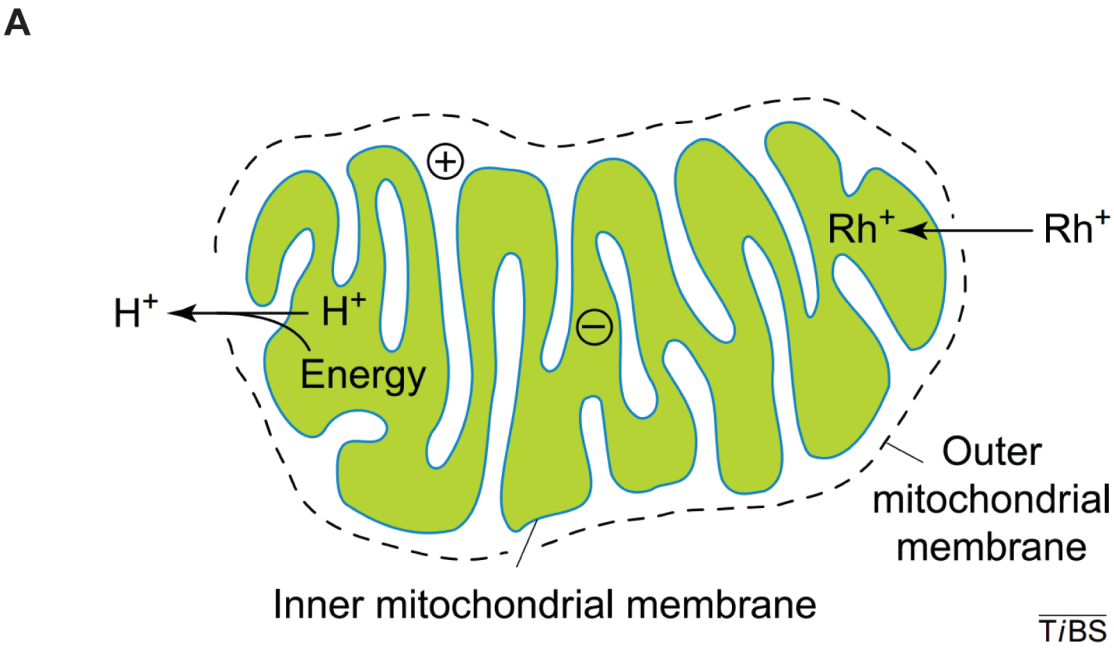

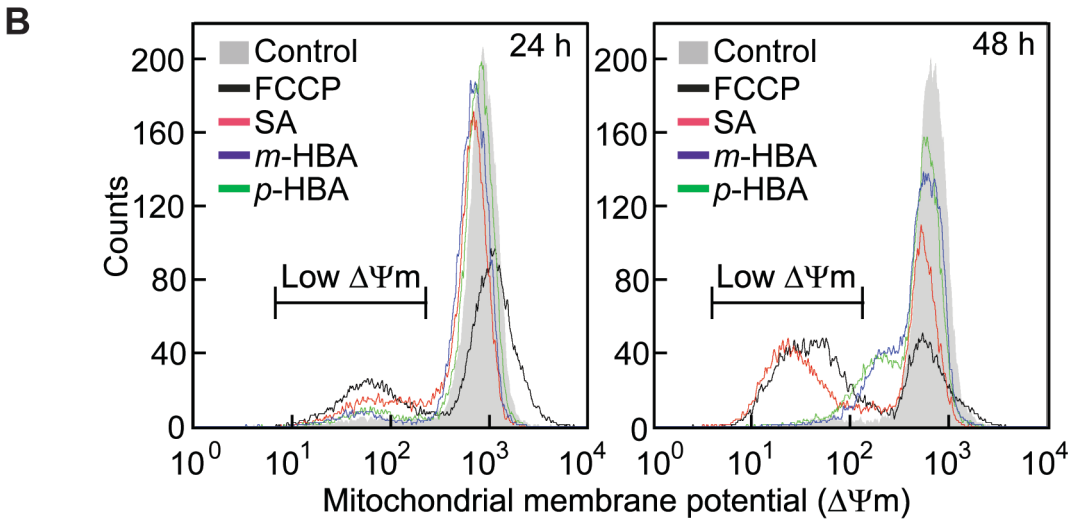

Figure 4-5: (A) A schematic representation of accumulation of rhodamine 123 by mitochondria. Cationic dye rhodamine 123 (Rh^+) is quenched by mitochondria, and accumulates electrophoretically inside mitochondria that pump out H^+ at the expense of respiration energy. Rhodamine 123 efflux is detected by FACS, which measures its fluorescence. Reduction in fluorescence is directly correlated with the change in the membrane potential hence disturbance in mitochondrial activity (adopted from Skulachev, 2001). (B) K562 cells were treated with SA (red), m-HBA (blue), or p-HBA (green) for 24 (left) or 48 h (right) and stained with Rhodamine 123 to measure mitochondrial membrane potential. FCCP (black), a known uncoupler, was

used as the positive control.

4.3.4 FECH is responsible for salicylic acid-induced inhibition of heme biosynthesis in zebrafish

A clear picture of salicylic acid mechanism can only be drawn when there is enough evidence to conclude that it inhibits heme production, at pharmacologically relevant concentration, in animals. To investigate inhibition of heme biosynthesis by salicylic acid *in vivo*, I used zebrafish (*Danio rerio*) as a model animal. Because of a short generation time, simple body structure, and a transparent periderm during development stages, zebrafish is one of the popular model organisms in developmental biology (Howe et al., 2013). Gene integrity of zebrafish is fairly close to humans and about 70% of human genes have at least one zebrafish ortholog (Howe et al., 2013). Moreover, gene manipulation for various specific purposes can be efficiently performed in zebrafish using antisense morpholino-modified oligonucleotides (*AMO*).

In a previous report, zebrafish mutant "*dracula"*, lacking FECH activity showed characteristic phenotype similar to erythropoietic protoporphyria disease caused by FECH deficiency (Childs et al., 2000). This includes phenotypic features like: accumulation of PpIX, light-dependent hemolysis and liver disease (Childs et al., 2000). Amino acid sequence of human and zebrafish FECH are ~ 79% identical. In addition, the W301 and L311 amino acid residues in human FECH, which are important for salicylic acid binding, are conserved in zFECH (**Figure 3-7**). Zebrafish FECH was cloned into the GST fusion expression vector pGEX-6P-1 (GE Healthcare) and used to produce the mature GST-tagged zFECH (GST-zFECH-WT). Binding assay was performed using *E. coli* extract expressing GST-zFECH. As shown in the **Figure 4-6**, GST-zFECH binds to salicylic acid-immobilized beads as efficiently as

human FECH (GST-hFECH-WT). Thus, these results support the use of zebrafish as a model animal to study the effect of salicylic acid on heme biosynthesis.

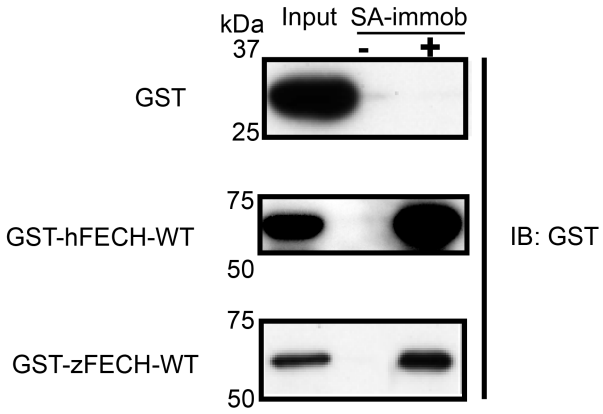

Figure 4-6: Salicylic acid binds zebrafish ferrochelatase (zFECH.) Cell lysates derived from *E. coli* expressing recombinant GST, GST-tagged full-length human FECH (GST-hFECH-WT), or GST-tagged full-length zebrafish FECH (GST-zFECH-WT) were subjected to affinity purification with salicylic acid-immobilized beads. Lysates (input) and affinity-purified material were immunoblotted (IB) with an anti-GST antibody.

Heme decrease in 48 hpf zebrafish embryos was visualized by *o*-dianisidine staining. *O*-dianisidine is readily oxidized by heme in the presence of hydrogen peroxide. Heme-rich hematocytes were stained in a granular pattern and based on the intensity of staining the embryos were divided into 3 classes: “strong”, “intermediate” and “weak” (**Figure 4-7A**). There were small embryo-to-embryo variation in appearance of *o*-dianisidine staining, which was due to (1) the different running patterns of the blood sinus, and (2) the image-to-image variations in the focal plane. Knockdown of FECH in zebrafish substantially decreased heme synthesis as shown by the decrease in percentage of strongly stained embryos (**Figure 4-7B**). This effect was successfully rescued by overexpression of zFECH mRNA, confirming that the decrease in heme staining was in fact because of FECH depletion (**Figure**

4-7B). Similarly, salicylic acid, at both 1 and 3 mM, was found to significantly decrease *o*-dianisidine staining in larger population of embryos (**Figure 4-7B)**. Also, no developmental defects were detected in salicylic acid or zFECH knockdown embryos.

Additional rescue experiments were performed to further confirm the effect of salicylic acid on heme biosynthesis. Salicylic acid treated embryos were injected with zFECH mRNA to rescue the salicylic acid induced heme depletion. Remarkably, overexpression of zFECH again partially restored the heme production in embryos exposed to pharmacological relevant concentration of salicylic acid (**Figure 4-7C)**. In the presence of 500 μM salicylic acid, FECH overexpression partially reversed the drug induced defects in heme biosynthesis, to an extent similar to that observed with 1 mM salicylic acid (**Figure 4-7C)**. In other words, the observed phenotypes were not clearly dependent on the drug concentration.

A

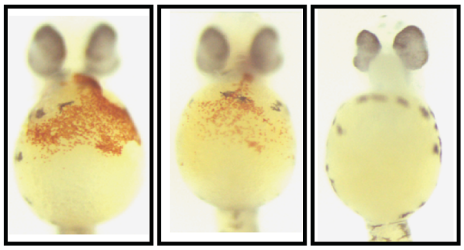

B

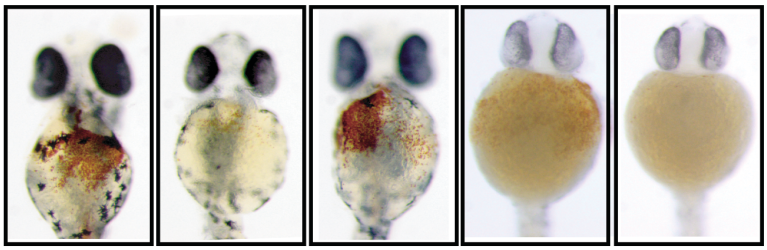

	Control	*zfech* AMO	*zfech* AMO + *zfech* mRNA	1 mM SA	3 mM SA
# of embryos	82	28	20	83	69
Strong	91%	0%	30%	21%	0%
Intermediate	5%	21%	70%	43%	33%
Weak	4%	79%	0%	36%	67%

*** *** *** ***

C

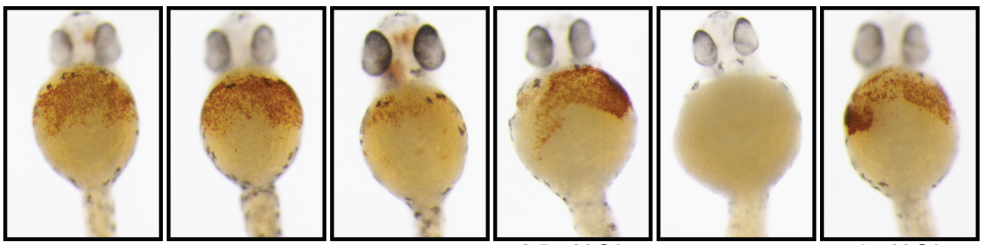

	Control	*zfech* mRNA	0.5 mM SA	0.5 mM SA + *zfech* mRNA	1 mM SA	1 mM SA + *zfech* mRNA
# of embryos	93	32	59	42	82	133
Strong	100%	100%	7%	24%	9%	32%
Intermediate	0%	0%	54%	50%	60%	52%
Weak	0%	0%	39%	26%	31%	16%

* ***

Figure 4-7: Salicylic acid inhibits heme synthesis in zebrafish. (A) Embryos at 48 hpf were stained with *o*-dianisidine and inspected under a microscope. Embryos were sorted into "strong," "intermediate," and "weak" categories, based on staining intensity and the illustrated diagnostic criteria. (B) An AMO against *zFECH* was injected into zebrafish embryos with or without *zFECH* mRNA. Alternatively, embryos were treated with the indicated concentrations of salicylic acid (SA). Shown below the images are the percentages of embryos sorted into "strong", "intermediate," and "weak" categories, and the total

number of embryos examined for each condition. (C) Zebrafish embryos were treated with 0.5 or 1 mM salicylic acid, with or without prior injection of *zFECH* mRNA, and analyzed as in (B). Statistical significance was determined by applying the chi-square contingency test. *p<0.05, ***p<0.0001.

The effect of salicylic acid on heme decrease in K562 cells is consistent with the heme decrease in zebrafish embryos. In accordance with the same data, salicylic acid isomers, *m*-HBA and *p*-HBA, had no significant effect on heme production in zebrafish (**Figure 4-8**). Thus, the results clearly show that salicylic acid specifically inhibits heme biosynthesis by inhibiting FECH activity during zebrafish development.

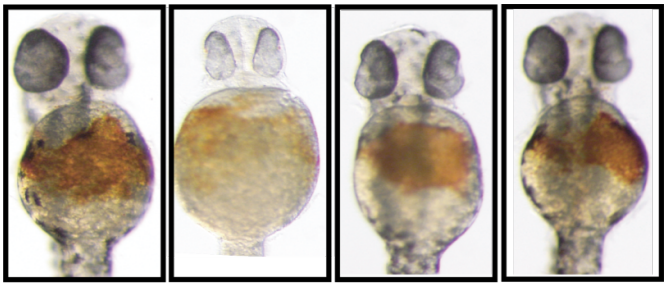

	Control	SA	*m*-HBA	*p*-HBA
# of embryos	18	20	20	25
Strong	100%	5%	95%	92%
Intermediate	0%	20%	5%	8%
Weak	0%	75%	0%	0%

***

Figure 4-8: In contrast to salicylic acid, its isomers *m*-HBA or *p*-HBA could not reduce heme biosynthesis in zebrafish. Zebrafish embryos 1 hpf were treated with 1 mM salicylic acid (SA), *m*-HBA, or p-HBA, respectively, and at 48 hpf the same embryos were stained with *o*-dianisidine and inspected under a microscope. They were then processed as in Figure 4-7B. Statistical significance was determined by applying the chi-square contingency test. *p<0.05, ***p<0.0001.

4.3.6 Salicylic acid causes PpIX accumulation in zebrafish embryos

Protoporphyrin IX is an auto-fluorescent compound, with a $\lambda_{excitation}$ of 387 nm and

$\lambda_{emission}$ of 633 nm that enable the visualization of its intracellular presence by fluorescence microscopy. PpIx is used as a substrate by FECH to produce heme and if the defect in heme synthesis by salicylic acid is indeed due to the inhibition of FECH, its substrate PpIX may be conversely accumulated in affected embryos. Hence, PpIX auto-fluorescence in zebrafish embryos was examined under a fluorescence microscope at an illumination peak of 520-550 nm. As expected, zFECH knockdown embryos showed a substantial accumulation of PpIX in the blood sinus covering the yolk, and this accumulation was reversed by simultaneous overexpression of zFECH (**Figure 4-9**). Similarly, salicylic acid-treated embryos showed a substantial increase in the PpIX level (**Figure 4-9**). Thus, these results indicate that salicylic acid inhibits heme biosynthesis by inhibiting FECH activity during zebrafish development.

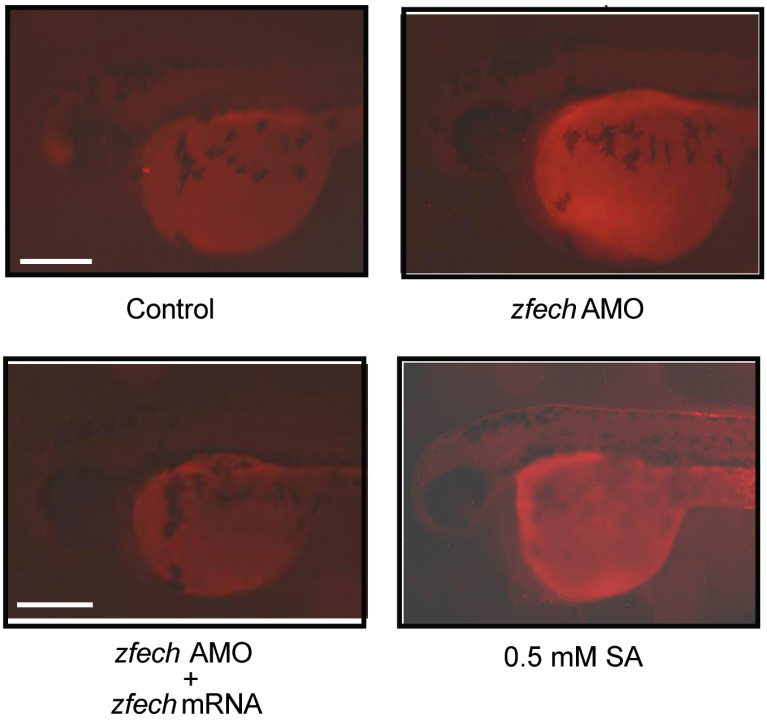

Figure 4-9: Concomitant reduction in heme biosynthesis by salicylic acid stimulates PpIX accumulation in zebrafish. Accumulation of PpIX in living 48-hpf embryos was detected by fluorescence microscopy using its auto-fluorescence with illumination peak at 520-550 nm. Scale bar, 150 μm.

4.4 Conclusions

Here, I showed that salicylic acid inhibits heme synthesis in K562, 293T and zebrafish. Similar effect was seen when FECH gene was knockdown in 293T and zebrafish. At cellular level salicylic acid induced heme decrease was clearly reduced by FECH knockdown in 293T cells. In zebrafish, the salicylic acid-induced decrease in heme content that was rescued by overexpression of FECH mRNA. Biologically germane concentrations of salicylic acid were employed in the cell culture and zebrafish experiments and were sufficient to inhibit heme biosynthesis and mitochondrial function. Moreover, similar differences in salicylic acid, *m*-HBA, and *p*-HBA inhibitory activity were observed *in vitro*, in various cell culture experiments, and in zebrafish. Thus, these results strongly point to the functional connection between salicylic acid and FECH.

Chapter 5. Discussion and perspective

5.1 Discussion

This study identified FECH as a novel salicylic acid-binding protein. Several lines of evidence support the idea that salicylic acid decreases heme biosynthesis by inhibiting FECH: (i) FECH binds to salicylic acid-immobilized beads (**Chapter 2**); (ii) salicylic acid inhibits the enzymatic activity of recombinant FECH in vitro (**Chapter 2**); (iii) salicylic acid binds to FECH at the dimer interface, which is thought to be critical for its activity (**Chapter 3**); (iv) salicylic acid decreases heme content in cultured human cells, and its inhibitory effect is abrogated by the knockdown of FECH (**Chapter 4**); (v) salicylic acid inhibits heme synthesis in zebrafish, which can be partially rescued by the overexpression of zFECH (**Chapter 4**); and (vi) salicylic acid isomers (*m*-HBA and *p*-HBA) are less effective than salicylic acid in all the assays examined (**Chapter 2 and 4**).

5.1.1 How FECH discriminate salicylic acid from its isomers?

Human FECH is an inner mitochondrial, homodimeric protein that faces the matrix side and contains a (2Fe-2S) cluster (Wu et al., 2001). The dimer interface is characterized by an extensive network of hydrogen bonds and hydrophobic interactions (Dailey et al., 2007; Medlock and Swartz et al., 2007; Medlock and Dailey et al., 2007; Medlock et al., 2009; Medlock et al., 2012; Wu et al., 2001). Based on the current structure, salicylic acid fits into the hydrophobic dimer interface channel formed by the pseudo 2-fold symmetry of FECH subunits. Salicylic acid is known to have higher lipid solubility than *m*-HBA and *p*-HBA (Kunze et al.,1972). This occurs

because the negative charge of the carboxylate of salicylic acid is delocalized through intramolecular hydrogen bonding between the carboxyl group and the hydroxyl group. Thus, salicylate may move into the hydrophobic dimer interface of FECH more easily than *meta*- or *para*-hydroxybenzoate. Another possibility may be that the hydrogen bond between the hydroxyl group of salicylic acid and FECH Ser281 contributes to isoform specificity. However, this idea is not consistent with our mutational analysis showing that the hydrogen bond is dispensable for their interaction (**Figure 3-4**). Yet another possibility is that the hydroxyl group of *m*-HBA and *p*-HBA causes steric hindrance with surrounding FECH molecules. However, this possibility was not supported by molecular modeling of *m*-HBA and *p*-HBA complexed with FECH (**Figure 5-1**).

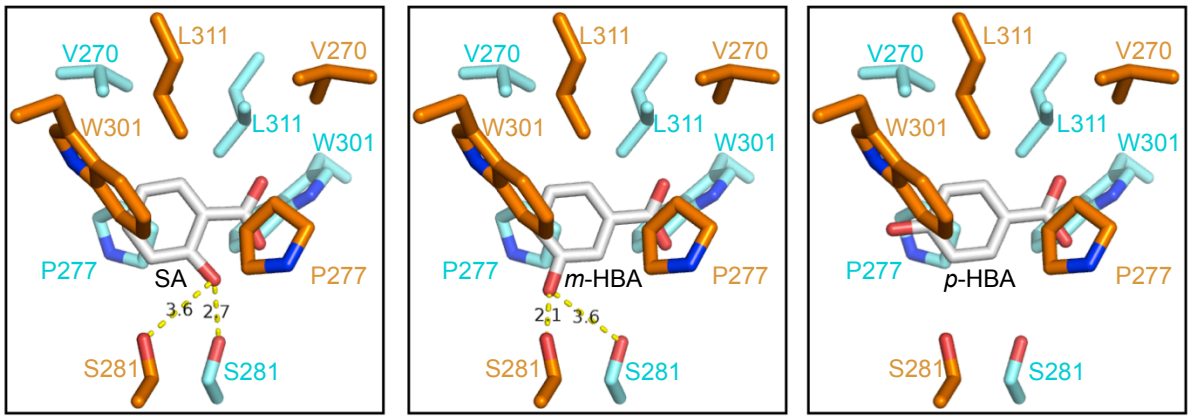

Figure 5-1: Molecular modeling of possible conformations of *meta*-hydroxybenzoic acid (*m*-HBA) and *para*-hydroxybenzoic acid (*p*-HBA) in salicylic acid (SA) binding site. Amino acids, present in salicylic acid binding site. are coloured in cyan (chain B) and orange (chain A), respectively, while salicylic acid, *m*-HBA and *p*-HBA are colored by elements.

5.1.2 How salicylic acid inhibits FECH activity?

Salicylic acid-binding site of FECH is located at a distance from its active site and is

instead found at the dimer interface (Figure 2A), which is believed to be critical to the enzymatic activity of FECH (Wu et al., 2001; Medlock and Swartz et al., 2007; Najahi-Missaoui and Dailey, 2005). This raises the possibility that salicylic acid affects the dimerization status of FECH, possibly causing (i) the dissociation of the dimer or (ii) a conformational change. Both of these possibilities are supported by the fact that salicylic acid caused a shift in the FECH peak on a gel filtration column (**Figure 3-8**). Because the shift was not as large as that caused by the V270A, W301A, or L311A point mutation (**Figure 3-8A and Figure 3-5**), salicylic acid may only cause a conformational change in the dimer rather than its complete dissociation. Salicylic acid is an organic acid with a pKa value of 3.0 and a hydrophobic benzene ring constituent. As mentioned earlier, salicylic acid may easily slip into the hydrophobic dimer interface of FECH. Because the salicylic acid-binding site of FECH is highly hydrophobic and contains no charged amino acids, it is reasonable to hypothesize that the negative charge on salicylic acid may have a destabilizing effect on the FECH dimer. Regardless, our findings suggest that salicylic acid binding to the dimer interface results in the allosteric inhibition of FECH.

The potential mechanism of action of salicylic acid discussed above apparently contradicts the co-crystal structure (**Figures 3-2 and Figure 3-3**), which shows that salicylic acid binds to the FECH dimer with no appreciable conformational change. Because dimer integrity is critical for the stability of FECH in solution (Najahi-Missaoui and Dailey, 2005), any change in FECH conformation by salicylic acid might lead to the protein precipitation while crystallization and, therefore, complex with structural changes may not have lent itself to crystallization. Eventually, the crystals obtained represent only an initial binding state of FECH•salicylic acid complex.

Based on my current co-crystal structure, one salicylic acid molecule

apparently binds to the dimer interface. By contrast, the findings from the experiments with monomeric FECH (bacterial FECH and a human FECH mutant, V270A) suggest that two salicylic acid molecules may bind to each of the two FECH protomers. We speculate that, after the salicylic acid-induced dissociation of the FECH dimer or the generation of conformational changes in the enzyme, salicylic acid may remain bound to one of the protomers and thereby continue to inhibit FECH function. It is possible that another salicylic acid molecule enters the dimer interface, binds to the other protomer, and stabilizes the new conformation (**Figure 5-2**).

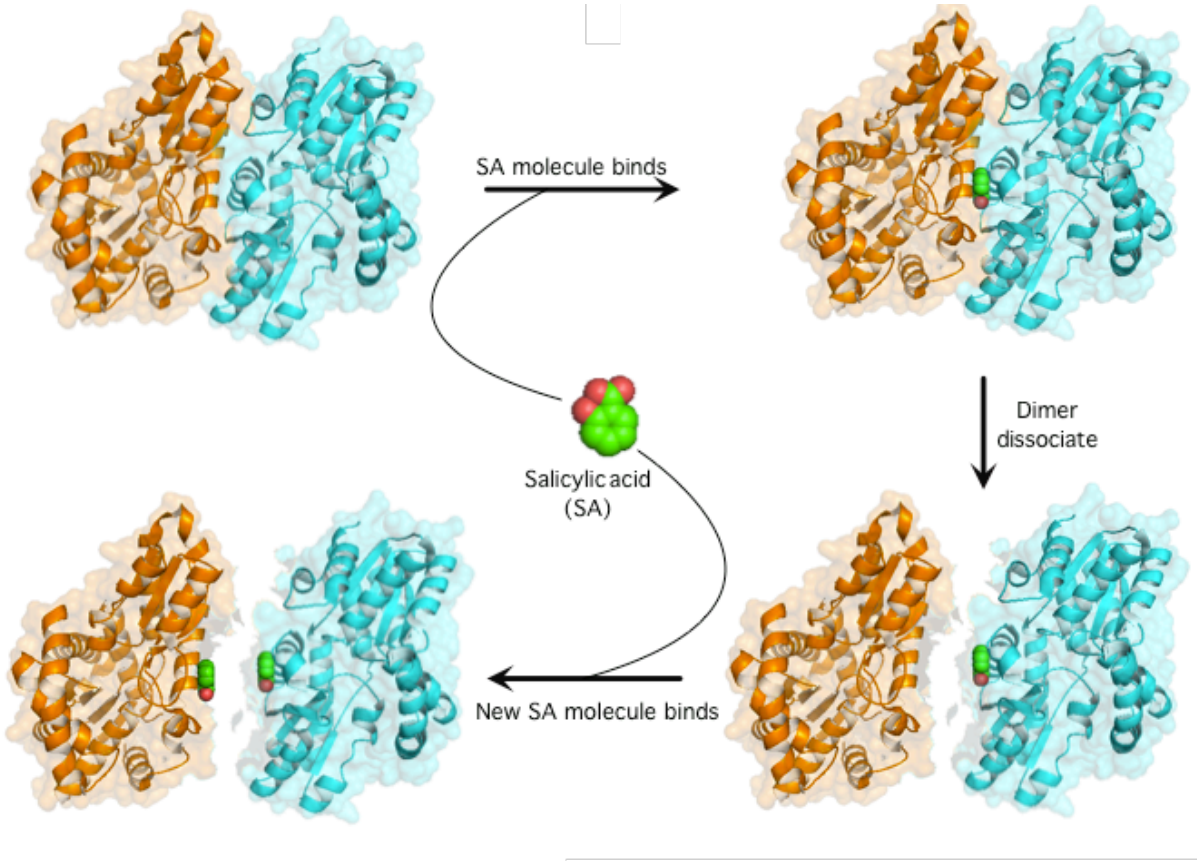

Figure 5-2: A possible mechanism of salicylic acid inhibition of FECH activity. (1) Salicylic acid binds to the FECH dimer at its dimer interface. (2) Negative charge on salicylate destabilizes the FECH dimer interface. This causes conformational changes in the FECH dimer and eventually results in its disruption. (3) During this process, another salicylic acid molecule may be

incorporated into the dimer so that salicylic acid binds to each protomer.

Another possible mechanism of salicylic acid action is that the drug inhibits the dynamic structural changes previously shown to play an important role in the catalytic cycle of FECH (Dailey et al., 2007; Medlock and Swartz et al., 2007; Medlock and Dailey et al., 2007; Medlock et al., 2009; Medlock et al., 2012; Najahi-Missaoui and Dailey, 2005). More specifically, PpIX binding to the active site results in substantial conformational changes, including those of the "lips" (upper and lower), which together serve as the substrate entry site (Medlock and Swartz et al., 2007; Wu et al., 2001) (**Figure 5-3**). The salicylic acid-binding site identified in this study is part of the mobile lower lip, although our structural data suggest that salicylic acid does not physically prevent the entry of the substrate (**Figure 5-3**). Because a single molecule of salicylic acid binds to the dimer interface and simultaneously interacts with two FECH molecules through Pro277, Trp301, and Leu311, the drug may inhibit conformational changes associated with the catalytic cycle by preventing the flexible movement of the dimer (**Figure 5-3**). No matter what the mechanism involved, our findings suggest that salicylic acid binds to the dimer interface of FECH, thereby inhibiting its activity in an allosteric manner either by causing the dissociation of the dimer or by affecting its conformational changes.

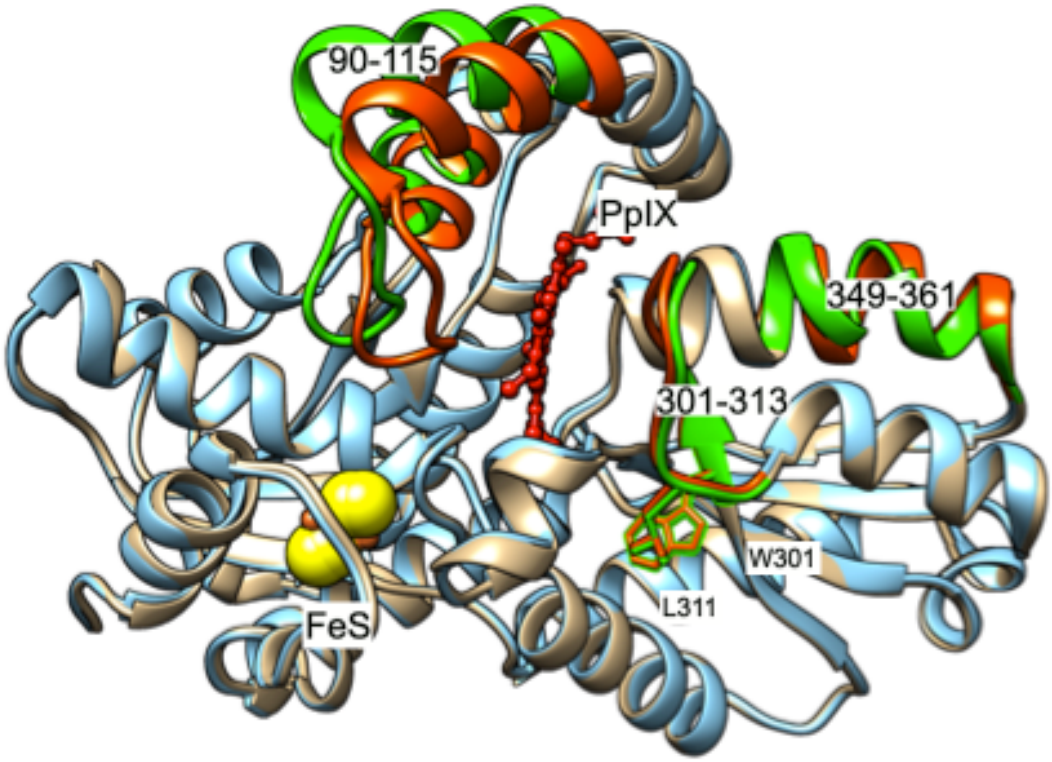

Figure 5-3: Structural alignment of the Protoporphyrin IX (PpIX)-bound (PDB: 2QD1) and substrate-free (PDB: 2HRC) forms of human ferrochelatase. Regions of significant movement in the substrate-bound form have been highlighted in red while substrate-free form have been highlighted in green for clarity and includes residues 90–115, 301–313, and 349–361. The [2Fe-2S] cluster is shown in yellow and PpIX is shown in red. Regions 90–115 and 301–313 form the "upper" and "lower" lip of FECH active site. Also shown are amino acids W301 and L311, which are important for salicylic acid interaction.

5.1.3 FECH mediates salicylic acid-induced mitochondrial dysfunction

Salicylic acid affects heme content, NAD(P)H content, and mitochondrial membrane potential at millimolar concentrations in K562 cells. Concordantly, previous studies showed that salicylic acid inhibited oxidative phosphorylation and decreased the ATP:AMP ratio at similar concentrations (Cronstein et al., 1999). These consequences are likely to result from the inhibition of FECH, because the down-regulation of FECH results in a reduction of heme content and a concomitant

reduction in the activity of heme proteins such as cytochromes, which are essential for the electron transport system, the generation of membrane potential, and ATP synthesis (Atamna et al., 2001; Atamna et al., 2002; Gatta et al., 2009; Möbius et al., 2010). It is also possible that other known targets of salicylic acid (*e.g.*, COX, AMPK, and IKK-β) are involved in mitochondrial dysfunction (**Figure 5-4**). In regard to COX, salicylic acid has little, if any, effect on the enzymatic activity of purified COX (Mitchell et al., 1993). Thus, it seems unlikely that COX plays a role in salicylic acid-induced mitochondrial dysfunction. On the other hand, salicylic acid activates AMPK, an essential regulator of energy metabolic homeostasis, thereby increasing mitochondrial ATP production (Hawley et al., 2012) (**Figure 5-4**). However, because salicylic acid conversely inhibits ATP synthesis by uncoupling mitochondrial respiration, the AMPK pathway is unlikely to be involved in salicylic acid-induced mitochondrial injury (**Figure 5-4**). Salicylic acid also inhibits the protein kinase activity of IKK-β and attenuates inflammatory and immune responses involving NF-κB (Kopp and Ghosh, 1994; Yin et al., 1998). NF-κB is a crucial regulator of cellular energy metabolism (Mauro et al., 2011), and therefore its inhibition by salicylic acid may affect mitochondrial energy metabolism (**Figure 5-4**). Hence, the mitochondrial dysfunction induced by salicylic acid may be due to a combination of inhibitory actions on FECH and the NF-κB pathway.

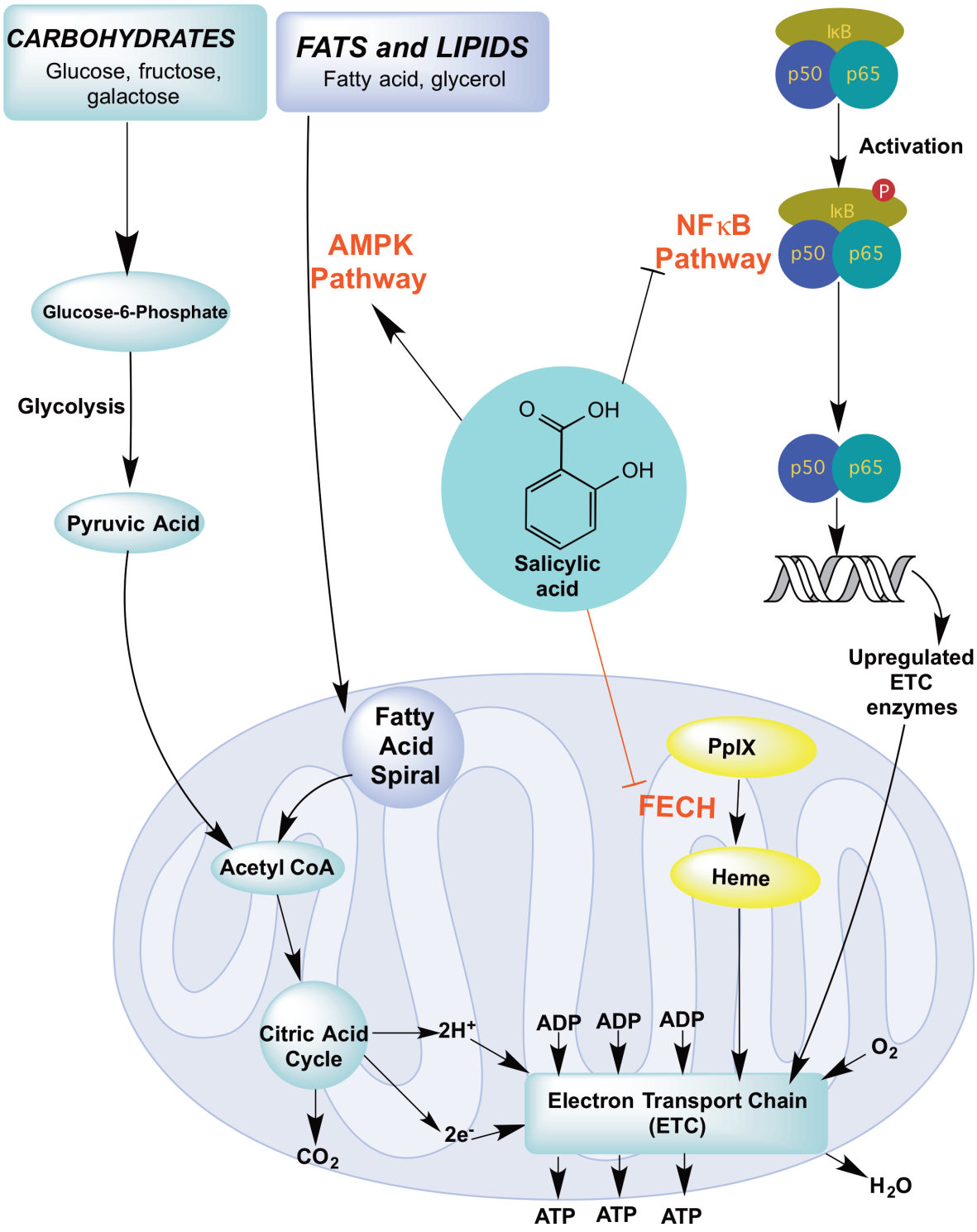

Figure 5-4: FECH mediates salicylic acid-induced mitochondrial injury. Inhibition of FECH by salicylic acid results in a reduction of heme content and a concomitant reduction in the activity of heme proteins such as cytochromes, which are essential for the electron transport system (ETC). Inhibition of NFκB pathway by salicylic acid can also induce the mitochondrial injury by blocking the expression of enzymes such as cytochrome c oxidase 2 (SCO2; Mauro et

al., 2011). But contrary to this, salicylic acid activates AMPK increasing fatty acid oxidation and energy production.

5.1.4 Possible relevance to the anti-inflammatory function of salicylic acid

Although highly speculative, the present findings may have relevance to the anti-inflammatory actions of salicylic acid. Aspirin (acetyl salicylic acid) inhibits COX by transferring its acetyl group to the active site of prostaglandin synthase (Loll et al., 1995). Despite the absence of the acetyl group and no significant effect on purified COX, salicylic acid has similar anti-inflammatory effects *in vivo* and can inhibit COX activity in cell-based assays (Mitchell et al., 1993). A few explanations have been proposed as to how salicylic acid might mitigate inflammation. For example, salicylic acid might inhibit the NF-κB pathway, which controls the expression of the COX-2 gene (Lim et al., 2001). Because heme is the prosthetic group of COX (Chen et al., 1989), our findings suggest that salicylic acid may also inhibit prostaglandin synthesis by blocking FECH activity and heme synthesis (**Figure 5-5**). Another possible explanation for the anti-inflammatory actions of salicylic acid is that it induces the release of cellular adenosine, an endogenous anti-inflammatory agent that acts on adenosine A2 receptors (Cronstein, 1994). A previous study showed that salicylic acid attenuates inflammation by an adenosine-dependent mechanism, even in mice lacking COX-2 or the p105 subunit of NF-κB (Cronstein et al., 1999), leading to the idea that there may be an additional target of salicylic acid. This target may be FECH, given that the inhibition of heme synthesis and the resultant inhibition of ATP synthesis might trigger the accumulation of adenosine and its release.

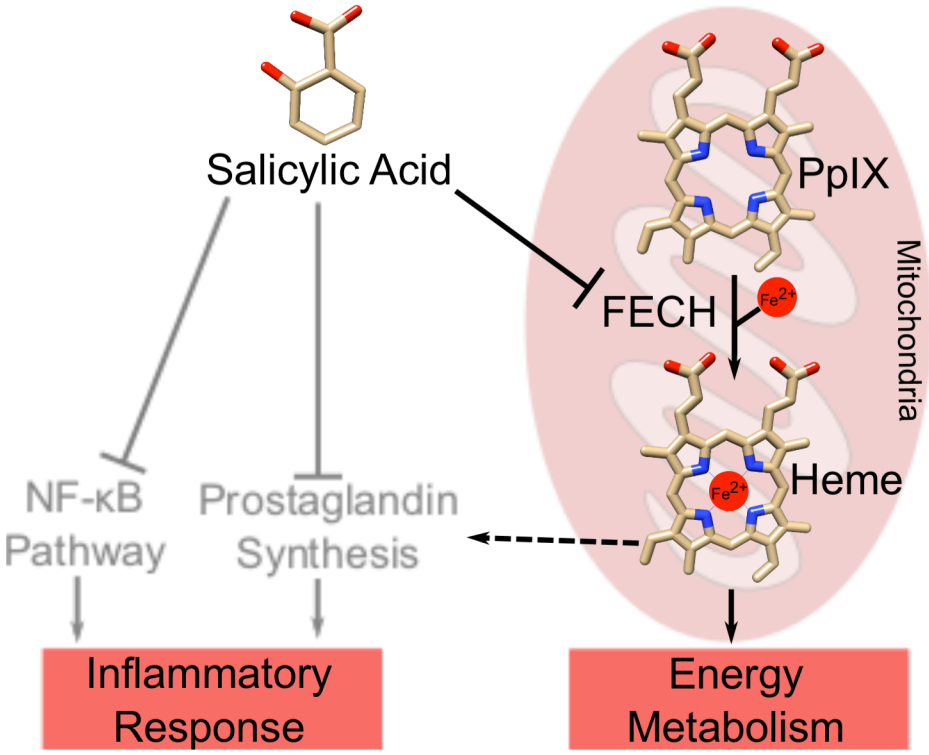

Figure 5-5: A hypothesis of how salicylic acid inhibits cyclooxygenase (COX) prostaglandin synthesis activity in intact cells. Heme is a prosthetic group of COX and is important for its activity. Thus, salicylic acid-induced heme decrease in cells indirectly inhibits COX activity.

5.2 Perspectives

In this study, we showed that FECH, a terminal enzyme in the heme biosynthesis pathway, is a new molecular target of salicylic acid that mediates its anti-mitochondrial activity. Given that heme serves as a prosthetic group of many hemoproteins, such as cytochromes in the electron transport chain and COXs in the prostaglandin synthesis pathway, a reduction of heme biosynthesis by salicylic acid may contribute to the other pharmacological effects of the drug. Although evidence was presented that salicylic acid inhibits FECH activity and mitochondria function, there is need for mitochondrial specific study designs. In addition, experiments should be designed to evaluate the potential impact of salicylic acid-mediated inhibition of mitochondrial ATP synthesis resulting in the release of adenosine, an endogenous anti-inflammatory agent, which may be partially responsible for its anti-inflammatory activity. Clearly, further investigation is required to determine the possible role of FECH in the many pharmacological actions of salicylic acid.

References

Afonine, P.V., Grosse-Kunstleve, R.W., Echols, N., Headd, J.J., Moriarty, N.W., Mustyakimov, M., Terwilliger, T.C., Urzhumtsev, A., Zwart, P.H., Adams, P.D. (2012). Towards automated crystallographic structure refinement with phenix.refine. Acta Crystallogr. D Biol. Crystallogr. 68, 352-367.

Al-Karadaghi, S., Hansson, M., Nikonov, S., Jonsson, B., and Hederstedt, L. (1997). Crystal structure of ferrochelatase: the terminal enzyme in heme biosynthesis. Structure 5, 1501-1510.

Amann, R., Peskar, B.A. (2002). Anti-inflammatory effects of aspirin and sodium salicylate. Eur J Pharmacol. 28, 1-9.

Andersson, L.C., Nilsson, K., Gahmberg, C.G. (1979). K562-a human erythroleukemic cell line. Int J Cancer 23, 143-7.

Antonicka, H., Mattman, A., Carlson, C.G., Glerum, D.M., Hoffbuhr, K.C., Leary, S.C., Kennaway, N.G., Shoubridge, E.A. (2003). Mutations in COX15 produce a defect in the mitochondrial heme biosynthetic pathway, causing early-onset fatal hypertrophic cardiomyopathy. Am. J. Hum. Genet. 72, 101-114.

Atamna, H., Killilea, D.W., Killilea, A.N. & Ames, B.N. (2002). Heme deficiency may be a factor in the mitochondrial and neuronal decay of aging. Proc. Natl. Acad. Sci. USA 99, 14807-14812.

Atamna, H., Liu, J. & Ames, B.N. (2001). Heme deficiency selectively interrupts assembly of mitochondrial complex IV in human fibroblasts: revelance to aging. J. Biol. Chem. 276, 48410-48416.

Baggott, J.E., Morgan, S.L., Ha, T., Vaughn, W.H. & Hine, R.J. (1992). Inhibition of

folate-dependent enzymes by non-steroidal anti-inflammatory drugs. Biochem. J. 282, 197-202.

Beinke, S., Robinson, M.J., Hugunin, M., Ley, S.C. (2004). Lipopolysaccharide activation of the TPL-2/MEK/extracellular signal-regulated kinase mitogen-activated protein kinase cascade is regulated by IkappaB kinase-induced proteolysis of NF-kappaB1 p105. Mol Cell Biol 24, 9658-9667.

Bellosillo, B., Piqué, M., Barragán, M., Castaño, E., Villamor, N., Colomer, D., Montserrat, E., Pons, G., Gil, J. (1998). Aspirin and salicylate induce apoptosis and activation of caspases in B-cell chronic lymphocytic leukemia cells. Blood. 92, 1406-1414

Berridge, M.V., Herst, P.M. & Tan, A.S. (2005). Tetrazolium dyes as tools in cell biology: new insights into their cellular reduction. Biotechnol. Annu. Rev. 11, 127-152.

Braun, F.K., Al-Yacoub, N., Plötz, M., Möbs, M., Sterry, W., Eberle, J. (2012). Nonsteroidal anti-inflammatory drugs induce apoptosis in cutaneous t-cell lymphoma cells and enhance their sensitivity for TNF-related apoptosis-inducing ligand. J. Invest. Dermatol. 132, 429-439.

Burden, A.E., Wu, C., Dailey, T.A., Busch, J.L., Dhawan, I.K., Rose, J.P., Wang, B., Dailey, H.A. (1999). Human ferrochelatase: crystallization, characterization of the (2Fe-2S) cluster and determination that the enzyme is a homodimer. Biochim. Biophys. Acta 1435, 191-197.

Chen, Y.N. & Marnett, L.J. (1989). Heme prosthetic group required for acetylation of prostaglandin H synthase by aspirin. FASEB J. 3, 2294-2297.

Childs, S., Weinstein, B.M., Mohideen, M.A., Donohue, S., Bonkovsky, H., Fishman M.C. (2000). Zebrafish dracula encodes ferrochelatase and its mutation provides a model for erythropoietic protoporphyria. Curr Biol 10, 1001-4.

Collaborative Computational Project, Number 4. (1994). The CCP4 suite: programs for protein crystallography. Acta Crystallogr. D Biol. Crystallogr. 50, 760-763.

Cronstein, B.N. (1994). Adenosine, an endogenous anti-inflammatory agent. J. Appl. Physiol. 76, 5-13.

Cronstein, B.N., Montesinos, M.C. & Weissmann, G. (1999). Salicylates and sulfasalazine, but not glucocorticoids, inhibit leukocyte accumulation by an adenosine-dependent mechanism that is independent of inhibition of prostaglandin synthesis and p105 of NFkappaB. Proc. Natl. Acad. Sci. USA 96, 6377-6381.

Dailey, H.A. (1988) Metal Inhibition of Ferrochelatase. Ann. NY Acad. Sci. 514:81-86.

Dailey, H.A., Wu, C.K., Horanyi, P., Medlock, A.E., Najahi-Missaoui, W., Burden, A.E., Dailey, T.A., Rose, J. (2007). Altered orientation of active site residues in variants of human ferrochelatase. Evidence for a hydrogen bond network involved in catalysis. Biochemistry 46, 7973-7979.

Doi, H. & Horie, T. (2010). Salicylic acid-induced hepatotoxicity triggered by oxidative stress. Chem. Biol. Interact. 183, 363-368.

Durner, J., Shah, J. & Klessig, D.F. (1997). Salicylic acid and disease resistance in plants. Trends. Plant. Sci. 2, 266-274.

Elder, D.J.E., Hague, A., Hicks, D.J., Paraskeva, C. (1996). Differential growth inhibition by the aspirin metabolite salicylate in human colorectal tumor cell lines: enhanced apoptosis in carcinoma and In vitro-transformed adenoma relative to adenoma cell lines. Cancer Research. 56, 2273-2276.

Emsley, P. & Cowtan, K. (2004). Coot: model-building tools for molecular graphics. Acta Crystallogr. D Biol. Crystallogr. 60, 2126-2132.

Gatta, L.B., Vitali, M., Verardi, R., Arosio, P. & Finazzi, D. (2009). Inhibition of heme

synthesis alters amyloid precursor protein processing. J. Neural. Transm. 116, 79-88.

Gora, M., Grzybowska, E., Rytka, J., Labbe-Bois, R. (1996). Probing the active-site residues in Saccharomyces cerevisiae ferrochelatase by directed mutagenesis. In vivo and in vitro analyses. J Biol Chem. 271, 11810-6.

Grosser, T., Emer, S., Garret, A.F.D. (2009). Anti-Inflammatory, Antipyretic, and Analgesic Agents; Pharmacotherapy of Gout. In The Pharmacological Basis of Therapeutics, L.L. Brunton, B.A. Chabner, B.C. Knollmann ed. (Goodman & Gilman's), pp. 959-1004.

Hardie, D.G., Ross, F.A., Hawley, S.A. (2012) AMP-activated protein kinase: a target for drugs both ancient and modern. Chem. Biol. 19, 1222–1236

Hawley, S.A., Fullerton, M.D., Ross, F.A., Schertzer, J.D., Chevtzoff, C., Walker, K.J., Peggie, M.W., Zibrova, D., Green, K.A., Mustard, K.J., Kemp, B.E., Sakamoto, K., Steinberg, G.R., Hardie, D.G. (2012). The ancient drug salicylate directly activates AMP-activated protein kinase. Science 336, 918-922.

Higgs, G.A., Salmon, J.A., Henderson, B., Vane, J.R., (1987). Pharmacokinetics of aspirin and salicylate in relation to inhibition of arachidonate cyclooxygenase and antiinflammatory activity. Proc. Natl. Acad. Sci. U.S.A. 84, 1417 – 1420.

Howe, K., Clark, M.D., Torroja, C.F., Torrance, J., Berthelot, C. et al. (2013). The zebrafish reference genome sequence and its relationship to the human genome. Nature 496, 498-503.

Huang, M., Camara, A.K., Stowe, D.F., Qi, F., Beard, D.A. (2007) Mitochondrial inner membrane electrophysiology assessed by rhodamine-123 transport and fluorescence. Ann Biomed Eng 35, 1276-1285.

Hunter, G.A., Sampson, M.P., Ferreira, G.C. (2008). Metal ion substrate inhibition of ferrochelatase. J Biol Chem 283, 23685-91

Ito, T., Ando, H., Suzuki, T., Ogura, T., Hotta, K., Imamura, Y., Yamaguchi, Y., Handa, H. (2010). Identification of a primary target of thalidomide teratogenicity. Science 327, 1345-1350.

Karlberg, T., Lecerof, D., Gora, M., Silvegren, G., Labbe-Bois, R., Hansson, M., and AlKaradaghi, S. (2002). Metal binding to Saccharomyces cerevisiae ferrochelatase. Biochemistry 41, 13499-13506.

Klampfer, L., Cammenga, J., Wisniewski, H.G. & Nimer, S.D. (1999). Sodium salicylate activates caspases and induces apoptosis of myeloid leukemia cell lines. Blood 93, 2386-2394.

Klein, E., Ben-Bassat, H., Neumann, H., Ralph, P., Zeuthen, J., Polliack, A., Vánky, F. (1976). Properties of the K562 cell line, derived from a patient with chronic myeloid leukemia. Int J Cancer 18, 421-31.

Kopp, E., Ghosh, S. (1994). Inhibition of NF-kappa B by sodium salicylate and aspirin. Science 265, 956-959.

Langenbach, R., Loftin, C.D., Lee, C. & Tiano, H. (1999). Cyclooxygenase-deficient mice. A summary of their characteristics and susceptibilities to inflammation and carcinogenesis. Ann. N. Y. Acad. Sci. 889, 52-61.

Li, F.M., Lim, C.K. & Peters, T.J. (1987). An HPLC assay for rat liver ferrochelatase activity. Biomed. Chromatogr. 2, 164-168.

Lim, J.W., Kim, H. & Kim, K.H. (2001). Nuclear factor-kappaB regulates cyclooxygenase-2 expression and cell proliferation in human gastric cancer cells. Lab. Invest. 81, 349-360.

Loll, P.J., Picot, D., Garavito, R.M. (1995). The structural basis of aspirin activity inferred from the crystal structure of inactivated prostaglandin H2 synthase. Nat.

Struct. Biol. 2, 637-643.

Mauro, C., Leow, S.C., Anso, E., Rocha, S., Thotakura, A.K., Tornatore, L., Moretti, M., De Smaele, E., Beg, A.A., Tergaonkar, V., Chandel, N.S., Franzoso, G. (2011). NF-kB controls energy homeostasis and metabolic adaptation by upregulating mitochondrial respiration. Nat. Cell. Biol. 13, 1272-1279.

Medlock, A., Swartz, L., Dailey, T.A., Dailey, H.A. & Lanzilotta, W.N. (2007). Substrate interactions with human ferrochelatase. Proc. Natl. Acad. Sci. USA 104, 1789-1793.

Medlock, A.E., Carter, M., Dailey, T.A., Dailey, H.A. & Lanzilotta, W.N. (2009). Product release rather than chelation determines metal specificity for ferrochelatase. J. Mol. Biol. 393, 308-319.

Medlock, A.E., Dailey, T.A., Ross, T.A., Dailey, H.A. & Lanzilotta, W.N. (2007). A pi-helix switch selective for porphyrin deprotonation and product release in human ferrochelatase. J. Mol. Biol. 373, 1006-1016.

Medlock, A.E., Najahi-Missaoui, W., Ross, T.A., Dailey, T.A., Burch, J., O'Brien, J.R., Lanzilotta, W.N., Dailey, H.A. (2012). Identification and characterization of solvent-filled channels in human ferrochelatase. Biochemistry 51, 5422-5433.

Mitchell, J.A., Akarasereenont, P., Thiemermann, C., Flower, R.J. & Vane, J.R. (1993). Selectivity of nonsteroidal anti-inflammatory drugs as inhibitors of constitutive and inducible cyclooxygenase. Proc. Natl. Acad. Sci. USA 90, 11693-11697.

Möbius, K., Arias-Cartin, R., Breckau, D., Hännig, A.L., Riedmann, K., Biedendieck, R., Schröder, S., Becher, D., Magalon, A., Moser, J., Jahn, M., Jahn, D. (2010). Heme biosynthesis is coupled to electron transport chains for energy generation. Proc. Natl. Acad. Sci. USA 107, 10436-10441.

Morrison, K.L., Weiss, G.A. (2006). The origins of chemical biology. Nat Chem Biol. 2,

3-6.

Najahi-Missaoui, W. & Dailey, H.A. (2005). Production and characterization of erythropoietic protoporphyric heterodimeric ferrochelatases. Blood 106, 1098-1104.

Needs, C.J. & Brooks, P.M. (1985). Clinical Pharmacokinetics of the salicylate. Clin. Pharmacokinet. 10, 64-177.

Nicolaou, K.C., Montagnon, T. (2008). Aspirin. In Molecules That Changed the World (WILEY-VCH, Weinheim), pp. 21-28.

Otwinowski, Z., Minor, W. (1997). Processing of x-ray diffraction data collected in oscillation mode. Methods Enzymol. 276, 307-326.

Piqué, M., Barragán, M., Dalmau, M., Bellosillo, B., Pons, G., Gil, J. (2000). Aspirin induces apoptosis through mitochondrial cytochrome c release. The Federation of European Biochemical Societies (FEBS) Letters. 480, 193-196.

Ransom, D.G., Haffter, P., Odenthal, J., Brownlie, A., Vogelsang, E., Kelsh, R.N., Brand, M., van Eeden, F.J., Furutani-Seiki, M., Granato, M., Hammerschmidt, M., Heisenberg, C.P., Jiang, Y.J., Kane, D.A., Mullins, M.C., Nüsslein-Volhard, C. (1996). Characterization of zebrafish mutants with defects in embryonic hematopoiesis. Development 123, 311-319.

Rothwell, P.M., Fowkes, F.G., Belch, J.F., Ogawa, H., Warlow, C.P., Meade, T.W. (2011). Effect of daily aspirin on long-term risk of death due to cancer: analysis of individual patient data from randomised trials. Lancet 377, 31-41.

Sakamoto, S., Kabe, Y., Hatakeyama, M., Yamaguchi, Y. & Handa, H. (2009). Development and application of high-performance affinity beads: toward chemical biology and drug discovery. Chem. Rec. 9, 66-85.

Shi, Z., Ferreira, G.C. (2004). Probing the active site loop motif of murine

ferrochelatase by random mutagenesis. J Biol Chem. 279, 19977-86.

Shimizu, N., Sugimoto, K., Tang, J., Nishi, T., Sato, I., Hiramoto, M., Aizawa, S., Hatakeyama, M., Ohba, R., Hatori, H., Yoshikawa, T., Suzuki, F., Oomori, A., Tanaka, H., Kawaguchi, H., Watanabe, H., Handa, H. (2000). High-performance affinity beads for identifying drug receptors. Nat. Biotechnol. 18, 877-881.

Skulachev, V.P. (2001). Mitochondrial filaments and clusters as intracellular power-transmitting cables. Trends Biochem Sci. 26:23-29.

Steinberg, G.R., Dandapani, M., Hardie, D.G. (2013). AMPK: mediating the metabolic effects of salicylate-based drugs ? Trends Endocrinol Metab. S1043-2760, 00104-5

Steinberg, G.R. and Kemp, B.E. (2009) AMPK in health and disease. Physiol. Rev. 89, 1025–1078

Steiner, R.A., Lebedev, A.A. & Murshudov, G.N. (2003). Fisher's information in maximum-likelihood crystallographic refinement. Acta Crystallogr. D Biol. Crystallogr. 59, 2114-2124.

Taketani, S., Adachi, Y., Nakahashi, Y. (2000). Regulation of the expression of human ferrochelatase by intracellular iron levels. Eur J Biochem. 267, 4685-4692.

Uga, H., Kuramori, C., Ohta, A., Tsuboi, Y., Tanaka, H., Hatakeyama, M., Yamaguchi, Y., Takahashi, T., Kizaki, M., Handa, H. (2006). A new mechanism of methotrexate action revealed by target screening with affinity beads. Mol. Pharmacol. 70, 1832-1839.

Vane, J.R. & Botting, R.M. (2003). The mechanism of action of aspirin. Thromb. Res. 110, 255-258.

Vane, J.R. (1971). Inhibition of prostaglandin synthesis as a mechanism of action for aspirin-like drugs. Nat. New. Biol. 231, 232-235.

Wagener, F.A., Volk, H.D., Willis, D., Abraham, N.G., Soares, M.P., Adema, G.J., Figdor, C.G. (2003). Different faces of the heme-heme oxygenase system in inflammation. Pharmacol Rev 55, 551-71.

Wu, C.K., Dailey, H.A., Rose, J.P., Burden, A., Sellers, V.M., Wang, B.C. (2001). The 2.0 Å structure of human ferrochelatase, the terminal enzyme of heme biosynthesis. Nat. Struct. Biol. 8, 156-160.

Yin, M.J., Yamamoto, Y. & Gaynor, R.B. (1998). The anti-inflammatory agents aspirin and salicylate inhibit the activity of I(kappa)B kinase-beta. Nature 396, 77-80.

You, K. (1983). Salicylate and mitochondrial injury in reye's syndrome. Science 221, 163-165.

Zimmermann, K.C., Waterhouse, N.J., Goldstein, J.C., Schuler, M., Green, D.R. (2000). Aspirin induces apoptosis through release of cytochrome c from mitochondria. Neoplasia. 2, 505–513

Publications/Presentations

Peer reviewed

Vipul Gupta, Shujie Liu, Hideki Ando, Ryohei Ishii, Shumpei Tateno, Yuki Kaneko, Masato Yugami, Satoshi Sakamoto, Yuki Yamaguchi, Osamu Nureki and Hiroshi Handa (2013). Salicylic acid induces mitochondrial injury by inhibiting ferrochelatase heme biosynthesis activity. Mol Pharmacol. [Epub ahead of print]

Shanthy Sundaram, Ashutosh Tripathi, **Vipul Gupta** (2010). Structure prediction and molecular simulation of gases diffusion pathways in hydrogenase. Bioinformation 5(4): 177-183.

Presentations (Oral/Poster)

Vipul Gupta, Shujie Liu, Yuki Yamaguchi and Hiroshi Handa, Identification of novel protein target of salicylic acid, International Symposium, Centre of Biotechnology, University of Allahabad, India, 2013; Oral.

Vipul Gupta, Shujie Liu and Hiroshi Handa, Development of high affinity purification nanobeads and their application in screening of paclitaxel, docetaxel and salicylic acid binding proteins, International Symposium-cum-training Workshop on "Recent trends in Bioinformatics, Systems Biology and Biomolecular Interactions", University of Allahabad, India, 2012; Oral.

Shujie Liu, **Vipul Gupta**, Hideki Ando, Yasuaki Kabe, Yuki Yamaguchi and Hiroshi Handa, Identification of a novel molecular target for salicylic acid, 第 34 回日本分子生物学会 横浜 2011 年 12 月;Poster.

Vipul Gupta, Shujie Liu and Hiroshi Handa, Development of high affinity purification nanobeads and their application in screening of paclitaxel, docetaxel and salicylic acid binding proteins, Molecular Biology Institute Research Conference, University of California Los Angeles, USA , 2011; Poster.

Vipul Gupta and Hiroshi Handa, Development of high affinity purification nanobeads and their application in screening of paclitaxel and docetaxel binding proteins, Bio-GCOE Summer School & International Conference, Kyoto University, 2011; Poster.

Vipul Gupta and Hiroshi Handa, *In silico* and *in vitro* approach to protein-drug interaction, GCOE Summer School "Evolving Education and Research Center for Spatio-Temporal Biological Network", Hayama, Shonan Village, Kanagawa, 2009; Poster.

Acknowledgement

It would not have been possible to conclude my doctoral thesis without acknowledging people whom I can only offer my words of appreciation.

First and foremost, I would like to express my deep gratitude to my supervisors Professor Hiroshi Handa and Professor Yuki Yamaguchi who with their help, support and great patience, guided me throughout my graduate studies. I will also like to convey my best regards to Dr. Hideki Ando for his guidance on zebrafish experiments. My sincere thanks to Dr. Satoshi Sakamoto and Dr. Takumi Ito for their insightful suggestions and advises. I will also like to thank Shujie Liu for her assistance with the experiments.

A PhD is always a pleasant experience when you have financial backing, for which I would like to acknowledge the Grants-in-aid for Scientific Research from the Ministry of Education, Culture, Sports, Science and Technology of Japan and Tokyo Institute of Technology for their financial support.

I would like to take this opportunity to convey my heartiest appreciations to my collaborators, Dr. Osamu Nureki and Dr. Ryohei Ishii (University of Tokyo) for their frequent feedbacks, successful experiments and providing me an opportunity to learn the impressive techniques of X-ray crystallography. My generous appreciation to Dr. Atsushi Kawakami for providing zebrafish embryos when they were needed the most. I will also like to thank Dr. Shun-ichiro Ogura for his support with fluorescence HPLC. I also thank the Material Analysis Suzukake-dai Center (Technical Department, Tokyo Institute of Technology) for technical support in heme analysis.

Life is never easy when you don’t have someone to share your worries especially as a foreigner, for which I think that I was lucky to have great friends who always helped and motivated me throughout my stay for which my special thanks go to Dr. Satoki Karasawa, Yuka Nishio, Shintaro Kawata, Dr. Ayumi Kawano, Dr. Mathew Kallumadil, Shujie Liu, Junko Kato, Alba and all the present and previous Handa-Yamaguchi lab members. I will also like to thank lab secretaries Ando san, Ishikawa san, Niji san and Kuroda san (not a secretary but still helped me with official work), for making the official work easier for me.

Apart from my nice lab mates, I was also gifted with some very nice friends outside the lab. A special thanks to Yasmine Assal for making me believe, during the lunch breaks, that I have a scientific mind. Yasmine, you are a true friend, a nice human and above all a person to rely on. Will miss you a lot. Thanks to Ashish Lahoti, Shruti Lahoti, Dr. Shashank Khurana and Dinesh Kumar for their support and love.

A big thanks to my parents who sacrificed many things in their life to make me what I am today. I also take this opportunity to thanks my brother Rahul and my sister Malya for all the love, inspiration, wishes and support. Last and most important, a big thanks and hug to my fiancé Dr. Archana Bajpai. Archana, you always stood by me, throughout encouraging and sorting out snags. I don't have words to express my emotions that how much I love you and how blessed I am to have a partner like you.

Finally, I would like to thank my referee for spending their valuable time to read this thesis.